5 61283 5 B p_s

NASA TN D-1793

NASA TN D-1793

56p.

N 63 17301

Code-1

TECHNICAL NOTE

D-1793

CENTER-LINE PRESSURE DISTRIBUTIONS ON TWO-DIMENSIONAL BODIES WITH LEADING-EDGE ANGLES GREATER THAN THAT FOR SHOCK DETACHMENT AT MACH NUMBER 6 AND ANGLES OF ATTACK UP TO 25°

By Theodore J. Goldberg, George C. Ashby, Jr., and James G. Hondros

Langley Research Center
Langley Station, Hampton, Va.

NATIONAL AERONAUTICS AND SPACE ADMINISTRATION

WASHINGTON June 1963

1

NATIONAL AERONAUTICS AND SPACE ADMINISTRATION

TECHNICAL NOTE D-1793

CENTER-LINE PRESSURE DISTRIBUTIONS ON TWO-DIMENSIONAL BODIES WITH LEADING-EDGE ANGLES GREATER THAN THAT FOR SHOCK DETACHMENT AT MACH NUMBER 6 AND ANGLES OF ATTACK UP TO 25°

By Theodore J. Goldberg, George C. Ashby, Jr.,
and James G. Hondros

17301

SUMMARY

Center-line pressure distributions were obtained for two-dimensional sharp-nose parabolic arc, circular arc, and wedge bodies having a leading-edge angle greater than that for shock detachment (aerodynamically blunt bodies) at Mach number of 6 for angles of attack up to 25°. The maximum pressure coefficient was found to increase continuously from the shock-attachment value to the stagnation value behind a normal shock between leading-edge deflection angles of 42° and 51°. Only the data for contoured bodies having leading-edge angles of 66° or greater are correlated very well by the generalized Newtonian theory. However, at all angles of attack for all aerodynamically blunt bodies having curved surfaces, the agreement between the generalized Newtonian theory and the measured values of pressure coefficient was reasonably good for surface-deflection angles above 30°. This theory can be used to predict pressures on most two-dimensional bodies by the methods shown herein. With few exceptions, at a given deflection angle the pressure distributions rearward of the maximum pressure on the lower and upper surfaces of aerodynamically blunt wedges are essentially coincident with those of wedges having higher and lower half-angles, respectively. In addition, the pressure distributions of these wedges are in good agreement aft of the maximum-pressure point with those of a flat plate at corresponding deflection angles to the lower surface above 53° and to the upper surface above 31°.

INTRODUCTION

There is a large amount of available experimental and theoretical information in the hypersonic speed range for bodies having either rounded leading edges and therefore detached shock waves or sharp leading edges with attached shock waves. However there is very little, if any, available data in this speed range for the class of bodies with sharp leading edges having detached shock waves. The purpose of the present investigation is to provide some information in that area.

This report presents the center-line pressure distributions on a series of two-dimensional bodies having leading-edge angles from 42^o to 90^o which were measured in the Langley 20-inch Mach 6 tunnel at angles of attack up to 25^o. In addition the means by which the pressure distributions can be predicted are also presented.

SYMBOLS

C_p	pressure coefficient, $\dfrac{p_l - p_\infty}{\frac{1}{2}(\gamma p_\infty M_\infty)}$
M_∞	free-stream Mach number
p_l	local pressure, lb/sq in.
p_t	total or stagnation pressure, lb/sq in.
p_∞	free-stream pressure, lb/sq in.
s	distance along body surface from nose, in.
s_w	total length of wedge surface, in.
t	half the maximum body thickness, in.
x,y	body coordinates
α	angle of attack, deg
γ	ratio of specific heats
δ	local inclination of the body surface referenced to wind axis, deg
θ	local inclination of body surface referenced to body axis, deg

Subscripts:

geom	geometric
l	lower surface
le	leading edge
max	maximum
stag	stagnation behind a normal shock
u	upper surface

APPARATUS AND METHODS

Wind Tunnel and Models

This investigation was conducted in the Langley 20-inch Mach 6 tunnel. The tunnel, which has been described in reference 1, is a blowdown-to-atmosphere type which operates at a maximum stagnation temperature of 600° F and a maximum stagnation pressure of 600 lb/sq in. The air is dried by an activated alumina dryer designed to provide a dewpoint temperature of -40° F at 600 lb/sq in.

The three groups of 5 two-dimensional models used in this investigation consisted of wedges and parabolic and circular arcs. Each group had leading-edge angles of 42°, 54°, 66°, 78°, and 90°. These models will herein be referred to by their leading-edge angles and contours. These contours were selected because they represent a large portion of the entire class of two-dimensional sharp-nose bodies having a leading-edge angle greater than that for shock detachment at a Mach number of 6. For a given deflection angle the wedge and the parabolic arc represent the minimum and maximum surface curvature of the present investigation, respectively, while the circular arc represents an intermediate curvature. Although the theoretical shock-detachment angle at Mach 6.0 is 42.4°, it was felt that a perfectly sharp leading edge could not be fabricated and that the shock for a 42°-leading-edge-angle model would be detached. This leading-edge angle would represent the lower limit of the aerodynamically blunt range. All models had a span of 4.00 inches and a thickness of 4.00 inches. The models were adapted with a 2.56-inch-long cylindrical section on the rear by using a "quick-disconnect" type connection to facilitate model changes. Photographs of the models and of the model attached to the support connection are shown in figures 1 and 2, respectively. Model dimensions are given in table I along with x,y locations of orifices, local inclinations at orifices, and surface distance-to-thickness ratios. Extensions, which were added to both sides of the 78° parabolic arc body to check the two dimensionality of the flow along the center line, were each 3 inches wide and contoured to match the basic body. A row of orifices on one of the extensions was located at the same position relative to the edge (2 inches inboard) as those on the basic body. This body was selected because it was the longest and any disturbance emanating from the tips of the models would affect the most rearward orifices. The 78° parabola with extensions is shown in figure 2. Model orifice sizes for the basic models and extensions were 0.021 inside diameter near the leading edges and 0.063 inside diameter at all other orifice locations.

The models were supported in the tunnel by the goose-neck support system shown in figure 3, which moved the model 25° in angle of attack in the horizontal plane. A mechanically operated counter geared to the vertical shaft of the support system was used to measure the angle of attack. Deflections due to air loads were negligible because of the stiffness of the sting support.

Tests

All models were tested in 5° increments over an angle-of-attack range of 0° to 25°. In addition, the 42°-leading-edge models were tested in 1° increments at angles of attack from 0° to 15°.

All tests reported herein were conducted at a stagnation pressure and temperature of 400 lb/sq in. absolute and 400° F which yields a Reynolds number of 7.6×10^6 per foot.

Pressure data were recorded by photographing a mercury manometer for pressures greater than 1 lb/sq in. absolute. For pressures of 1 lb/sq in. absolute or less a butyl phthalate manometer was used to obtain greater accuracy because of the low specific gravity of the fluid. Tunnel stagnation pressures were measured with a 0 to 600 lb/sq in. Bourdon gage. All pressures were photographically recorded simultaneously.

Data Reduction and Accuracy

Previous tunnel calibrations have shown that at any instant the Mach number throughout the test section varies by only ±0.02. However, the Mach number level varies from 5.94 to 6.04 depending upon time - the time during each run, the time between runs, and the total time elapsed. This fact makes it extremely difficult, if not impossible, to obtain an exact calibration curve of Mach number against time. The data, therefore, were initially reduced at an average Mach number of 6. This procedure resulted in sufficient data scatter to make difficult an analysis of data trends. One obvious trend emerged, however, which led to a better definition of test Mach numbers. This trend is shown in figure 4 where the maximum pressure coefficients obtained on the various bodies are presented as a function of the flow-deflection angles at which they were obtained. At flow-deflection angle for shock detachment ($\delta = 42^\circ$) the data agree with oblique shock theory. At higher flow-deflection angles the data approach and even exceed the stagnation-pressure-coefficient value at flow-deflection angles considerably less than 90°. The degree by which the data exceed $C_{p,stag}$, of course, is indicative of the data scatter. Since the data exceed $C_{p,stag}$ by as much as 4 percent which is much greater than measuring accuracy, the scatter is attributed to a true Mach number variation different from the assumed constant value of 6.0. By using the data trend shown in figure 4, a more representative Mach number variation for reducing the data was obtained by the following procedure. For each model the ratio of maximum-local to tunnel-stagnation pressure was assumed to be equal to the total pressure ratio across a normal shock. This ratio was then used to compute the corresponding Mach number for each model and α combination. At the angles of attack where the resulting Mach numbers fell within the known tunnel range these values of Mach number were used to reduce the data. The Mach numbers so obtained were applicable to all bodies except the 42° wedge at angles of attack below 7° and the 42° parabolic and circular arc bodies below $\alpha = 10^\circ$. For the 42° bodies at 0° angle of attack, the Mach numbers were computed by assuming the measured maximum pressure to be given by oblique shock theory. Since these Mach numbers again fell within the known range of tunnel Mach number, they were used to reduce the data for these models. For the angles of attack of the 42° bodies between 0° and 7° or 10°, as the case may be, a linear variation of Mach number with angle of attack between these limits was assumed. This assumption appears to be justifiable because the variation of tunnel Mach number with time is quasi-linear and in the same direction.

The center line of the body was considered to be the dividing line between the upper and lower surfaces at all angles of attack. The location of the maximum pressure point was determined from faired curves of P_l/P_t against θ on the upper and lower surfaces. Where no peak occurred beyond the first orifice, the values of P_l/P_t and θ at the first orifice were used to compute $C_{p,max}$ and δ_{max}. Where a peak occurred downstream of the first orifice, the faired values were used to compute $C_{p,max}$ and δ_{max}.

It should be noted that the data for the 78° parabolic arc body is the least reliable at angles of attack below 15° because the first orifice on the lower surface was inadvertently plugged. At 0° angle of attack the first orifice on the upper surface was used but it was located at an angle of about 8° less than that of the leading edge. At 5° and 10° angle of attack, the second orifice on the lower surface, which was located at an angle of about 12° less than the leading edge, was used. Therefore, the free-stream Mach number computed from the pressures at these orifices for these angles of attack is too high and results in a value of C_p which is too high. It is only this error in Mach number which raises a question as to the reliability of the data for the 78° body.

The maximum error of the measured pressures is believed to be less than 1 percent of the maximum measured value on the body. Model alinement and angles of attack are believed to be accurate to about ±1/2°. The accuracy of the x,y coordinates of the model orifices is ±0.001 inch. The measured coordinates were used to compute the slopes for all orifices.

RESULTS AND DISCUSSION

Experimental Results

Basic data.- The pressure distributions of the 78° parabolic arc model with and without extension pieces at $\alpha = -10^\circ$, 0°, and 10° are presented in figure 5 to show the two dimensionality of the flow. Flow blockage prevented any measurements at higher angles of attack; therefore, the agreement between the distributions on the body with and without the extensions establishes only that the flow along the center line of this, the longest, body is two dimensional up to $\alpha = 10^\circ$. However, all other bodies have the same span but are shorter; therefore, the flow along their center line, with the possible exception of the wedges having higher leading-edge angles, should also be two dimensional up to $\alpha = 10^\circ$.

Pressure distributions of the 15 models tested are presented in figures 6, 7, and 8 for angles of attack up to 25°. In addition, schlieren photographs of all the bodies near 0° angle of attack are presented in figure 9 to show the variation of the shock shape with changes in leading-edge angle and body contour.

Maximum pressure coefficient.- One of the most important results of these tests is that stagnation pressure occurs on all of the bodies in this investigation having a leading-edge deflection angle greater than about 51° and that the maximum pressure coefficient for all bodies has its locus along a single representative curve. (See fig. 10.) The portion of the curve between shock-detachment angle and 51° may be questionable because of the small uncertainty in the value of free-stream Mach number and the inability to locate the first orifice directly at the apex of the nose. However, if the maximum known tunnel Mach numbers were used to compute the pressure coefficients for this portion of the curve, it would shift the deflection angle at which stagnation occurs only about 2° to approximately 49°. In reference 2 stagnation pressure on a flat plate was measured at a deflection angle of 45°. The unrealistic maximum pressure coefficients that are predicted for bodies in this investigation by two modifications to the Newtonian theory are also shown in figure 10 for comparison.

On the upper surface, figure 11 shows that all measured values of $C_{p,max}$ do not lie along a single curve but vary with leading-edge angle and angle of attack. However, for each leading-edge angle the values of $C_{p,max}$ for all shapes tested generally fall along the same curve with the exception of the 78° and 90° bodies. As the leading-edge angle increases, the variation of $C_{p,max}$ with deflection angle approaches that predicted by modified Newtonian theory until at $\delta_{le} = 90^{\circ}$ the curved-surface bodies agree with this theory.

Location of maximum pressure coefficients.- The location of the maximum pressures would be expected to occur at the point where the slope relative to the flow is the greatest - herein referred to as the geometric location. A comparison of the geometric and measured slopes at which the maximum pressures occurred on both the lower and upper surfaces of the parabolic and circular arc bodies is shown in figure 12. It must be remembered that physical limitations prevented the installation of the first orifice exactly at the leading edge. Therefore, in comparing the measured with the geometric location of $C_{p,max}$, they will be considered to coincide whenever the measured values differ from the geometric by the same difference as that indicated at 0° angle of attack. On the lower surface (fig. 12(a)) only for the 90° circular arc body do the measured and geometric locations coincide over the angle-of-attack range investigated. For all other bodies the measured location of $C_{p,max}$ moves off the nose before its angle relative to the flow becomes 90°. This result is attributed to the pressure bleed-off around the sharp leading edge. For bodies having leading-edge angles up to and including 66°, the measured location of $C_{p,max}$ moves off the nose when its angle relative to the flow becomes approximately 67°. This is also true for the wedges, as can be seen in figures 8(b) to (f). However, the maximum difference between the geometric and measured location for any body through the angle-of-attack range of the tests is only about 8°. On the upper surface the location of the maximum pressure might be expected to remain at the nose over the angle-of-attack range of the test. Figure 12(b) shows this to be true only for the 78° and 90° bodies. For bodies having leading-edge angles below 78° the location of $C_{p,max}$ is seen to move off the nose at angles of attack less than 20°. This result can be attributed to leading-edge separation around the nose followed by flow reattachment as indicated in figures 6, 7, and 8.

Comparison of center-line pressure distributions on wedges and a flat plate at corresponding deflection angles.- Another important result which can be obtained from these tests is the effect of leading-edge angle on the pressure distributions over the wedge surfaces at a given inclination to the flow. The lower- and upper-surface pressure distributions, in terms of $C_p/C_{p,max}$ against s/s_w for wedges at approximately constant surface-deflection angles are presented in figure 13. The surface-deflection angles are only approximately constant because the wedge angles were varied in 12° increments whereas the angle of attack was varied in 5° increments. It can be seen that the maximum pressure point moves rearward on the lower surface with decreasing wedge angle only for deflection angles greater than about 66° and on the upper surface with increasing wedge angle only for deflection angles less than about 66°. The effect of leading-edge angle on wedge surface-pressure distributions is seen to be slight because, with few exceptions, at a given deflection angle, the pressure distributions rearward of the maximum pressure point on the lower and upper surfaces are essentially coincident with those of corresponding surfaces of wedges having higher and lower half-angles, respectively. Thus the wedge-surface pressure distributions are primarily a function only of flow-deflection angles. The effect of leading edge is confined to those regions ahead of the location of the maximum pressure coefficient. Since the value of $C_{p,max}$ on the lower surface is a constant (as shown in fig. 13), the pressure coefficients aft of the maximum pressure point on the lower surface at a given location of all wedges at the same deflection angles are also coincident. However, on the upper surface the value of $C_{p,max}$ varies not only with deflection angle but also with wedge angle at the same deflection angle; therefore, the pressure coefficients at a given location on the upper surface of wedges at the same deflection angles are not coincident. It should be noted that at $\delta = 66^{\circ}$ and above, the distributions on the lower and upper surfaces for the same δ agree. This can be seen from figures 13(a) and 13(b) since the data for each body at $\alpha = 0$ are presented in both.

Also included in figure 13 are flat-plate pressure distributions from reference 2 at approximately the same deflection angles as the wedge surfaces. In general, the pressure distributions of the wedges are in good agreement aft of the maximum pressure point with those of the flat plate at deflection angles of the lower surface above 53° and of the upper surface above 31°. This agreement might not be envisioned since in a subsonic-flow field behind a normal shock, the upper surface would be expected to affect the pressures on the lower surface of the wedge. It is interesting to note that for deflection angles from 27° to 37° the values of $C_{p,max}$ for the upper surface of wedges at angles of attack other than 0° are about the same as those for a flat plate at corresponding deflection angles.

Prediction of Pressures on Aerodynamically Blunt Bodies

Having obtained the pressure data on these bodies it is of interest to determine if there is a simple method of predicting pressures on two-dimensional aerodynamically blunt bodies. Probably the most widely used method of predicting pressures and forces (because of its simplicity and ease of calculating) is some form of the Newtonian theory

$$C_p = K \sin^2\delta$$

Various modifications of this theory have been found to give reasonably good predictions of the pressure distribution on different bodies, if the proper value of K is chosen. For example, it is shown in reference 3 that with $K = (\gamma + 1)$, the theory is applicable only to bodies having small leading-edge angles; and in reference 4, with $K = C_{p,stag}$, theory is limited to bodies having 90° leading-edge slopes. As can be seen in figure 10, neither of these modifications is applicable to the bodies of this investigation.

A more recent consideration of the Newtonian theory is presented in reference 5 which suggests that in the general case K has the form $\frac{C_{p,max}}{\sin^2\delta_{max}}$, thus acknowledging that K is not necessarily constant. This resulted in the generalized Newtonian theory

$$\frac{C_p}{C_{p,max}} = \frac{\sin^2\delta}{\sin^2\delta_{max}}$$

which was shown to predict the surface-pressure distribution reasonably well for pointed-nose bodies having a leading-edge angle less than that for shock detachment, as well as for bodies having a 90° leading-edge slope. (Unpublished work also shows that this generalized form of Newtonian theory can be derived by resorting to the tangent-wedge or tangent-cone approximations.) Therefore, it was decided to investigate this method for use in predicting the pressures on the two-dimensional aerodynamically blunt bodies studied herein.

Wedges.- Since the prediction of the pressure distribution for any body by means of the generalized Newtonian theory is basically dependent upon the body having a changing slope, it obviously cannot be applied in the same manner to wedges as to bodies having curved surfaces. However, it is shown in reference 5, that by using pressures computed from attached shock theory, the generalized Newtonian theory is applicable from one wedge to another, for wedge angles less than shock detachment at 0° angle of attack. For the aerodynamically blunt wedges of the present investigation it is apparent from figure 8 that the large and varied pressure gradients require any correlation with generalized Newtonian theory from one wedge to another, or from one surface to another for the same wedge at angle of attack, to be made at more than one point along the surface of the bodies. Even if this could be done with reasonably good results, the pressure distribution of one wedge would first have to be known. In view of the fact that experimental values must be resorted to, and since the data of the present investigation cover the range of aerodynamically blunt wedges, the pressure distribution of any wedge in this regime can be obtained by interpolating these data. In addition, the good agreement in pressure distribution from wedge to wedge at the same deflection angles, as well as the agreement from wedges to a flat plate at corresponding deflection angles (fig. 13), enables the pressure distribution to be obtained for either of the two types of bodies if one is known.

Parabolic and circular arc bodies.- Since the lower and upper surfaces of the bodies of the present investigation are separated by a sharp leading edge, which is shown in figures 6 and 7 to result in flow separation and reattachment at some angles of attack and, therefore, a difference in the value of K between the two surfaces, the theory might not be expected to apply from surface to surface. Therefore, the data for each surface are reduced in the generalized Newtonian form by using their respective measured $C_{p,max}$ values. The results for the parabolic and circular arc models together with the generalized Newtonian theory prediction using the measured $C_{p,max}$ and its associated δ_{max} are presented in figures 14 and 15.

As can be seen from figures 14 and 15, the data for both the parabolic arc and circular arc bodies can be divided into two distinct correlation groups; bodies having a leading-edge angle closest to that for shock attachment (42° and 54°) and bodies having leading-edge angles much greater than shock attachment (66° to 90°). The data for the former group are not correlated with any consistency by the generalized Newtonian theory, whereas the data of the latter group were in general correlated very well for both surfaces by the theory.

The agreement between the measured and theoretical values in percent of the measured C_p cannot be made directly from figures 14 and 15 because the $C_{p,max}$ values are not constant for all bodies on either surface. Therefore, a majority of the measured and predicted values of C_p together with their differences in percent of measured C_p are presented in table II. As might be expected the agreement is best near the nose where the body slope is high and becomes progressively poorer as the surface inclination decreases; however, the disagreement does not in general become poorer than about 20 percent of measured C_p down to a surface inclination of 30° (the limit to which modified Newtonian theory is known to predict the pressures very well on cylinders). The very high percentage errors at inclinations below 30° may not be very significant because the pressures are very low over this region. There are points between the nose and the maximum pressure point on both surfaces of some bodies at angle of attack which cannot be predicted by the generalized Newtonian theory because the value of $\dfrac{\sin^2\delta}{\sin^2\delta_{max}}$ becomes greater than 1. But considering all points above deflection angles of 30°, the theory predicts about 85 percent of them within 10 percent of the measured C_p. It should be noted that whereas the data for the lower surface appear to be in better agreement with the theory than those of the upper surface in figures 14 and 15, table II shows that, on the basis of the percentage of measured C_p, both surfaces show about the same agreement for inclinations above 30°. The agreement for the circular arc bodies was, in general, better than that for the parabolic arc bodies and indicated that for the same leading-edge angle the gradient of slope along the body may be the important factor in determining how well the generalized Newtonian theory predicts the pressure distribution for two-diminensional aerodynamically blunt bodies, that is, the more rapidly the slope changes, the poorer the correlation.

Application of Generalized Newtonian Theory to Any Two-Dimensional Aerodynamically Blunt Body Having Curved Surfaces

It has been shown that the pressure distributions of the aerodynamically blunt bodies having curved surfaces of the present investigation agree reasonably well with the generalized Newtonian theory. However, in order to use this theory to predict the pressures on any body without resorting to experimentation, it is necessary to know a pressure at a given slope on the surface. Since the measured locations of the maximum pressures are shown in figure 12 to occur reasonably close to the geometric locations and because the maximum pressure on the lower surface is equal to stagnation value for the majority of deflection angles between shock detachment and 90° (fig. 10), it would be convenient to utilize the maximum pressure on the lower surface to predict the pressures over the whole body. An analysis shows that this can be accomplished as follows:

On the lower surface $C_{p,max} = C_{p,stag}$ for $\delta_{le} \geqq 51^{\circ}$, while for $\delta < 51^{\circ}$, $C_{p,max}$ for deflection angles between 42° and 51° can be obtained from

$$\frac{C_{p,max}}{C_{p,stag}} = \frac{\sin^2\delta_{le}}{\sin^2 51^{\circ}}$$

The values of $C_{p,max}$ obtained in this manner for these deflection angles are shown in figure 10 and are in good agreement with the measured values. For deflection angles equal to or less than shock detachment, $C_{p,max}$ is obtained from oblique shock theory.

The pressure distribution for the lower surface at each angle of attack can then be computed from

$$\frac{C_p}{C_{p,max}} = \frac{\sin^2\delta}{\sin^2\delta_{max,geom}}$$

and the pressure distributions for the upper surface can be obtained at any angle of attack from

$$\frac{C_p}{C_{p,max(\alpha=0^{\circ})}} = \frac{\sin^2\delta}{\sin^2\delta_{le(\alpha=0^{\circ})}}$$

The pressure coefficients predicted by this method for the parabolic and circular arc bodies are presented in table II. In general, these values are about the same as those obtained from the generalized Newtonian theory by using the values of $C_{p,max}$ at their actual locations on each surface and are within about 20 percent of the measured C_p at deflection angles above 30°. Some of the points between the nose and the actual location of the maximum pressure point, which could not be predicted by the generalized Newtonian theory by using $C_{p,max}$ at its actual location for each surface, are not predicted by this method within this accuracy. However, on the whole, about 85 percent of all points at deflection angles above 30° are predicted within 10 percent of the measured C_p value.

The good agreement between the generalized Newtonian theory and the data of the present investigation as well as the results for bodies having a leading-edge angle less than that for shock detachment in reference 5 indicate that this theory may be applicable to all two-dimensional bodies except aerodynamically blunt wedges.

CONCLUSIONS

An investigation of the center-line pressure distributions on two-dimensional sharp-nose bodies having a leading-edge angle greater than that for shock detachment at a Mach number of 6 and angles of attack up to 25° has resulted in the following conclusions:

1. Stagnation pressure behind a normal shock was measured on all bodies having a leading-edge deflection angle greater than about 51° and the maximum pressure coefficient for all bodies has its locus along a single representative curve which continuously increases with increasing deflection angle between shock detachment and about 51°.

2. With few exceptions the center-line pressure distributions rearward of the maximum pressure point on the lower and upper surfaces of aerodynamically blunt wedges are primarily a function only of surface-deflection angle and essentially independent of leading-edge angle. In addition, the pressure distributions of these wedges are in good agreement aft of the maximum pressure point with those of a flat plate at corresponding deflection angles to the lower surface above 53° and to the upper surface above 31°.

3. Only the data for contoured bodies having leading-edge angles of 66° or greater are correlated very well by the generalized Newtonian theory. However, at all angles of attack for all aerodynamically blunt bodies having curved surfaces, the agreement between the generalized Newtonian theory and the measured values of C_p was reasonably good for surface-deflection angles above 30° (for 85 percent of the points in this region the theoretical values of C_p were within 10 percent of the measured C_p).

4. The generalized Newtonian theory can be used to predict the center-line pressures on aerodynamically blunt contoured bodies because the maximum pressures and their locations can be predetermined.

Langley Research Center,
National Aeronautics and Space Administration,
Langley Station, Hampton, Va., February 27, 1963.

REFERENCES

1. Ashby, George C., Jr., and Fitzgerald, Paul E., Jr.: Longitudinal Stability and Control Characteristics of Missile Configurations Having Several Highly Swept Cruciform Fins and a Number of Trailing-Edge and Fin-Tip Controls at Mach Numbers From 2.21 to 6.01. NASA TM X-335, 1961.

2. Hondros, James G.: Pressure Distributions on Two-Dimensional Sharp-Leading-Edge Flat Plates With Sweep Angles of 0°, 30°, and 45° at a Mach Number of 6 and Angles of Attack From 0° to 90°. NASA TN D-1371, 1962.

3. Laitone, Edmund V.: Exact and Approximate Solutions of Two-Dimensional Oblique Shock Flow. Jour. Aero. Sci., vol. 14, no. 1, Jan. 1947, pp 25-41.

4. Lees, Lester: Hypersonic Flow. Fifth International Aeronautical Conference (Los Angeles, Calif., June 20-23, 1955), Inst. Aero. Sci., Inc., 1955, pp 241-276.

5. Love, E. S.: Generalized-Newtonian Theory. Jour. Aero/Space Sci. (Reader's Forum), vol. 26, no. 5, May 1959, pp. 314-315.

TABLE I.- MODEL DIMENSIONS AND ORIFICE LOCATIONS

(a) Parabolic arc models

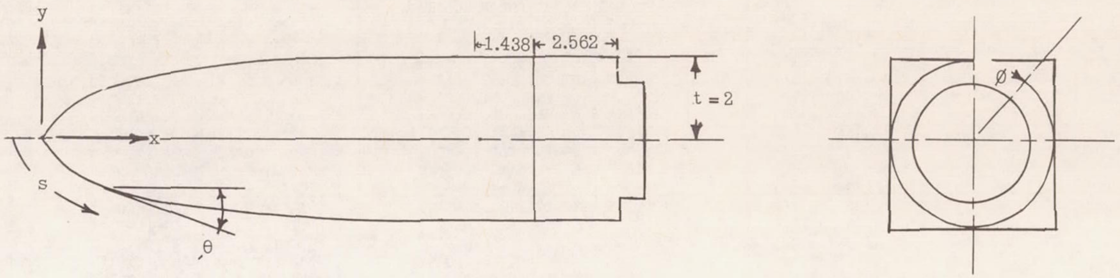

42° parabolic arc				
Orifice location		Slope θ, deg	s/t	ϕ, deg
x, in.	y, in.			
0.067	-0.060	41.23	0.045	180
.226	-.196	39.44	.149	
.407	-.342	37.46	.265	
.565	-.457	35.80	.363	
.726	-.568	34.15	.411	
1.227	-.880	29.33	.756	
1.512	-1.033	26.80	.918	
1.861	-1.199	23.88	1.110	
2.255	-1.358	20.82	1.324	
2.698	-1.512	17.66	1.558	
3.829	-1.792	10.75	2.142	
4.306	-1.873	8.26	2.383	
4.774	-1.933	6.02	2.619	
5.241	-1.975	3.97	2.854	
5.720	-1.999	2.03	3.093	
6.999	-2.000	0	3.733	
.172	.148	40.0	.114	0
.282	.236	38.82	.185	
.412	.338	37.41	.268	
.571	.456	35.73	.367	
.730	.569	34.11	.464	
.968	.725	31.76	.606	
1.226	.877	29.44	.755	
1.518	1.034	26.90	.921	
1.862	1.197	23.87	1.111	
2.257	1.359	20.81	1.325	
2.702	1.512	17.64	1.560	
3.836	1.794	10.71	2.113	
4.305	1.871	8.26	2.383	
4.776	1.932	6.01	2.620	
5.242	1.972	3.97	2.854	
5.718	1.994	2.05	3.092	
6.174	2.000	.35	3.321	
6.431	2.000	0	3.449	

54° parabolic arc				
Orifice location		Slope θ, deg	s/t	ϕ, deg
x, in.	y, in.			
0.036	-0.052	53.04	0.030	180
.140	-.180	50.39	.114	
.275	-.332	47.19	.217	
.415	-.476	44.12	.317	
.610	-.654	40.21	.448	
.792	-.799	36.92	.565	
1.106	-1.065	31.89	.755	
1.446	-1.206	27.22	.951	
1.875	-1.403	22.27	1.187	
2.422	-1.601	17.10	1.477	
3.497	-1.850	9.54	2.029	
3.972	-1.923	6.96	2.269	
4.564	-1.975	4.21	2.567	
5.097	-1.996	2.09	2.834	
5.427	-1.997	.90	2.999	
6.701	-1.998	0	3.636	
.122	.156	50.83	.100	0
.194	.242	49.08	.156	
.275	.332	47.19	.217	
.419	.481	44.03	.320	
.610	.655	40.21	.448	
.793	.802	36.90	.565	
1.100	1.062	31.97	.752	
1.451	1.212	27.17	.953	
1.872	1.405	22.30	1.185	
2.423	1.602	17.10	1.478	
3.502	1.852	9.51	2.032	
4.030	1.924	6.37	2.298	
4.566	1.973	4.21	2.569	
5.097	1.988	2.09	2.834	
5.432	1.999	.89	3.002	
5.909	1.999	0	3.240	

66° parabolic arc				
Orifice location		Slope θ, deg	s/t	ϕ, deg
x, in.	y, in.			
0.026	-0.068	64.19	0.031	180
.105	-.202	59.35	.114	
.195	-.335	54.70	.197	
.293	-.468	50.37	.278	
.402	-.592	46.23	.360	
.664	-.829	38.33	.536	
.985	-1.051	31.22	.732	
1.446	-1.291	23.96	.992	
2.155	-1.521	16.54	1.369	
3.049	-1.761	10.53	1.829	
3.569	-1.846	7.99	2.092	
4.092	-1.910	5.90	2.355	
4.612	-1.958	4.16	2.616	
5.128	-1.987	2.69	2.875	
5.655	-1.998	1.38	3.138	
6.182	-2.000	.25	3.402	
7.263	-2.000	0	3.950	
.073	.147	61.21	.082	0
.134	.251	57.75	.142	
.196	.341	54.65	.198	
.299	.475	50.12	.282	
.406	.595	46.09	.362	
.667	.832	38.25	.538	
.988	1.053	31.17	.733	
1.448	1.291	23.94	.993	
2.055	1.518	17.41	1.317	
3.059	1.764	10.48	1.833	
3.567	1.846	8.00	2.091	
4.095	1.911	5.89	2.357	
4.617	1.958	4.15	2.619	
5.138	1.989	2.66	2.871	
5.653	1.999	1.39	3.138	
6.193	1.999	.22	3.407	
6.461	1.999	0	3.541	

78° parabolic arc				
Orifice location		Slope θ, deg	s/t	ϕ, deg
x, in.	y, in.			
0.015	-0.069	73.93	0.031	180
.052	-.164	66.82	.086	
.108	-.267	59.51	.148	
.406	-.615	39.79	.375	
.777	-.862	28.87	.599	
1.309	-1.104	20.75	.891	
2.035	-1.331	14.74	1.272	
3.251	-1.583	9.47	1.893	
3.876	-1.678	7.56	2.197	
4.500	-1.754	6.17	2.523	
5.021	-1.805	5.20	2.785	
5.749	-1.863	4.07	3.150	
6.363	-1.902	3.28	3.458	
6.999	-1.934	2.56	3.776	
7.620	-1.957	1.95	4.087	
8.246	-1.975	1.40	4.400	
8.865	-1.988	.92	4.710	
9.491	-1.998	.48	5.023	
10.177	-1.999	.05	5.366	
11.256	-1.999	0	5.905	
.025	.084	70.56	.048	0
.062	.183	65.35	.098	
.102	.260	60.19	.142	
.230	.438	49.06	.252	
.381	.591	40.86	.359	
.782	.865	28.77	.602	
1.316	1.107	20.67	.895	
2.045	1.334	14.68	1.277	
3.249	1.584	9.35	1.892	
3.871	1.675	7.58	2.207	
4.502	1.751	6.16	2.524	
5.025	1.803	5.19	2.787	
5.748	1.861	4.08	3.150	
6.377	1.902	3.26	3.465	
7.000	1.933	2.56	3.777	
7.625	1.957	1.94	4.090	
8.251	1.974	1.40	4.403	
8.871	1.987	.92	4.713	
9.499	1.995	.48	5.027	
10.183	1.998	.05	5.369	
10.465	1.998	0	5.510	

90° parabolic arc				
Orifice location		Slope θ, deg	s/t	ϕ, deg
x, in.	y, in.			
0.000	-0.007	89.62	0.004	180
.005	-.117	83.50	.051	
.019	-.214	77.79	.099	
.055	-.333	70.43	.167	
.124	-.480	61.21	.252	
.345	-.765	44.48	.433	
.665	-1.015	32.22	.636	
.958	-1.176	25.64	.803	
1.415	-1.362	19.16	1.050	
2.164	-1.574	12.93	1.439	
3.447	-1.794	7.20	2.090	
4.193	-1.874	5.12	2.465	
4.938	-1.930	3.52	2.839	
5.693	-1.967	2.23	3.217	
6.444	-1.992	1.16	3.593	
7.381	-1.999	.09	4.061	
8.457	-1.999	0	4.599	
.005	.110	83.90	.051	0
.040	.213	77.53	.143	
.057	.339	70.54	.169	
.125	.482	61.09	.253	
.335	.757	44.92	.426	
.662	1.014	32.27	.634	
.955	1.175	25.69	.801	
1.419	1.363	19.13	1.050	
2.163	1.574	12.93	1.439	
3.446	1.793	7.21	2.090	
4.198	1.874	5.11	2.468	
4.949	1.931	3.49	2.795	
5.695	1.967	2.22	3.218	
6.447	1.990	1.16	3.594	
7.384	1.998	.09	4.063	
8.167	1.999	0	4.454	

TABLE I.- MODEL DIMENSIONS AND ORIFICE LOCATIONS - Continued

(b) Circular arc models

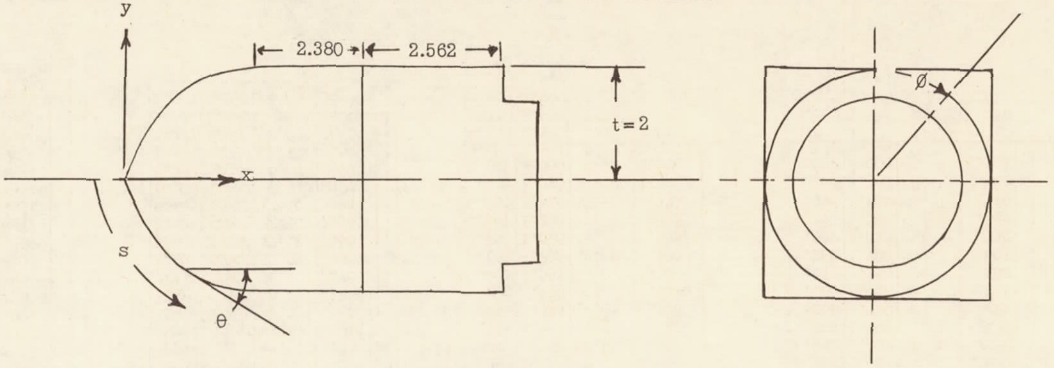

42° circular arc				
Orifice location		Slope θ, deg	s/t	φ, deg
x, in.	y, in.			
0.082	-0.075	41.19	0.056	180
.203	-.179	40.01	.136	
.278	-.239	39.30	.183	
.481	-.399	37.41	.312	
.675	-.542	35.63	.432	
.979	-.751	32.91	.618	
1.226	-.906	30.77	.764	
1.488	-1.053	28.56	.913	
1.979	-1.298	24.51	1.188	
2.27	-1.423	22.19	1.345	
3.036	-1.690	16.21	1.752	
3.567	-1.823	12.18	2.022	
4.082	-1.918	8.33	2.289	
4.609	-1.980	4.42	2.575	
5.121	-1.997	.66	2.749	
6.212	-1.998	0	3.293	
.162	.139	40.43	.105	0
.287	.243	39.24	.187	
.363	.305	38.51	.236	
.592	.480	36.39	.380	
.747	.592	34.99	.476	
.979	.749	32.92	.616	
1.233	.910	30.71	.768	
1.583	1.104	27.76	.967	
1.979	1.298	24.51	1.188	
2.273	1.424	22.16	1.347	
3.037	1.690	16.20	1.751	
3.567	1.823	12.18	2.022	
4.083	1.919	8.32	2.292	
4.609	1.982	4.42	2.586	
5.127	1.997	.62	2.738	
5.410	1.999	0	2.879	

54° circular arc				
Orifice location		Slope θ, deg	s/t	φ, deg
x, in.	y, in.			
0.046	-0.064	53.07	0.040	180
.117	-.154	51.71	.097	
.195	-.247	50.29	.156	
.302	-.370	48.36	.237	
.422	-.500	46.27	.326	
.538	-.619	44.31	.409	
.721	-.789	41.36	.535	
.941	-.973	37.96	.679	
1.149	-1.127	34.91	.808	
1.376	-1.275	31.71	.943	
1.592	-1.399	28.77	1.067	
2.430	-1.762	17.96	1.524	
2.905	-1.890	12.15	1.769	
3.375	-1.967	6.52	2.002	
3.843	-1.995	.97	2.177	
4.932	-1.998	0	2.722	
.081	.105	52.44	.066	0
.183	.231	50.53	.146	
.285	.351	48.66	.225	
.342	.415	47.65	.268	
.472	.554	45.40	.364	
.605	.685	43.19	.457	
.736	.803	41.11	.545	
.919	.955	38.30	.664	
1.121	1.107	35.32	.791	
1.362	1.317	31.59	.984	
1.591	1.402	28.76	1.069	
2.434	1.765	17.91	1.529	
2.905	1.892	12.14	1.773	
3.377	1.968	6.49	2.005	
3.849	1.999	.90	2.226	
4.125	1.999	0	2.363	

66° circular arc				
Orifice location		Slope θ, deg	s/t	φ, deg
x, in.	y, in.			
0.016	-0.039	65.28	0.021	180
.060	-.128	63.59	.070	
.111	-.225	61.74	.125	
.177	-.341	59.45	.192	
.253	-.465	56.98	.265	
.382	-.647	53.19	.376	
.495	-.794	50.05	.469	
.611	-.922	47.10	.555	
.763	-1.079	43.39	.665	
.906	-1.207	40.12	.761	
1.111	-1.366	35.71	.891	
1.342	-1.517	31.04	1.028	
2.027	-1.834	18.18	1.411	
2.506	-1.952	9.79	1.656	
3.018	-1.997	1.04	1.876	
4.094	-2.000	0	2.414	
.058	.126	63.64	.070	0
.116	.238	61.49	.133	
.159	.314	60.01	.176	
.245	.455	57.37	.259	
.340	.595	54.33	.343	
.436	.722	51.63	.423	
.533	.839	49.04	.499	
.643	.958	46.29	.579	
.761	1.076	43.45	.663	
.906	1.208	40.12	.762	
1.108	1.366	35.76	.891	
1.325	1.510	31.33	1.022	
2.016	1.830	18.37	1.404	
2.497	1.950	9.94	1.652	
3.004	1.998	1.29	1.891	
3.361	2.000	0	2.069	

78° circular arc				
Orifice location		Slope θ, deg	s/t	φ, deg
x, in.	y, in.			
0.004	-0.042	77.04	0.023	180
.022	-.128	75.05	.068	
.047	-.214	73.02	.112	
.089	-.329	70.27	.173	
.149	-.474	66.70	.251	
.208	-.599	63.57	.319	
.274	-.722	60.39	.389	
.382	-.899	55.70	.493	
.493	-1.051	51.43	.588	
.597	-1.171	47.83	.667	
.750	-1.325	42.90	.776	
.967	-1.506	36.49	.917	
1.174	-1.644	30.85	1.042	
2.072	-1.968	9.06	1.521	
2.386	-1.997	1.89	1.665	
3.470	-1.999	0	2.207	
.028	.124	75.11	.066	0
.056	.218	72.89	.114	
.091	.319	70.46	.167	
.147	.456	67.10	.241	
.205	.584	63.91	.311	
.273	.714	60.56	.385	
.351	.845	57.11	.461	
.445	.981	53.34	.544	
.544	1.105	49.76	.623	
.643	1.216	46.37	.698	
.744	1.315	43.16	.768	
.950	1.490	37.03	.904	
1.152	1.628	31.47	1.026	
2.039	1.964	9.82	1.507	
2.373	1.997	2.19	1.659	
2.678	1.999	0	1.811	

90° circular arc				
Orifice location		Slope θ, deg	s/t	φ, deg
x, in.	y, in.			
0.001	-0.003	89.91	0.001	180
.002	-.073	87.90	.036	
.011	-.190	84.53	.095	
.028	-.323	80.71	.162	
.056	-.461	76.64	.232	
.089	-.582	73.06	.295	
.134	-.714	69.05	.365	
.215	-.897	63.31	.465	
.279	-1.014	59.47	.532	
.373	-1.156	54.59	.616	
.503	-1.322	48.54	.722	
.611	-1.538	44.00	.802	
.822	-1.614	36.11	.939	
1.523	-1.940	13.80	1.326	
1.929	-1.996	2.04	1.507	
3.004	-2.000	0	2.045	
.004	.089	87.45	.044	0
.009	.170	85.13	.085	
.021	.275	82.07	.138	
.042	.390	78.73	.196	
.071	.518	74.97	.261	
.112	.648	71.05	.330	
.176	.813	65.96	.418	
.239	.941	61.88	.489	
.318	1.076	57.39	.568	
.397	1.190	53.40	.637	
.505	1.322	48.51	.722	
.618	1.439	43.82	.803	
.826	1.614	36.02	.939	
1.508	1.934	14.27	1.314	
1.924	1.995	2.17	1.503	
2.204	1.999	0	1.643	

TABLE I.- MODEL DIMENSIONS AND ORIFICE LOCATIONS - Concluded

(c) Wedge models

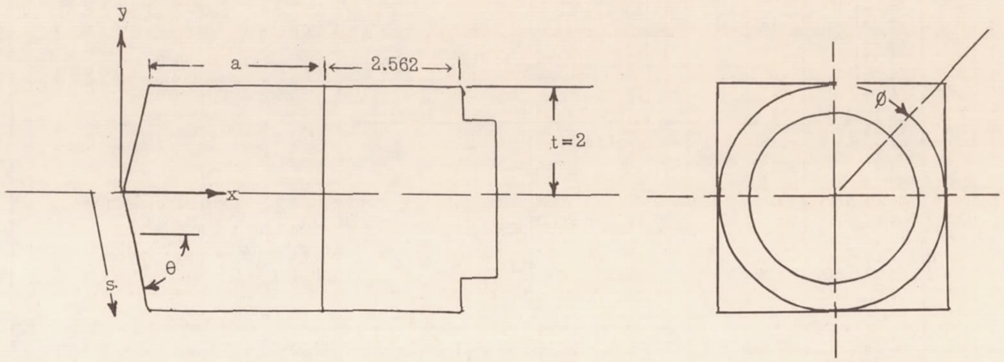

42° wedge				
Orifice location		Slope θ, deg	s/t	Ø, deg
x, in.	y, in.			
0.054	-0.048	42.00	0.036	180
.203	-.183		.136	
.357	-.321		.240	
.459	-.413		.308	
.573	-.516		.386	
.761	-.684		.512	
.944	-.850		.635	
1.125	-1.012		.756	
1.320	-1.188		.888	
1.498	-1.349		1.008	
1.687	-1.518		1.134	
2.145	-1.931		1.443	
3.216	-2.000	0	1.992	
.149	.134	42.00	.100	0
.256	.230		.172	
.364	.328		.245	
.476	.428		.320	
.575	.517		.386	
.765	.689		.514	
.949	.855		.638	
1.141	1.027		.767	
1.326	1.192		.891	
1.510	1.358		1.015	
1.691	1.523		1.138	
2.155	1.941		1.450	
2.417	2.000	0	1.592	

a = 1.438

54° wedge				
Orifice location		Slope θ, deg	s/t	Ø, deg
x, in.	y, in.			
0.046	-0.063	54.00	0.039	180
.132	-.181		.112	
.231	-.318		.196	
.318	-.438		.270	
.410	-.565		.349	
.560	-.771		.476	
.704	-.970		.599	
.934	-1.285		.794	
1.037	-1.428		.882	
1.146	-1.579		.976	
1.406	-1.936		1.196	
2.448	-2.000	0	1.734	
.099	.137	54.00	.084	0
.164	.226		.140	
.231	.318		.196	
.324	.446		.276	
.417	.574		.354	
.564	.777		.480	
.714	.982		.607	
.932	1.284		.794	
1.042	1.435		.887	
1.148	1.581		.977	
1.412	1.944		1.201	
1.548	2.000	0	1.284	

a = 2.063

66° wedge				
Orifice location		Slope θ, deg	s/t	Ø, deg
x, in.	y, in.			
0.025	-0.057	66.00	0.031	180
.077	-.172		.095	
.138	-.309		.169	
.198	-.445		.244	
.255	-.574		.314	
.359	-.806		.441	
.453	-1.017		.557	
.547	-1.229		.672	
.634	-1.424		.779	
.844	-1.895		1.037	
1.876	-2.000	0	1.588	
.046	.102	66.00	.056	0
.094	.210		.115	
.136	.304		.166	
.190	.428		.234	
.266	.597		.326	
.355	.796		.436	
.452	1.016		.556	
.547	1.228		.672	
.630	1.415		.774	
.837	1.878		1.028	
1.101	2.000	0	1.200	

a = 2.625

78° wedge				
Orifice location		Slope θ, deg	s/t	Ø, deg
x, in.	y, in.			
0.002	-0.011	78.00	0.005	180
.028	-.133		.068	
.061	-.288		.147	
.087	-.411		.210	
.117	-.548		.280	
.168	-.788		.403	
.219	-1.030		.526	
.274	-1.288		.658	
.325	-1.531		.782	
.404	-1.898		.970	
1.422	-2.000	0	1.520	
.022	.102	78.00	.052	0
.044	.208		.106	
.068	.320		.164	
.089	.418		.214	
.117	.552		.282	
.168	.788		.403	
.222	1.041		.532	
.274	1.290		.660	
.297	1.400		.716	
.408	1.921		.982	
.622	2.000	0	1.121	

a = 3.090

90° wedge				
Orifice location		Slope θ, deg	s/t	Ø, deg
x, in.	y, in.			
0.000	0.000	90.00	0.000	180
	-.109		.054	
	-.199		.100	
	-.314		.157	
	-.449		.224	
	-.696		.348	
	-.945		.472	
	-1.096		.548	
	-1.246		.623	
	-1.394		.697	
	-1.915		.958	
.995	-2.000	0	1.498	
.000	.112	90.00	.056	0
	.200		.100	
	.333		.167	
	.455		.228	
	.700		.350	
	.958		.479	
	1.079		.540	
	1.206		.603	
	1.335		.668	
	1.930		.965	
.198	2.000	0	1.099	

a = 3.515

TABLE II.- MEASURED AND THEORETICAL VALUES OF PRESSURE COEFFICIENTS FOR

TWO-DIMENSIONAL AERODYNAMICALLY BLUNT BODIES

(a) Parabolic arc bodies - lower surface

$\theta_{le} = 42^\circ$

α, deg	δ, deg	$C_{p,meas}$	C_p (a)	C_p (b)	$\frac{C_{p,meas} - C_p}{C_{p,meas}}$ (a)	$\frac{C_{p,meas} - C_p}{C_{p,meas}}$ (b)
0	41.232	1.2822	1.2822	1.2441	0	0.02971
	39.441	1.1226	1.1908	1.1551	-.06075	-.02913
	35.800	.93906	1.0099	.97988	-.07543	-.04347
	29.332	.65852	.70248	.68158	-.06676	-.03502
	26.800	.57012	.60001	.58214	-.05243	-.02108
	23.884	.46761	.48380	.46940	-.03462	-.00383
	10.753	.14409	.10268	.09961	.28739	.30870
	3.976	.05815	.01426	.01382	.75477	.76234
	0	.01764	0	0	1.0000	1.0000
5	46.232	1.6314	1.6314	1.5906	0	.02501
	44.441	1.4039	1.5332	1.4949	-.09210	-.06482
	40.800	1.1608	1.3357	1.3022	-.15067	-.12181
	34.332	.83187	.99511	.97021	-.19623	-.16630
	31.800	.72034	.86866	.84692	-.20590	-.17572
	28.884	.60192	.72989	.71163	-.21260	-.18227
	15.753	.22472	.23048	.22473	-.02563	-.00004
	8.979	.10756	.07627	.07436	.29091	.30866
	5.000	.05117	.01523	.01485	.70236	.70979
10	51.232	1.8190	1.8190	1.7809	0	.02095
	49.441	1.5955	1.7267	1.6904	-.08223	-.05948
	45.800	1.3371	1.5379	1.5056	-.15018	-.12602
	39.332	.98596	1.2021	1.1768	-.21922	-.19356
	36.800	.86787	1.0737	1.0511	-.23717	-.21088
	33.884	.73834	.93000	.92046	-.25958	-.23312
	27.667	.50660	.64511	.63156	-.27341	-.24666
	16.029	.21390	.22825	.22345	-.06709	-.04465
	10.000	.09771	.07321	.07169	.25074	.26630
15	56.232	1.8186	1.8186	1.7868	0	.01749
	54.441	1.6716	1.7413	1.7108	-.04170	-.02345
	50.800	1.4362	1.5804	1.5527	-.10040	-.08112
	44.332	1.0984	1.2852	1.2627	-.17007	-.14958
	41.800	.98350	1.1691	1.1487	-.18871	-.16797
	38.884	.86305	1.0370	1.0188	-.20155	-.18046
	32.667	.62216	.76667	.75325	-.23227	-.21070
	25.753	.40783	.49670	.48800	-.21791	-.19658
	18.979	.24477	.27848	.27361	-.13772	-.11782
	15.000	.15212	.15404	.15133	-.01262	.00519
20	61.232	1.8170	1.8170	1.7909	0	.01436
	59.441	1.7523	1.7532	1.7279	-.00051	.01392
	55.800	1.5496	1.6176	1.5943	-.04388	-.02885
	49.332	1.2352	1.3605	1.3409	-.10144	-.08557
	46.800	1.1192	1.2566	1.2385	-.12277	-.10659
	43.884	1.0062	1.1363	1.1199	-.12930	-.11300
	37.667	.75410	.88297	.87027	-.17089	-.15405
	30.753	.53493	.61818	.60929	-.15563	-.13901
	26.026	.39756	.45550	.44896	-.14574	-.12929
	20.000	.24067	.25064	.24702	-.04143	-.02638
25	66.232	1.8187		1.7978		.01149
	64.441	1.8138	1.7902	1.7466	.01301	.03705
	60.800	1.6619	1.6763	1.6355	-.00866	.01589
	54.332	1.3774	1.4520	1.4167	-.05416	-.02853
	51.800	1.2632	1.3586	1.3255	-.07552	-.04932
	48.880	1.1490	1.2486	1.2182	-.08668	-.06023
	42.667	.88970	1.0105	.98588	-.13578	-.10810
	35.753	.65514	.75094	.73266	-.14623	-.11833
	31.029	.50699	.58469	.57047	-.15326	-.12521
	28.979	.45822	.51653	.50394	-.12725	-.09978
	25.000	.32612	.36394	.35508	-.11597	-.08880

$\theta_{le} = 54^\circ$

α, deg	δ, deg	$C_{p,meas}$	C_p (a)	C_p (b)	$\frac{C_{p,meas} - C_p}{C_{p,meas}}$ (a)	$\frac{C_{p,meas} - C_p}{C_{p,meas}}$ (b)
0	53.041	1.8182	1.8178	1.7734	0.00022	0.02464
	50.391	1.6148	1.6897	1.6484	-.04638	-.02808
	44.120	1.2832	1.3799	1.3462	-.07536	-.04910
	40.217	1.0886	1.1872	1.1581	-.09058	-.06384
	36.920	.94213	1.0273	1.0022	-.09040	-.06376
	31.892	.73125	.79519	.77575	-.08744	-.06085
	27.229	.55603	.59632	.58173	-.07246	-.04622
	17.108	.27568	.24620	.24018	.10694	.12877
	9.546	.13049	.07840	.07647	.39919	.41398
	0	.01598	0	0	1.0000	1.0000
5	58.041	1.8177	1.8174	1.7805	.00017	.02047
	55.391	1.6749	1.7103	1.6756	-.02114	-.00042
	49.120	1.3674	1.4434	1.4141	-.05558	-.03415
	45.218	1.1874	1.2721	1.2463	-.07133	-.04960
	41.920	1.0532	1.1270	1.1041	-.07007	-.04833
	36.892	.84084	.91032	.89185	-.08263	-.06067
	32.229	.66268	.71836	.70378	-.08402	-.06202
	27.272	.50222	.53000	.51926	-.05531	-.03393
	14.546	.19411	.15936	.15612	.17902	.19571
	9.219	.06354	.06476	.06346	-.01920	.00126
	5.000	.01534	.01919	.01880	-.25098	-.22555
10	63.041	1.8185	1.8182	1.7882	.00016	.01666
	60.391	1.7524	1.7299	1.7013	.01284	.02916
	54.120	1.4905	1.5026	1.4777	-.00812	.00859
	50.217	1.3295	1.3517	1.3294	-.01670	.00038
	46.920	1.1924	1.2210	1.2008	-.02399	-.00704
	41.892	.98312	1.0209	1.0040	-.03853	-.02124
	37.229	.80196	.83798	.82413	-.04491	-.02764
	32.272	.62755	.65237	.64158	-.03955	-.02236
	27.107	.47149	.47501	.46715	-.00747	.00920
	16.968	.21078	.19493	.19171	.07520	.09047
	10.000	.08348	.06901	.06787	.17333	.18699
15	68.041	1.8089		1.7936		.00846
	65.391	1.8176	1.7890	1.7236	.05172	.05172
	59.120	1.6138	1.5942	1.5360	.01215	.04821
	55.217	1.4651	1.4601	1.4067	.00341	.03986
	51.920	1.3319	1.3410	1.2920	-.00683	.02996
	46.892	1.1392	1.1540	1.1118	.01299	.02405
	42.229	.95019	.97791	.94217	-.02917	.00844
	37.272	.77671	.79366	.76465	-.02182	.01552
	32.107	.59270	.61122	.58888	-.03125	.00645
	24.546	.36841	.37366	.36001	-.01425	.02280
	19.219	.24883	.23449	.22591	.05763	.09211
	15.000	.14102	.14501	.13970	-.02829	.00936
20	73.041	1.7527		1.7997		-.02682
	70.391	1.8177	1.8175	1.7454	.00011	.03978
	64.120	1.6870	1.6581	1.5923	.01713	.05614
	60.217	1.5650	1.5430	1.4818	.01406	.05316
	56.920	1.4517	1.4381	1.3810	.00937	.04870
	51.892	1.2666	1.2685	1.2182	-.00150	.03821
	47.229	1.0883	1.1040	1.0602	-.01443	.02582
	42.272	.91303	.92665	.88989	-.01492	.02534
	37.107	.72789	.74533	.71577	-.02396	.01665
	29.546	.47774	.49823	.47847	-.04289	-.00153
	24.219	.34337	.34465	.33097	-.00373	.03611
	20.000	.21458	.23963	.23012	-.11674	-.07242
25	78.041	1.7269		1.8054		-.04546
	75.391	1.8178		1.7664		.02828
	69.120	1.7818	1.7315	1.6468	.02823	.07577
	65.217	1.6839	1.6350	1.5550	.02904	.07655
	61.920	1.5880	1.5439	1.4684	.02777	.07531
	56.892	1.4182	1.3920	1.3239	.01847	.06649
	52.229	1.2496	1.2395	1.1789	.00808	.05658
	47.272	1.0747	1.0701	1.0178	.00428	.05295
	42.107	.87839	.89152	.84791	-.01495	.03470
	34.546	.61134	.63796	.60675	-.04354	.00751
	31.968	.52485	.55596	.52876	-.05927	-.00745
	29.219	.45289	.47257	.44945	-.04345	.00760
	25.000	.31147	.35427	.33695	-.13741	-.08181

$\theta_{le} = 66^\circ$

α, deg	δ, deg	$C_{p,meas}$	C_p (a)	C_p (b)	$\frac{C_{p,meas} - C_p}{C_{p,meas}}$ (a)	$\frac{C_{p,meas} - C_p}{C_{p,meas}}$ (b)
0	64.196	1.8179	1.8180	1.7656	-0.00006	0.02877
	59.356	1.6746	1.6600	1.6122	.00872	.03726
	50.375	1.3699	1.3303	1.2919	.02891	.05694
	46.236	1.1989	1.1697	1.1360	.02476	.05246
	38.334	.91565	.86281	.83792	.05771	.08489
	31.229	.66833	.60305	.58565	.09768	.12371
	23.969	.44057	.37007	.35940	.16002	.18424
	16.548	.28411	.18199	.17674	.35944	.37792
	5.907	.08221	.02371	.02301	.71159	.72011
	0	.01218	0	0	1.0000	1.0000
5	69.196	1.8176	1.8177	1.7767	-.00006	.02250
	64.356	1.7371	1.6902	1.6521	.02700	.04893
	55.375	1.4719	1.4082	1.3764	.04328	.06488
	51.236	1.3232	1.2645	1.2360	.04436	.06590
	43.334	1.0450	.97952	.95744	06266	.08379
	36.229	.79406	.72669	.71030	.08484	.10548
	28.969	.55118	.48786	.47687	.11488	.13482
	15.534	.20918	.14917	.14581	.28688	.30294
	9.165	.10137	.05278	.05160	.47933	.49097
	5.000	.03693	.01581	.01545	.57189	.58164
10	74.196	1.8187		1.7885		.01661
	69.356	1.8069	1.7528	1.6915	.02994	.06387
	60.375	1.5978	1.5123	1.4595	.05351	.08656
	56.236	1.4638	1.3833	1.3350	.05499	.08799
	48.334	1.1946	1.1171	1.0780	.06488	.09706
	41.229	.94583	.86965	.83926	.08054	.11267
	33.969	.69831	.62485	.60303	.10520	.13644
	26.548	.48615	.39991	.38595	.17739	.20611
	17.998	.23864	.19115	.18447	.19900	.22699
	14.165	.16171	.11991	.11571	.25849	.28446
	10.000	.07548	.06034	.05823	.20058	.22854
15	79.196	1.7631		1.7986		-.02013
	74.356	1.8184	1.8038	1.7284	.00803	.04949
	65.375	1.6861	1.6074	1.5402	.04668	.00865
	61.236	1.5736	1.4948	1.4323	.05008	.08979
	53.334	1.3349	1.2516	1.1993	.06240	.10158
	46.229	1.0857	1.0145	.97212	.06558	.10461
	38.969	.83585	.76935	.73718	.07956	.11805
	31.548	.61086	.53259	.51033	.12813	.16457
	25.534	.39769	.36143	.34631	.09118	.12920
	19.165	.22864	.20968	.20092	.08284	.12124
	15.000	.12920	.13032	.12487	-.00867	.03351
20	84.196	1.6818		1.8081		-.07510
	79.356	1.8179		1.7644		.02943
	70.375	1.7671	1.6946	1.6205	.04103	.08296
	66.236	1.6856	1.6000	1.5305	.05078	.09225
	58.334	1.4741	1.3838	1.3233	.06126	.10230
	51.229	1.2370	1.1613	1.1106	.06120	.10218
	43.969	.98858	.92068	.88046	.06868	.10937
	36.548	.75520	.67746	.64788	.10294	.14211
	30.534	.52810	.49303	.47149	.06641	.10720
	27.998	.44090	.42101	.40263	.04511	.08680
	24.165	.33299	.32015	.30617	.03856	.08054
	20.000	.20627	.22346	.21369	-.08334	-.03597
25	89.196	1.6187		1.8185		-.12343
	84.356	1.8062		1.8012		.00277
	75.375	1.8188	1.7624	1.7027	.03101	.06383
	71.236	1.7621	1.6877	1.6306	.04222	.07463
	63.334	1.5922	1.5033	1.4530	.05583	.08743
	56.229	1.3890	1.3009	1.2569	.06343	.09510
	48.969	1.1328	1.0712	1.0349	.05438	.08642
	41.548	.90941	.82817	.80014	.08933	.12015
	35.534	.66082	.63585	.61434	.03779	.07034
	32.998	.57524	.55841	.53951	.02926	.06211
	30.907	.51230	.49646	.47965	.03092	.06373
	29.165	.45189	.44712	.43198	.01056	.04406
	25.000	.30903	.33624	.32486	-.08805	-.05122

[a,b]See footnotes at end of table.

TABLE II.- MEASURED AND THEORETICAL VALUES OF PRESSURE COEFFICIENTS FOR

TWO-DIMENSIONAL AERODYNAMICALLY BLUNT BODIES - Continued

(a) Parabolic arc bodies - lower surface - Concluded

$\theta_{le} = 78^\circ$

α, deg	δ, deg	$C_{p,meas}$	C_p (a)	C_p (b)	$\frac{C_{p,meas} - C_p}{C_{p,meas}}$ (a)	$\frac{C_{p,meas} - C_p}{C_{p,meas}}$ (b)
0	70.560	1.8192	1.8192	1.6909	0	0.07053
	66.612	1.7205	1.7236	1.6018	-.00180	.06899
	59.517	1.5597	1.5195	1.4122	.02577	.09457
	39.792	.95817	.83825	.77900	.12516	.18699
	28.875	.60391	.47732	.44358	.20962	.26549
	20.759	.38482	.25718	.23899	.33169	.37896
	14.743	.23748	.13260	.12323	.44164	.48109
	9.470	.13178	.05538	.02019	.57975	.84679
	6.172	.07668	.02361	.02194	.69210	.71388
	2.565	.02607	.00366	.00382	.85961	.85347
	0	.00237	0	0	1.0000	1.0000
5	71.612	1.8185	1.8187	1.6623	-.00011	.08589
	64.517	1.6917	1.6457	1.5043	.02719	.11078
	44.792	1.1250	1.0027	.91651	.10871	.18532
	33.875	.74707	.62727	.57374	.15982	.23201
	25.759	.50109	.38161	.34882	.23844	.30388
	19.743	.33110	.23046	.19072	.30396	.42398
	12.569	.15467	.09560	.08738	.38191	.43506
	7.565	.05873	.03502	.03201	.40317	.45496
	5.000	.02002	.01535	.01402	.30291	.36331
10	76.612	1.8184	1.8184	1.7231	0	.05241
	69.517	1.7405	1.6862	1.5977	.03120	.08205
	49.792	1.2537	1.1209	1.0621	.10593	.15283
	38.875	.88814	.75715	.71741	.14749	.19223
	30.759	.61804	.50281	.47642	.18644	.22914
	24.743	.42646	.33679	.31911	.21027	.25172
	15.207	.16201	.13207	.12514	.18480	.22758
	12.565	.10359	.09096	.08619	.12192	.16797
	10.000	.05209	.05793	.05490	-.11211	-.05395
15	81.612	1.8182	1.8182	1.7795	0	.02128
	74.520	1.7862	1.7254	1.6887	.03404	.05459
	54.792	1.3880	1.2405	1.2141	.10627	.01253
	43.875	1.0448	.89268	.87368	.14560	.16378
	35.759	.76556	.63464	.62113	.17101	.18866
	29.743	.55391	.45742	.44770	.17420	.19175
	17.565	.16819	.17173	.16807	-.02105	.00071
	15.000	.10432	.12446	.12180	-.19306	-.16342
20	86.612	1.8000		1.8125		-.00694
	79.517	1.8188	1.7851	1.7586	.01853	.03310
	59.792	1.5289	1.3791	1.3586	.09798	.11139
	48.875	1.1989	1.0478	1.0323	.12603	.13896
	40.759	.91897	.78719	.77550	.14340	.15612
	34.743	.69355	.59984	.59093	.13512	.14796
	29.470	.48378	.44684	.44020	.07636	.09008
	25.207	.33538	.33470	.32973	.00203	.01685
	22.565	.24709	.27189	.26785	-.10037	-.08402
	20.000	.17383	.21596	.21276	-.24236	-.22395
25	91.612	1.7420		1.8187		-.04403
	84.517	1.8189		1.8023		.00913
	64.792	1.6607	1.5248	1.4892	.08183	.10327
	53.875	1.3812	1.2154	1.1870	.12004	.14060
	45.759	1.1029	.95616	.93379	.13305	.15333
	39.743	.86458	.76154	.74371	.11918	.13980
	34.470	.64194	.59658	.58263	.07066	.09239
	32.569	.56252	.53965	.52703	.04066	.06309
	30.207	.47497	.47126	.46024	.00781	.03101
	29.079	.43369	.44005	.42975	-.01466	.00908
	27.565	.37490	.39888	.38955	-.06396	-.03908
	25.000	.28922	.33266	.32487	-.15020	-.12326

$\theta_{le} = 90^\circ$

α, deg	δ, deg	$C_{p,meas}$	C_p (a)	C_p (b)	$\frac{C_{p,meas} - C_p}{C_{p,meas}}$ (a)	$\frac{C_{p,meas} - C_p}{C_{p,meas}}$ (b)
0	89.633	1.8183	1.8183	1.8182	0	0.00011
	83.508	1.7990	1.7951	1.7950	.00217	.00222
	77.797	1.7330	1.7372	1.7371	-.00242	-.00237
	70.437	1.6129	1.6144	1.6144	-.00093	-.00093
	61.219	1.4225	1.3968	1.3967	.01807	.01814
	44.481	1.0019	.89279	.89275	.10890	.10894
	32.224	.63411	.51682	.51680	.18654	.18500
	25.648	.46671	.34073	.34071	.26993	.26997
	19.168	.30430	.19599	.19599	.35593	.35593
	12.935	.18482	.09108	.09108	.50720	.50720
	5.121	.06340	.01446	.01446	.77192	.77192
	0	.00436	0	0	1.0000	1.0000
5	94.633	1.8180		1.8061		.00655
	88.508	1.8180	1.8180	1.8167	0	.00072
	82.797	1.7992	1.7907	1.7894	.00472	.00545
	75.437	1.7164	1.7042	1.7030	.00711	.00781
	66.219	1.5597	1.5234	1.5223	.02327	.02398
	49.481	1.1610	1.0514	1.0507	.09440	.09500
	37.224	.79419	.66552	.66506	.16201	.16259
	30.648	.60297	.47281	.47248	.21557	.21641
	24.168	.41550	.30490	.30470	.26619	.26667
	17.935	.26629	.17247	.17236	.35232	.35274
	10.121	.10892	.05612	.05609	.48476	.48503
	5.000	.02867	.01383	.01382	.51761	.51796
10	99.633	1.7827		1.7677		.00841
	93.508	1.8098		1.8118		-.00111
	87.797	1.8186	1.8186	1.8159	0	.00148
	80.437	1.7840	1.7710	1.7684	.00729	.00874
	71.219	1.6661	1.6325	1.6300	.02017	.02167
	54.481	1.3089	1.2066	1.2048	.07816	.07953
	42.224	.94529	.82232	.82110	.13009	.13138
	35.648	.73546	.61867	.61776	.15880	.16004
	29.168	.53445	.43257	.43194	.19063	.19180
	15.121	.16457	.12386	.12368	.24737	.24847
	10.000	.06628	.05490	.05483	.17170	.17275
15	104.63	1.7142		1.7023		.00694
	98.508	1.7648		1.7787		-.00788
	92.797	1.8096		1.8141		-.00249
	85.437	1.8184	1.8184	1.8069	0	.00632
	76.219	1.7502	1.7261	1.7152	.01377	.02000
	59.481	1.4579	1.3581	1.3495	.06845	.07435
	47.224	1.1050	.98572	.97948	.10795	.11359
	40.648	.89607	.77658	.77167	.13335	.13883
	34.168	.67826	.57718	.57352	.14903	.15442
	27.935	.47119	.40158	.39903	.14773	.15314
	20.121	.25086	.21646	.21510	.13713	.14255
	15.000	.12145	.12260	.12181	-.00947	-.00296
20	109.663	1.6230		1.6135		.00585
	103.508	1.6991		1.7198		-.01218
	97.797	1.7764		1.7854		-.00507
	90.437	1.8189		1.8136		.00291
	81.219	1.8180	1.7861	1.7765	.01755	.02283
	64.481	1.5830	1.4894	1.4814	.05913	.06418
	52.224	1.2673	1.1423	1.1361	.09863	.10353
	45.648	1.0574	.93510	.93008	.11566	.12041
	39.168	.82781	.69831	.69457	.15644	.16095
	32.935	.59699	.54054	.53761	.09456	.09947
	27.206	.34969	.38210	.38004	-.09268	-.08679
	22.230	.22350	.26181	.26041	-.17141	-.16515
	20.000	.19370	.21392	.21277	-.10439	-.09845
25	114.633	1.5031		1.5029		.00013
	108.508	1.5944		1.6358		-.02597
	102.797	1.6982		1.7296		-.01849
	95.437	1.7878		1.8026		-.00828
	86.219	1.8189	1.8189	1.8110	0	.00434
	69.481	1.6820	1.6025	1.5955	.04727	.05143
	57.224	1.3993	1.2913	1.2856	.07718	.08125
	50.648	1.2092	1.0924	1.0876	.09659	.10056
	44.168	.97590	.88690	.88300	.09120	.09519
	37.935	.74263	.69042	.68738	.07003	.07440
	30.121	.47246	.45996	.45794	.02646	.03073
	28.521	.40930	.41638	.41456	-.01730	-.01285
	25.000	.29548	.32631	.32487	-.10434	-.09947

[a,b] See footnotes at end of table.

TABLE II.- MEASURED AND THEORETICAL VALUES OF PRESSURE COEFFICIENTS FOR TWO-DIMENSIONAL AERODYNAMICALLY BLUNT BODIES - Continued

(b) Parabolic arc bodies - upper surface

$\theta_{le} = 42^\circ$

α, deg	δ, deg	$C_{p,meas}$	C_p (a)	C_p (c)	$\frac{C_{p,meas} - C_p}{C_{p,meas}}$ (a)	$\frac{C_{p,meas} - C_p}{C_{p,meas}}$ (c)
0	40.044	1.0974	1.0976	1.1854	-0.00018	-0.08019
	38.824	1.0514	1.0416	1.1256	.00932	-.07057
	37.413	.99001	.97869	1.0571	.01143	-.06777
	35.735	.93783	.90415	.97681	.03591	-.04156
	34.110	.86294	.83395	.90055	.03359	-.04358
	31.761	.75797	.73473	.79348	.03066	-.04685
	29.441	.66589	.64015	.69187	.03866	-.03905
	26.900	.56767	.54264	.58617	.04409	-.03259
	17.641	.28897	.24325	.26300	.15822	.08987
	10.714	.13734	.09167	.09898	.33253	.27931
	3.970	.05386	.01270	.01373	.76420	.74508
	0	.02193	0	0	1.0000	1.0000
5	35.044	.86132	.86149	.94422	-.00020	-.09625
	33.824	.82310	.80906	.88735	.01706	-.07806
	32.413	.77736	.75064	.82283	.03437	-.05849
	30.735	.73162	.68221	.74797	.06754	-.02235
	29.110	.66269	.61847	.67775	.06673	-.02273
	26.761	.56370	.52979	.58059	.06016	-.02996
	24.441	.48851	.44634	.49027	.08632	-.00360
	21.900	.40204	.36340	.39840	.09611	.00905
	12.641	.19528	.12493	.13715	.36025	.29768
	5.714	.08813	.02591	.02839	.70600	.67786
	-1.030	.02548				
	-5.000	.02293				
10	30.044	.66342	.66355	.71782	-.00020	-.08200
	28.824	.64183	.61481	.66567	.04210	-.03714
	27.413	.59295	.56106	.60703	.05378	-.02375
	25.735	.54914	.49887	.53992	.09154	.01679
	24.110	.49517	.44180	.47784	.10778	.03500
	21.761	.41072	.36389	.39362	.11402	.04163
	19.441	.34596	.29294	.31724	.15325	.08302
	16.900	.27803	.22364	.24200	.19563	.12959
	7.641	.12310	.04668	.05063	.62080	.58871
	.714	.04882	.00042	.00044	.99140	.99099
	-6.030	.00818				
	-10.000	-.00071				
15	25.044	.50172	.50187	.51315	-.00030	-.02278
	23.824	.45663	.45648	.46726	.00033	-.02328
	22.413	.41957	.40710	.41630	.02972	.00779
	20.735	.38807	.35085	.35897	.09591	.07499
	19.110	.35101	.30024	.30693	.14464	.12558
	16.761	.29603	.23297	.23816	.21302	.19549
	14.441	.24106	.17393	.17809	.27848	.26122
	11.900	.18980	.11903	.12176	.37287	.35848
	2.641	.07429	.00591	.00608	.92045	.91816
	-4.286	.02241				
	-11.030	-.00035				
	-15.000	-.00122				
20	20.044	.36460	.38458	.33640	-.05480	.07735
	18.824	.36460	.34039	.29815	.06640	.18225
	17.413	.33468	.29314	.25647	.12412	.23369
	15.735	.29866	.24059	.21061	.19444	.29482
	14.110	.25776	.19465	.17018	.24484	.33977
	11.761	.21075	.13608	.11898	.35431	.43544
	9.441	.17046	.08789	.07655	.48440	.55092
	6.900	.13566	.04722	.04133	.65192	.69534
	-2.359	.05568				
	-9.286	.01905				
	-16.030	.00135				
	-20.000	-.00029				
25	15.044	.20452	.34618	.19293	-.69265	.05667
	13.824	.26378	.29285	.16350	-.11021	.38017
	12.413	.25884	.23739	.13233	.08287	.48876
	10.735	.23230	.17808	.09936	.23341	.57228
	9.110	.20452	.12889	.07179	.36979	.64898
	6.761	.16254	.07127	.03969	.56152	.75581
	4.441	.12859	.03071	.01717	.76118	.86647
	1.900	.09835	.00565	.00315	.94255	.96797
	-7.359	.03353				
	-14.286	.00822				
	-21.030	-.00023				
	-25.000	-.00029				

$\theta_{le} = 54^\circ$

α, deg	δ, deg	$C_{p,meas}$	C_p (a)	C_p (c)	$\frac{C_{p,meas} - C_p}{C_{p,meas}}$ (a)	$\frac{C_{p,meas} - C_p}{C_{p,meas}}$ (c)
0	50.839	1.6530	1.6530	1.6701	0	-0.07034
	49.090	1.5541	1.5700	1.5863	-.01023	-.02072
	47.190	1.4446	1.4794	1.4947	-.02409	-.03469
	44.035	1.2882	1.3284	1.3421	-.03121	-.04184
	40.217	1.0998	1.1462	1.1581	-.04219	-.05301
	36.901	.94839	.99117	1.0015	-.04511	-.05600
	31.979	.74752	.77136	.77936	-.03189	-.04259
	22.307	.42712	.39589	.40000	.07312	.06350
	17.101	.27693	.23772	.24018	.14159	.13271
	6.374	.09608	.03382	.03417	.64800	.64436
	2.094	.03725	.00369	.00372	.90094	.90013
	0	.02286	0	0	1.0000	1.0000
5	45.839	1.3601	1.3598	1.4299	.00022	-.05132
	44.080	1.2734	1.2791	1.3441	-.00448	-.05552
	32.190	1.1825	1.1917	1.2527	-.00778	-.05937
	39.035	1.0355	1.0482	1.1018	-.01226	-.06403
	35.217	.86403	.87887	.92379	-.01718	-.06916
	31.901	.73224	.73800	.77577	-.00787	-.05945
	26.979	.56201	.54408	.57186	.03190	-.01753
	17.307	.29478	.23371	.24571	.20717	.16646
	12.101	.18678	.11613	.12207	.37825	.34645
	1.374	.04585	.00151	.00159	.96707	.96532
	-2.906	.00364				
	-5.000	.02284				
10	40.839	1.1025	1.1023	1.1881	.00018	-.07764
	39.080	1.0290	1.0247	1.1037	.00418	-.07259
	37.190	.95802	.94170	1.0148	.01704	-.05927
	34.035	.83930	.80758	.87020	.03779	-.03682
	30.217	.67895	.65300	.70361	.03822	-.03632
	26.901	.57124	.52774	.56867	.07615	.00460
	21.979	.42314	.36128	.38922	.14619	.080163
	12.307	.20955	.11700	.12614	.44166	.39804
	7.101	.12387	.03939	.042447	.68201	.65733
	-3.626	.02167				
	-7.906	-.00097				
	-10.000	-.01138				
15	35.839	.81574		.95246		-.16760
	34.080	.83929	.82578	.87208	.01610	-.03906
	32.190	.75379	.74594	.78820	.01041	-.04565
	29.035	.64908	.61931	.65433	.04586	-.00808
	25.217	.53507	.47727	.50424	.10802	.05762
	21.901	.42913	.36580	.38649	.14758	.09936
	16.979	.30459	.22434	.23695	.26347	.22207
	7.307	.13916	.04247	.04491	.69481	.67728
	2.101	.07163	.00353	.00373	.95072	.94793
	-10.789	-.00706				
	-15.000	-.02007				
20	30.839	.47898		.73011		-.52430
	29.080	.58734		.65639		-.11756
	27.190	.57310	.53493	.57988	.06660	-.01183
	24.035	.49136	.42515	.46082	.13475	.06215
	20.217	.37310	.30609	.33176	.17960	.11080
	16.901	.29755	.21661	.23479	.27202	.21092
	11.979	.21211	.11050	.11969	.47904	.43572
	2.307	.08765	.00413	.00450	.95288	.94866
	-2.899	.04121				
	-13.626	-.01266				
	-17.956	-.01947				
	-20.000	-.02381				
25	25.839	.24493		.52777		-1.1548
	24.080	.30892		.46236		-.49670
	22.190	.41235	.41212	.39621	.00056	.03914
	19.035	.36456	.30744	.29548	.15668	.18949
	15.217	.27643	.19915	.19139	.27956	.30764
	11.901	.21223	.12292	.11814	.42082	.44334
	6.979	.14304	.04273	.04103	.70127	.71316
	-2.693	.04102				
	-7.899	.01380				
	-18.626	-.02418				
	-22.906	-.03003				
	-25.000	-.03052				

$\theta_{le} = 66^\circ$

α, deg	δ, deg	$C_{p,meas}$	C_p (a)	C_p (c)	$\frac{C_{p,meas} - C_p}{C_{p,meas}}$ (a)	$\frac{C_{p,meas} - C_p}{C_{p,meas}}$ (c)
0	61.215	1.7390	1.7390	1.6732	0	0.03784
	57.757	1.6153	1.6193	1.5582	-.00248	.03535
	54.654	1.5037	1.5061	1.4492	-.00160	.03624
	50.129	1.3428	1.3337	1.2831	.00678	.04446
	46.096	1.1951	1.1754	1.1308	.01648	.05380
	38.256	.90556	.86773	.83510	.04178	.07781
	31.171	.65950	.60637	.58355	.08056	.11516
	23.941	.43805	.37258	.35869	.14946	.18117
	17.410	.28789	.20282	.19501	.29549	.32262
	8.007	.10934	.04386	.04226	.59887	.61350
	4.150	.06076	.01186	.01141	.80481	.81221
	0	.01786	0	0	1.0000	1.0000
5	56.215	1.5499	1.5499	1.5047	0	.02916
	52.757	1.4112	1.4216	1.3802	-.00737	.02197
	49.654	1.2965	1.3031	1.2653	-.00509	.02406
	45.129	1.1485	1.1271	1.0941	.01863	.04737
	41.096	1.0035	.96959	.94118	.03379	.06210
	33.256	.72095	.67452	.65503	.06440	.09143
	26.171	.50348	.43633	.42373	.13337	.15840
	18.941	.31822	.23622	.22950	.25768	.27880
	12.410	.19678	.10372	.10060	.47291	.48877
	3.007	.06234	.00615	.00599	.90135	.90391
	-.850	.02702				
	-5.000	-.00334				
10	51.215	1.3739	1.3739	1.3236	0	.03661
	47.757	1.2312	1.2389	1.1937	-.00625	.03046
	44.654	1.1226	1.1167	1.0759	.00526	.04160
	40.129	.97499	.93943	.90484	.03647	.07195
	36.096	.84223	.78495	.75607	.06801	.10230
	28.256	.57424	.50656	.48818	.11786	.14987
	21.171	.38504	.29480	.28411	.23437	.26213
	13.941	.23615	.13081	.12643	.44607	.46462
	7.410	.13132	.03767	.03623	.71314	.72411
	-1.993	.03082				
	-5.850	.00601				
	-10.000	-.01571				
15	46.215	1.1758		1.1353		.03444
	42.757	1.1541	1.0650	1.0039	.07720	.13014
	39.654	.96823	.94108	.88705	.02804	.08384
	35.129	.80788	.76543	.72125	.05254	.10723
	31.096	.67301	.61666	.58104	.08373	.13665
	23.256	.44306	.36014	.33958	.18715	.23356
	16.171	.29017	.17917	.16896	.38253	.41772
	8.941	.17768	.05572	.05262	.68640	.70385
	2.410	.08694	.00412	.00385	.95261	.95572
	-10.850	-.01002				
	-15.000	-.02307				
20	41.215	1.0507		.94568		.099952
	37.757	1.0024	.97334	.81665	.02899	.18531
	34.654	.75834	.73947	.70426	.02485	.07131
	30.129	.64102	.65447	.54882	.02098	.14383
	26.096	.52434	.50262	.42148	.04142	.19617
	18.256	.32546	.25468	.21375	.21748	.34324
	11.171	.19623	.09741	.08176	.50359	.58335
	3.941	.10777	.01223	.01029	.88652	.90452
	-2.590	.04504				
25	36.215	.61803		.76037		-.23031
	32.757	.76970	.73943	.63771	.03933	.17148
	29.654	.59663	.61835	.53320	-.03640	.10631
	25.129	.49216	.61835	.39283	-.25640	.20182
	21.096	.39462	.45579	.28220	-.15501	.28488
	13.256	.23855	.13273	.11453	.44360	.51989
	6.171	.14100	.02916	.02517	.79319	.82148
	-1.059	.06800				
	-7.590	.02269				
	-16.993	-.01633				
	-20.850	-.02388				
	-25.000	-.02640				

[a,c]See footnotes at end of table.

TABLE II.- MEASURED AND THEORETICAL VALUES OF PRESSURE COEFFICIENTS FOR

TWO-DIMENSIONAL AERODYNAMICALLY BLUNT BODIES - Continued

(b) Parabolic arc bodies - upper surface - Concluded

$\theta_{le} = 78^{\circ}$

α, deg	δ, deg	$C_{p,meas}$	C_p (a)	C_p (c)	$\frac{C_{p,meas} - C_p}{C_{p,meas}}$ (a)	$\frac{C_{p,meas} - C_p}{C_{p,meas}}$ (c)
0	70.560	1.8192	1.8192	1.6908	0	0.07058
	65.353	1.6853	1.6899	1.5707	-.00273	.06800
	60.192	1.5546	1.5405	1.4316	.00907	.07912
	40.864	1.0113	.87584	.81393	.13395	.19516
	28.773	.60519	.47381	.44053	.21709	.27208
	20.678	.38354	.25522	.23709	.33457	.38184
	14.680	.24004	.13144	.12211	.45242	.49129
	9.350	.13306	.05399	.05019	.59424	.62280
	6.168	.07860	.02361	.02195	.69962	.72074
	2.563	.02735	.00411	.00380	.84973	.86106
	0	.00237	0	0	1.0000	1.0000
5	65.560	1.7451	1.7451	1.5760	0	.09690
	60.353	1.5739	1.5902	1.4362	-.01036	.08749
	55.192	1.4155	1.4197	1.2818	-.00297	.09445
	35.864	.85203	.72279	.65261	.15168	.23405
	23.773	.48178	.34199	.30897	.29015	.35869
	15.678	.29118	.15385	.13885	.47163	.52315
	9.680	.17656	.05956	.05376	.66266	.69551
	4.350	.08384	.01211	.01094	.85556	.86951
	1.168	.04198	.00086	.000790	.97951	.98118
	-2.437	.00399				
	-5.000	-.00824				
10	60.560	1.5646	1.5646	1.4421	0	.07829
	55.353	1.3718	1.3961	1.2868	-.01771	.06196
	50.192	1.2003	1.2177	1.1220	-.01450	.06523
	30.864	.66515	.54299	.50039	.18366	.24770
	18.773	.35673	.21352	.19693	.40145	.44796
	10.678	.20786	.07091	.06528	.65886	.68594
	4.680	.11490	.01375	.01266	.88033	.88982
	-.650	.04643				
	-3.832	.01565				
	-7.437	-.01010				
	-10.000	-.01450				
15	55.560	1.3955	1.3955	1.2914	0	.07460
	50.353	1.1863	1.2163	1.1273	-.02529	.04973
	45.192	1.0167	1.0330	.95706	-.01603	.05866
	25.864	.52699	.39053	.36185	.25894	.31336
	13.773	.26274	.11619	.10777	.55778	.58982
	5.678	.14126	.02012	.01861	.85757	.86826
	-.320	.06988				
	-5.650	.02041				
	-8.832	-.00150				
	-12.437	-.01653				
	-15.000	-.01841				
20	50.560	1.2277	1.2277	1.1341	0	.07624
	45.353	1.0217	1.0418	.96241	-.01967	.05803
	40.192	.84446	.85757	.79189	-.01552	.06225
	20.864	.40457	.26116	.24117	.35448	.40389
	8.773	.18015	.04782	.04423	.73455	.75448
	.678	.09217	.00028	.000266	.99696	.99711
	-5.320	.03519				
	-10.650	.00263				
	-13.832	-.01151				
	-17.437	-.01810				
	-20.000	-.02203				
25	45.560	1.0266	1.0266	.96929	0	.05583
	40.353	.83832	.84420	.79718	-.00701	.04907
	35.192	.66946	.66914	.63153	.00048	.05666
	15.864	.29398	.15053	.14207	.48796	.51674
	3.773	.12925	.00469	.00823	.96371	.93632
	-4.322	.05808				
	-10.320	.01315				
	15.650	-.00870				
	-18.832	-.01821				
	-22.437	-.02119				
	-25.000	-.01838				

$\theta_{le} = 90^{\circ}$

α, deg	δ, deg	$C_{p,meas}$	C_p (a)	C_p (c)	$\frac{C_{p,meas} - C_p}{C_{p,meas}}$ (a)	$\frac{C_{p,meas} - C_p}{C_{p,meas}}$ (c)
0	83.900	1.7990	1.7990	1.7978	0	0.000667
	77.532	1.7474	1.7348	1.7336	.00721	.00790
	70.540	1.6279	1.6175	1.6165	.00639	.00700
	61.096	1.4344	1.3946	1.3935	.02775	.02851
	44.922	.99129	.90713	.90666	.08490	.08537
	32.279	.63784	.51907	.51858	.18621	.18697
	25.692	.46547	.34219	.34175	.26485	.26584
	19.131	.31799	.19544	.19530	.38539	.38583
	12.938	.19416	.09114	.09115	.53059	.53054
	7.217	.09459	.02871	.02870	.69648	.69659
	3.497	.04357	.00666	.00676	.84714	.84485
	0	.00250	0	0	1.0000	
5	78.900	1.7522	1.7522	1.7509	0	.00074
	72.532	1.6563	1.6557	1.6545	.00036	.00109
	65.540	1.5152	1.5075	1.5066	.00508	.00568
	56.096	1.2945	1.2536	1.2525	.03160	.03244
	39.922	.84121	.74922	.74883	.10935	.10982
	27.279	.51394	.38235	.38195	.25604	.25682
	20.692	.36347	.22735	.22702	.37450	.37541
	14.131	.23745	.10844	.10838	.54331	.54357
	7.932	.13275	.03466	.03463	.73891	.73913
	2.217	.05626	.00273	.00272	.95148	.95165
	-1.503	.01739				
	-5.000	-.01145				
10	73.900	1.6661	1.6661	1.6785	0	-.00744
	67.532	1.5433	1.5413	1.5527	.00130	-.00609
	60.540	1.3681	1.3682	1.3785	-.00007	- 00760
	51.096	1.1337	1.0932	1.1012	.03572	.02867
	34.922	.68190	.59132	.59588	.13283	.12615
	22.279	.39205	.27104	.26134	.30866	.33340
	15.692	.26917	.13216	.13302	.50901	.50581
	9.131	.16457	.04547	.04579	.72370	.72176
	2.932	.08140	.00473	.00476	.94189	.94152
	-6.503	-.00115				
	-10.000	-.01816				
15	68.900	1.5476	1.5476	1.5827	0	-.02268
	62.532	1.4005	1.3998	1.4315	.00050	-.02213
	55.540	1.2067	1.2086	1.2362	-.00157	-.02445
	46.096	.96804	.92314	.94391	.04638	.02493
	29.922	.55642	.44227	.45243	.20515	.18689
	17.279	.29948	.15694	.16042	.47596	.46434
	10.692	.19973	.06128	.06259	.69319	.68663
	4.131	.10693	.00922	.00944	.92240	.91171
	-2.062	.04821				
	-7.783	.00781				
	-11.503	-.01366				
	-15.000	-.02186				
20	63.900	1.4309	1.4309	1.4664	0	-.02481
	57.532	1.2622	1.2630	1.2943	-.00063	-.02543
	50.540	1.0599	1.0575	1.0839	.00226	-.02264
	41.096	.79420	.76675	.78563	.03456	.01079
	24.922	.43339	.31493	.32286	.27333	.25504
	12.279	.21843	.07853	.08224	.64048	.62348
	5.692	.13029	.01750	.01789	.86568	.86269
	-.869	.06624				
	-7.062	.02122				
	-12.783	-.00732				
	-16.503	-.02254				
	-20.000	-.02507				
25	58.900	1.2823	1.2823	1.3332	0	-.03969
	52.532	1.1041	1.1018	1.1454	.00208	-.03741
	45.540	.89836	.89075	.92630	.00847	-.031101
	36.096	.63757	.60714	.63111	.04773	.01013
	19.922	.32800	.20295	.21110	.38125	.35640
	7.279	.14664	.02811	.02919	.80831	.80094
	.692	.08159	.00026	.00027	.99681	.99669
	-5.869	.03407				
	-12.062	.00092				
	-17.783	-.01784				
	-21.503	-.02722				
	-25.000	-.02660				

[a,c]See footnotes at end of table.

TABLE II.- MEASURED AND THEORETICAL VALUES OF PRESSURE COEFFICIENTS FOR

TWO-DIMENSIONAL AERODYNAMICALLY BLUNT BODIES - Continued

(c) Circular arc bodies - lower surface

$\theta_{le} = 42^\circ$

α, deg	δ, deg	$C_{p,meas}$	C_p (a)	C_p (b)	$\frac{C_{p,meas} - C_p}{C_{p,meas}}$ (a)	$\frac{C_{p,meas} - C_p}{C_{p,meas}}$ (b)
0	41.19	1.2802	1.2798	1.2397	0.00031	0.03164
	40.01	1.1786	1.2205	1.1822	-.03555	-.00305
	39.30	1.1341	1.1842	1.1470	-.04418	-.01137
	37.41	1.0375	1.0898	1.0556	-.05041	-.01745
	35.63	.96749	1.0019	.97047	-.03557	-.00308
	32.91	.85232	.87173	.84432	-.02277	.00939
	30.77	.74025	.77243	.74819	-.04347	-.01023
	28.56	.64427	.67496	.65377	-.04764	-.01475
	24.51	.49071	.50828	.49231	-.03581	-.00326
	16.21	.24303	.23021	.22299	.05275	.08246
	12.18	.16563	.13148	.12734	.20618	.23118
	8.33	.11362	.06201	.06007	.45423	.47131
	0	.01926	0	0	1.0000	1.0000
5	46.19	1.6295	1.6292	1.5862	.00018	.02657
	45.01	1.4691	1.5654	1.5241	-.06555	-.03744
	44.30	1.4045	1.5214	1.4860	-.08323	-.05803
	42.41	1.2767	1.4236	1.3861	-.11506	-.08569
	40.63	1.1796	1.3270	1.2919	-.12496	-.09520
	35.77	.90016	1.0690	1.0407	-.18757	-.15613
	33.56	.78926	.95660	.93134	-.21202	-.18002
	29.51	.61382	.75953	.73947	-.23738	-.20470
	27.19	.52673	.65304	.63580	-.23980	-.20707
	21.21	.33939	.40982	.39900	-.20752	-.17564
	17.18	.24415	.27310	.26590	-.11857	-.08908
	13.33	.17961	.16640	.16200	.07355	.09805
	5.00	.05367	.02377	.02316	.55711	.56847
10	51.19	1.8178	1.8174	1.7772	.00022	.02233
	50.01	1.6617	1.7576	1.7187	-.05771	-.03430
	49.30	1.5900	1.7207	1.6826	-.08220	-.05824
	47.41	1.4529	1.6230	1.5870	-.11708	-.09230
	45.63	1.3432	1.5300	1.4960	-.13907	-.11376
	40.77	1.0507	1.2765	1.2482	-.02149	-.18797
	38.56	.94025	1.1636	1.1378	-.23754	-.21010
	34.51	.76004	.96125	.93997	-.26474	-.23674
	32.19	.66614	.84929	.83048	-.27479	-.24670
	26.21	.45674	.58426	.57132	-.27920	-.25086
	18.33	.26449	.29619	.28963	-.11985	-.09505
	14.42	.19342	.18558	.18147	.04053	.06178
	10.00	.09951	.09025	.08825	.09306	.11315
15	56.19	1.8183	1.8180	1.7844	-.00016	.01864
	55.01	1.7100	1.7680	1.7353	-.03392	-.01480
	54.30	1.6527	1.7369	1.7048	-.05095	-.03152
	52.41	1.5283	1.6540	1.6235	-.08225	-.06229
	50.63	1.4200	1.5742	1.5450	-.10859	-.08803
	45.77	1.1422	1.3521	1.3272	-.18377	-.16197
	43.56	1.0425	1.2510	1.2279	-.20000	-.17784
	39.51	.86761	1.0664	1.0467	-.22912	-.20642
	37.19	.77032	.96203	.94424	-.24887	-.22578
	31.21	.55542	.70746	.69439	-.27374	-.25021
	27.18	.43288	.54967	.53951	-.26980	-.24633
	19.42	.25369	.29106	.28569	-.14731	-.12614
	15.00	.15271	.17643	.17317	-.15533	-.01340
20	61.19	1.8176	1.8174	1.7897	.00011	.01529
	60.01	1.7728	1.7761	1.7492	-.00186	.01331
	59.30	1.7335	1.7503	1.7238	-.00969	.00560
	57.41	1.6268	1.6808	1.6553	-.03319	-.01752
	55.63	1.5299	1.6130	1.5885	-.05432	-.03830
	50.77	1.2728	1.4203	1.3988	-.11589	-.09899
	48.56	1.1728	1.3307	1.3105	-.13464	-.11741
	44.51	.99858	1.1636	1.1461	-.16545	-.14773
	42.19	.90594	1.0675	1.0513	-.17833	-.16045
	36.21	.68324	.82643	.81388	-.20957	-.19121
	32.18	.54888	.67160	.66141	-.22358	-.20502
	28.33	.44398	.53325	.52516	-.20107	-.18285
	20.00	.22312	.27693	.27230	-.24117	-.22042
25	66.19	1.8187		1.7964		.01226
	65.01	1.8187	1.8018	1.7635	.00929	.03035
	64.30	1.7939	1.7805	1.7427	.00747	.02854
	62.41	1.7195	1.7228	1.6862	-.00192	.01937
	60.63	1.6390	1.6656	1.6302	-.01623	-.00537
	55.77	1.4077	1.4989	1.4671	-.06479	-.04220
	53.56	1.3141	1.4195	1.3894	-.08021	-.05730
	47.19	1.0475	1.1800	1.1549	-.12649	-.10253
	41.21	.82246	.95209	.93188	-.15761	-.13304
	37.18	.67925	.80099	.78399	-.17923	-.15420
	33.33	.57014	.66219	.64813	-.16145	-.13679
	29.42	.45110	.52902	.51780	-.17273	-.14786
	25.00	.31657	.39168	.38336	-.23726	-.21098

$\theta_{le} = 54^\circ$

α, deg	δ, deg	$C_{p,meas}$	C_p (a)	C_p (b)	$\frac{C_{p,meas} - C_p}{C_{p,meas}}$ (a)	$\frac{C_{p,meas} - C_p}{C_{p,meas}}$ (b)
0	53.07	1.8182	1.8181	1.7749	0.00005	0.02381
	51.71	1.6974	1.7532	1.7117	-.03287	-.00842
	50.29	1.6008	1.6836	1.6437	-.05172	-.02680
	48.36	1.5092	1.5895	1.5518	-.05321	-.02823
	46.27	1.3802	1.4856	1.4504	-.07637	-.05086
	41.36	1.1214	1.2428	1.2133	-.10826	-.08195
	37.96	.95296	1.0769	1.0513	-.13006	-.10319
	34.91	.82137	.93223	.91012	-.13497	-.10805
	31.71	.69740	.78643	.76777	-.12766	-.10090
	28.77	.58170	.65901	.64337	-.13290	-.10602
	17.96	.28418	.27075	.26433	.04726	.06985
	6.52	.10808	.03665	.03578	.66090	.66895
	0	.03561	0	0	1.0000	1.0000
5	58.07	1.8185	1.8184	1.7826	.00005	.01974
	56.71	1.7330	1.7644	1.7296	-.01812	.00196
	55.29	1.6500	1.7058	1.6723	-.03382	-.01352
	53.36	1.5603	1.6258	1.5938	-.04198	-.02147
	51.27	1.4457	1.5363	1.5060	-.06267	-.04171
	49.31	1.3542	1.4519	1.4233	-.07215	-.05103
	46.36	1.2069	1.3225	1.2965	-.09578	-.07424
	42.96	1.0506	1.1728	1.1497	-.11631	-.09433
	39.91	.93361	1.0395	1.0191	-.11342	-.09157
	33.77	.68149	.77995	.76461	-.14448	-.12197
	22.96	.35907	.38439	.37683	-.07052	-.04946
	11.52	.15361	.10064	.09865	.34483	.35779
	5.00	.06331	.01919	.01880	.69689	.70305
10	63.07	1.8175	1.8174	1.7883	.00022	.01607
	61.71	1.7915	1.7731	1.7447	.01027	.02612
	60.29	1.7334	1.7246	1.6970	.00508	.02100
	58.36	1.6572	1.6575	1.6310	-.00018	.01578
	56.27	1.5573	1.5814	1.5560	-.01548	.00083
	54.31	1.4745	1.5085	1.4844	-.02306	-.00671
	51.36	1.3347	1.3953	1.3729	-.04540	-.02862
	47.96	1.1907	1.2614	1.2412	-.05938	-.04241
	44.91	1.0716	1.1399	1.1217	-.06374	-.04675
	38.77	.81687	.89645	.88207	.09742	-.07982
	27.96	.46181	.50285	.49480	.08887	-.07144
	16.52	.21796	.18480	.18184	.15214	.16572
	10.00	.10725	.06894	.06783	.35720	.36755
15	68.07	1.8005		1.7951		.00300
	66.71	1.8182	1.8105	1.7602	.00423	.03190
	65.29	1.7889	1.7707	1.7214	.01017	.03773
	63.36	1.7321	1.7146	1.6669	.01010	.03764
	61.27	1.6539	1.6499	1.6040	.00242	.03017
	56.36	1.4561	1.4875	1.4461	-.02156	.00687
	52.96	1.3182	1.3674	1.3294	-.03732	-.00850
	49.91	1.2077	1.2561	1.2212	-.04008	-.01118
	43.77	.96531	1.0267	.99817	-.06360	-.03404
	32.96	.58741	.63537	.61770	-.08165	-.05157
	27.15	.42868	.44682	.43439	-.04232	-.01332
	27.52	.30047	.28866	.28062	.03931	.06606
	15.00	.16616	.14375	.13975	.15590	.15894
20	73.07	1.7619		1.8007		-.02202
	71.71	1.8181		1.7739		.02431
	70.29	1.8138	1.8065	1.7436	.00402	.03870
	68.36	1.7814	1.7615	1.7002	.01117	.04558
	66.27	1.7259	1.7085	1.6490	.01008	.04456
	61.36	1.5609	1.5704	1.5157	-.00609	.02896
	57.96	1.4363	1.4650	1.4140	-.01998	.01553
	54.91	1.3306	1.3651	1.3176	-.02593	.00977
	48.77	1.0967	1.1476	1.1077	-.04641	-.01003
	37.96	.71364	.77153	.74468	-.08112	-.04350
	32.15	.54504	.57726	.55716	-.05911	-.02224
	26.52	.39782	.40633	.39218	-.02139	.01418
	20.00	.24082	.23848	.23017	.00972	.04422
25	78.07	1.7024		1.8054		-.06050
	76.71	1.7966		1.7865		.05622
	75.29	1.8174		1.7644		.02916
	73.36	1.8112	1.7951	1.7315	.00889	.04400
	71.27	1.7807	1.7536	1.6915	.01522	.05009
	66.36	1.6571	1.6411	1.5830	.00966	.04472
	62.96	1.5501	1.5514	1.4964	-.00084	.03464
	59.91	1.4516	1.4640	1.4122	-.00854	.02714
	53.77	1.2351	1.2673	1.2224	-.02607	.01028
	42.96	.85284	.90830	.87615	-.06454	-.02733
	37.15	.67486	.71309	.68785	-.05665	-.01925
	31.52	.50911	.53430	.51540	-.04948	-.01235
	25.00	.34418	.34923	.33687	-.01467	.02124

$\theta_{le} = 66^\circ$

α, deg	δ, deg	$C_{p,meas}$	C_p (a)	C_p (b)	$\frac{C_{p,meas} - C_p}{C_{p,meas}}$ (a)	$\frac{C_{p,meas} - C_p}{C_{p,meas}}$ (b)
0	65.28	1.8182	1.8184	1.7977	-0.00011	0.01127
	63.59	1.7647	1.7674	1.7474	-.00153	.00980
	61.74	1.6997	1.7094	1.6900	-.00571	.00571
	59.45	1.6256	1.6343	1.6157	-.00535	.00609
	56.98	1.5290	1.5493	1.5318	-.01328	-.00183
	50.05	1.2580	1.2950	1.2803	-.02941	-.01773
	47.10	1.1468	1.1825	1.1691	-.03113	-.01945
	40.12	.88377	.91486	.90452	-.03518	-.02348
	35.71	.71487	.75097	.74246	-.05050	-.03859
	31.04	.57028	.58566	.57902	-.02697	-.01533
	18.18	.26044	.21458	.21215	.17609	.18542
	9.79	.14440	.06362	.06289	.55942	.56447
	0	.03990	0	0	1.0000	1.0000
5	70.28	1.8181	1.8437	1.8022	-.01408	.00875
	68.59	1.8127	1.8031	1.7625	.00530	.02769
	66.74	1.7746	1.7558	1.7163	.01059	.03285
	64.45	1.7208	1.6934	1.6553	.01592	.03806
	61.98	1.6422	1.6214	1.5849	.01267	.03489
	55.05	1.3931	1.3977	1.3663	-.00330	.01924
	52.10	1.2909	1.2954	1.2663	-.00349	.01906
	45.12	1.0303	1.0445	1.0210	-.01378	.00903
	40.71	.85804	.88527	.86536	-.03174	-.00853
	36.04	.70447	.71991	.70373	-.02192	.00105
	23.18	.34715	.32242	.31517	.07124	.09212
	14.79	.18814	.13547	.13241	.27995	.29622
	5.00	.07327	.01582	.01545	.78409	.78914
10	75.28	1.7535		1.8062		-.03005
	73.59	1.8178		1.7766		.02266
	71.74	1.8178	1.8123	1.7411	.00303	.04219
	69.45	1.7929	1.7621	1.6929	.01718	.05578
	66.98	1.7359	1.7025	1.6356	.01924	.05778
	60.05	1.5231	1.5088	1.4496	.00939	.04826
	57.10	1.4285	1.4168	1.3612	.00819	.04711
	50.12	1.1786	1.1834	1.1369	-.00407	.03538
	45.71	1.0131	1.0300	.98956	-.01668	.02324
	41.04	.85841	.86616	.83215	-.00903	.03059
	28.18	.46181	.44829	.43069	.02928	.06739
	19.79	.27200	.23022	.22119	.15360	.18680
	10.00	-.11978	.06059	.05821		
15	80.28	1.6593		1.8100		-.09082
	78.59	1.7882		1.7901		-.00106
	76.74	1.8175		1.7650		.02889
	74.45	1.8175	1.8046	1.7292	.00710	.04858
	71.98	1.7845	1.7584	1.6849	.01426	.05581
	65.05	1.6214	1.5984	1.5316	.01419	.05538
	62.10	1.5432	1.5186	1.4551	.01594	.05709
	55.12	1.3160	1.3084	1.2537	.00578	.04734
	50.71	1.1596	1.1649	1.1162	-.00457	.03743
	46.04	1.0057	1.0072	.96513	-.00149	.04034
	33.19	.58905	.58245	.55810	.01120	.05254
	24.79	.36119	.34167	.32739	.05404	.09358
	15.00	.16571	.13026	.12481	.21393	.24682
20	85.28	1.5702		1.8136		-.15501
	83.95	1.7387		1.8032		-.03710
	79.45	1.8171		1.7648		.02878
	76.98	1.8171	1.8029	1.7334	.00781	.04606
	73.19	1.7681	1.7402	1.6731	.01578	.05373
	70.05	1.7019	1.6781	1.6134	.01398	.05200
	67.10	1.6339	1.6116	1.5495	.01365	.05166
	60.12	1.4360	1.4277	1.3727	.00578	.04408
	55.71	1.2902	1.2966	1.2466	-.00496	.03379
	51.04	1.1437	1.1481	1.1039	-.00385	.03480
	38.19	.72156	.72579	.69780	-.00586	.03293
	29.79	.47523	.46859	.45053	.01397	.05197
	20.00	.24362	.22218	.21360	.08801	.12322
25		1.4945		1.8178		-.21633
	88.59	1.6764		1.8167		-.08369
	86.74	1.7584		1.8119		-.03043
	81.98	1.8086		1.8008		.00431
	78.19	1.8043	1.7852	1.7416	-.01059	.03475
	75.05	1.7572	1.7394	1.6968	.01013	.03437
	72.10	1.7082	1.6874	1.6461	.01218	.03635
	65.12	1.5404	1.5335	1.4960	.00448	02882
	60.71	1.4106	1.4176	1.3829	-.00496	.01964
	56.04	1.2716	1.2817	1.2504	-.00794	.01667
	43.19	.85333	.87265	.85129	-.00264	.00239
	34.79	.59062	.60642	.59158	-.02675	-.00163
	25.00	.34261	.33282	.32468	.02857	.05233

[a,b]See footnotes at end of table.

TABLE II.- MEASURED AND THEORETICAL VALUES OF PRESSURE COEFFICIENTS FOR

TWO-DIMENSIONAL AERODYNAMICALLY BLUNT BODIES - Continued

(c) Circular arc bodies - lower surface - Concluded

$\theta_{le} = 78^\circ$							$\theta_{le} = 90^\circ$						
α, deg	δ, deg	$C_{p,meas}$	C_p (a)	C_p (b)	$\frac{C_{p,meas} - C_p}{C_{p,meas}}$ (a)	$\frac{C_{p,meas} - C_p}{C_{p,meas}}$ (b)	α, deg	δ, deg	$C_{p,meas}$	C_p (a)	C_p (b)	$\frac{C_{p,meas} - C_p}{C_{p,meas}}$ (a)	$\frac{C_{p,meas} - C_p}{C_{p,meas}}$ (b)
0	77.04	1.8190	1.8189	1.8055	0.00005	0.00742	0	89.91	1.8176	1.8179	1.8176	-0.00017	0
	75.05	1.7967	1.7879	1.7747	.00490	.01224		87.90	1.8176	1.8152	1.8152	.00132	.00132
	73.02	1.7657	1.7519	1.7390	.00782	.01512		84.53	1.8042	1.8011	1.8011	.00172	.00172
	66.70	1.6364	1.6157	1.6037	.01265	.01998		76.64	1.7181	1.7204	1.7204	-.00134	-.00134
	60.39	1.4588	1.4523	1.4416	.00446	.01179		73.06	1.6582	1.6634	1.6634	-.00314	-.00314
	55.70	1.3029	1.3071	1.2974	-.00322	.00422		69.05	1.5685	1.5852	1.5852	-.01065	-.01065
	51.43	1.1581	1.1709	1.1623	-.01105	-.00363		63.31	1.4311	1.4511	1.4511	-.01398	-.01398
	47.83	1.0442	1.0522	1.0445	-.00766	-.00029		59.47	1.3242	1.3485	1.3485	-.01835	-.01835
	42.90	.88394	.88753	.88098	-.00406	.00335		54.59	1.1845	1.2072	1.2072	-.01916	-.01916
	36.49	.68963	.67714	.67214	.01811	.02536		44.00	.87192	.87708	.87708	-.00592	-.00592
	30.85	.53554	.50366	.49993	.05953	.06649		36.11	.62711	.63149	.63149	-.00698	-.00698
	9.06	.14198	.04757	.04720	.66495	.66756		13.80	.17350	.10342	.10342	.40392	.40392
	0	.04235	0	0	1.0000	1.0000		0	.04591	0	0	1.0000	1.0000
5	82.04	1.8105		1.8104		.00006	5	94.91	1.7989		1.8044		-.00306
	80.05	1.8185	1.8185	1.7908	0	.01523		92.90	1.8117		1.8131		-.00077
	78.02	1.8123	1.7937	1.7663	.01026	.02538		89.53	1.8178	1.8177	1.8177	.00006	.00006
	71.70	1.7289	1.6897	1.6639	.02267	.03760		85.71	1.8062	1.8077	1.8077	-.00083	-.00083
	65.39	1.5193	1.5492	1.5256	.01906	.03400		81.64	1.7800	1.7793	1.7793	.00039	.00039
	60.70	1.4409	1.4255	1.4038	.01069	.02575		74.05	1.6648	1.6805	1.6805	-.00943	-.00943
	56.43	1.3055	1.3014	1.2816	.00314	.01831		68.31	1.5491	1.5697	1.5697	-.01330	-.01330
	52.83	1.1986	1.1903	1.1722	.00692	.02203		64.47	1.4540	1.4801	1.4801	-.01795	-.01795
	47.90	1.0348	1.0319	1.0162	.00280	.01701		59.59	1.3279	1.3519	1.3519	-.01807	-.01807
	41.49	.83891	.82249	.80994	.01957	.03453		49.00	1.0238	1.0354	1.0354	-.01133	-.01133
	35.85	.66956	.64259	.63315	.04028	.05438		41.11	.76661	.78607	.78607	-.02538	-.02538
	14.06	.18934	.11073	.10904	.41518	.42410		18.80	.25046	.18880	.18880	.24619	.24619
	5.00	.07747	.01424	.01402	.81619	.81903		5.00	.08288	.01382	.01382	.83325	.83325
10	87.04	1.7380		1.8163		-.04505	10	99.91	1.7530		1.7738		-.01187
	85.05	1.7992		1.8076		-.00467		97.90	1.7775		1.7832		-.03207
	83.02	1.8190	1.8312	1.7943	-.00671	-.01358		90.71	1.8175	1.8172	1.8172	.00017	.00017
	80.27	1.8172	1.8055	1.7692	.00644	.02641		86.64	1.8101	1.8110	1.8110	-.00050	-.00050
	76.70	1.7875	1.7743	1.7386	.00738	.02736		83.06	1.7898	1.7910	1.7910	-.00067	-.00067
	70.39	1.6743	1.6492	1.6159	.00150	.03488		79.05	1.7394	1.7519	1.7519	-.00719	-.00719
	65.70	1.5612	1.5439	1.5128	.01108	.03100		73.31	1.6522	1.6677	1.6677	-.00938	-.00938
	57.83	1.3373	1.3319	1.3050	.00404	.02415		69.47	1.5742	1.5939	1.5939	-.01251	-.01251
	52.90	1.1814	1.1824	1.1586	-,00085	.01930		64.59	1.4600	1.4827	1.4827	-.01555	-.01555
	46.49	.99343	.97744	.95774	.01610	.03593		54.00	1.1663	1.1896	1.1896	-.01998	-.01998
	40.85	.81038	.79518	.87021	.01876	-.07383		46.11	.92740	.94415	.94415	-.01806	-.01806
	19.03	.26369	.19834	.19434	.24783	.26300		23.80	.33772	.29598	.29598	.12359	.12359
	10.00	.12392	.05604	.05492	.54777	.55681		10.00	.13256	.05480	.05480	.58660	.58660
15	92.04	1.6225		1.8162		-.11938	15	104.91	1.6839		1.6984		-.00861
	92.05	1.7374		1.8185		-.04668		102.90	1.7167		1.7282		-.00670
	88.02	1.7911		1.8163		-.01407		99.53	1.7613		1.7690		-.00437
	81.70	1.8185	1.8016	1.7806	.00929	.02084		91.64	1.8189	1.8174	1.8174	.00082	.00082
	78.57	1.7948	1.7677	1.7471	.01510	.02658		88.06	1.8189	1.8168	1.8168	.00115	.00115
	75.39	1.7511	1.7228	1.7027	.01616	.02764		84.05	1.7985	1.7993	1.7993	-.00044	-.00044
	70.70	1.6675	1.6390	1.6198	.01709	.02861		78.31	1.7477	1.7443	1.7443	.00195	.00195
	62.83	1.4740	1.4564	1.4394	.01194	.02347		74.47	1.6895	1.6884	1.6884	.00065	.00065
	57.90	1.3291	1.3204	1.3050	.00655	.01813		69.51	1.5947	1.5976	1.5976	-.00182	-.00182
	51.49	1.1419	1.1264	1.1133	.01357	.02505		59.00	1.3248	1.3364	1.3364	-.00876	-.00876
	45.85	.96148	.94726	.93622	.01479	.02627		51.11	1.0913	1.1022	1.1022	-.00999	-.00999
	24.06	.35848	.30598	.30242	.14645	.15638		28.80	.45542	.42215	.42215	.07305	.07305
	15.00	.17059	.12326	.12182	.27745	.28589		15.00	.17617	.12185	.12185	.30834	.30834
20	97.04	1.4640		1.7911		-.02234	20	109.91	1.5903		1.6076		-.01088
	95.05	1.6404		1.8043		-.09991		107.90	1.6327		1.6468		-.00868
	93.02	1.7303		1.8134		-.04805		100.71	1.7568		1.7557		.00057
	86.70	1.8184		1.8124		.00330		93.06	1.8186	1.8134	1.8134	.00286	.00286
	83.60	1.8184	1.8093	1.7956	.00500	.01254		89.05	1.8136	1.8181	1.8181	-.00248	-.00248
	80.39	1.7940	1.7812	1.7676	.00713	.01472		83.31	1.7899	1.7939	1.7940	-.00223	-.00223
	75.70	1.7390	1.7205	1.7075	.01064	.01811		79.47	1.7550	1.7578	1.7578	-.00160	-.00160
	67.83	1.5846	1.5715	1.5595	.00827	.01584		74.59	1.6864	1.6901	1.6901	-.00219	-.00219
	62.90	1.4615	1.4521	1.4410	.00643	.01403		64.00	1.4599	1.4691	1.4691	-.00626	-.00626
	56.49	1.2809	1.2736	1.2640	.00570	.01319		56.11	1.2441	1.2534	1.2534	-.00742	-.00742
	50.85	1.1065	1.1120	1.0936	.00407	.01166		33.80	.57656	.56278	.56278	.00656	.00656
	29.06	.46776	.43249	.42920	.07540	.08244		22.04	.33389	.25588	.25588	.23364	.23364
	20.00	.25463	.21435	.21272	.15819	.16459		20.00	.26465	.21274	.21274	.19615	.19615
25	102.04	1.2941		1.7389		-.34371	25	114.91	1.4797		1.4952		-.01048
	100.05	1.5237		1.7625		-.15672		112.90	1.5272		1.5425		-.00992
	98.02	1.6442		1.7825		-.08411		109.53	1.6009		1.6146		-.00856
	91.70	1.7954		1.8163		-.01164		101.64	1.7447		1.7439		.00046
	88.57	1.8179		1.8168		.00061		94.05	1.8084		1.8087		-.00017
	85.39	1.8129	1.8111	1.8061	.000993	.00374		88.31	1.8178	1.8162	1.8162	.00088	.00088
	80.70	1.7847	1.7753	1.7704	.00527	.00801		84.47	1.0828	1.8009	1.8009	.00105	.00105
	72.82	1.6711	1.6641	1.6594	.00419	.00700		79.59	1.7597	1.7584	1.7584	.00074	.00074
	67.90	1.5657	1.5649	1.5606	.00051	.00326		69.00	1.5778	1.5843	1.5843	-.00412	-.00412
	61.49	1.4058	1.4074	1.3127	-.00114	.06623		61.11	1.3847	1.3937	1.3937	-.00650	-.00650
	55.85	1.2370	1.2484	1.2450	-.00922	-.00647		38.80	.71465	.71372	.71372	.00130	.00130
	34.06	.58832	.57198	.57042	.02777	.03043		27.04	.44090	.37552	.37552	.14829	.14829
	25.00	.35181	.32559	.32470	.07453	.07706		25.00	.36465	.32468	.32468	.10961	.10961

[a,b]See footnotes at end of table.

22

TABLE II.- MEASURED AND THEORETICAL VALUES OF PRESSURE COEFFICIENTS FOR

TWO-DIMENSIONAL AERODYNAMICALLY BLUNT BODIES - Continued

(d) Circular arc bodies - upper surface

$\theta_{le} = 42^\circ$

α, deg	δ, deg	$C_{p,meas}$	C_p (a)	C_p (c)	$\frac{C_{p,meas} - C_p}{C_{p,meas}}$ (a)	$\frac{C_{p,meas} - C_p}{C_{p,meas}}$ (c)
0	40.43	1.1724	1.1725	1.2027	-0.00009	-0.02584
	39.24	1.1241	1.1151	1.1438	.00801	-.01753
	38.51	1.0938	1.0810	1.1088	.01170	-.01371
	34.99	.92910	.91634	.93990	.01384	-.01162
	32.92	.83437	.82318	.84433	.01341	-.01194
	30.71	.73467	.72731	.74601	.01002	-.01544
	27.76	.60836	.60502	.62055	.00549	-.02004
	24.51	.48762	.47999	.49231	.01565	-.00962
	16.20	.24303	.21699	.22255	.10715	.08427
	12.18	.16440	.12416	.12734	.24477	.22543
	4.42	.06285	.01653	.01695	.73699	.73031
	0	.02570	0	0	1.0000	1.0000
5	35.43	.91207	.91225	1.0222	-.00020	-.12075
	34.24	.87886	.85893	.90588	.02268	-.03074
	33.51	.85505	.82750	.87212	.03222	-.01996
	31.39	.75605	.73601	.77572	.02651	-.02602
	29.99	.69590	.67782	.71491	.02598	-.027317
	27.92	.61320	.59491	.62733	.02983	-.02304
	22.76	.43525	.40081	.42825	.07913	.01608
	17.16	.28675	.23642	.24890	.17552	.13200
	11.20	.16645	.10240	.10794	.38480	.35152
	7.18	.10442	.04245	.04471	.59347	.57183
	-.58	.02798				
	-5.00	.000414				
10	30.43	.69342	.69356	.73358	-.00020	-.05792
	29.24	.67312	.64469	.68273	.04224	-.01428
	28.51	.64647	.61608	.65188	.04701	-.00836
	26.39	.56525	.53377	.56487	.05569	.00067
	24.99	.51512	.48218	.51066	.06395	.00866
	20.71	.37743	.33826	.35784	.10378	.05190
	17.76	.29685	.25168	.26623	.15216	.10315
	12.16	.18517	.12007	.12686	.35157	.31490
	6.20	.09570	.03152	.03338	.67064	.65120
	2.18	.05510	.00392	.00414	.92886	.92486
	-5.58	.00351				
	-10.00	-.01426				
15	25.43	.50788	.50803	.52760	-.00030	-.03883
	24.24	.47537	.46403	.48231	.02386	-.01460
	23.51	.44766	.43852	.45511	.02042	-.01664
	21.39	.38239	.36617	.38031	.04242	.00544
	19.99	.35099	.32169	.33440	.08348	.04727
	15.71	.24754	.20212	.20978	.18349	.15254
	12.76	.18966	.13450	.13959	.29084	.26400
	7.16	.10653	.04286	.04442	.59767	.58303
	1.20	.04680	.00121	.001254	.97415	.97321
	-2.82	.01909				
	-10.58	-.00134				
	-15.00	-.00241				
20	20.43	.32802	.40880	.34862	-.24627	-.06280
	19.24	.36422	.36395	.31072	.00074	.14689
	18.51	.34950	.33829	.28840	.03207	.17482
	16.39	.28324	.26685	.22765	.05998	.19626
	14.99	.24520	.22419	.19142	.08569	.21933
	10.71	.16115	.11599	.09882	.28024	.38678
	7.76	.11882	.06125	.05216	.48451	.56102
	2.16	.06115	.00480	.00406	.92150	.93361
	-3.88	.01925				
	-7.82	-.00007				
	-15.58	-.02185				
	-20.00	-.02879				
25	15.43	.16158		.20254		-.25350
	14.24	.25148		.17314		.31152
	13.51	.25148	.25171	.15616	-.00091	.37904
	11.39	.21552	.17951	.11152	.16708	.48255
	9.99	.18700	.13846	.08611	.25957	.53952
	5.71	.11446	.04571	.02833	.60065	.75249
	2.76	.07727	.01074	.006634	.86101	.91415
	-2.84	.03077				
	-8.80	-.00054				
	-12.82	-.01356				
	-20.58	-.02726				
	-25.00	-.02838				

$\theta_{le} = 54^\circ$

α, deg	δ, deg	$C_{p,meas}$	C_p (a)	C_p (c)	$\frac{C_{p,meas} - C_p}{C_{p,meas}}$ (a)	$\frac{C_{p,meas} - C_p}{C_{p,meas}}$ (c)
0	52.44	1.7737	1.7734	1.7454	0.00017	0.01596
	50.53	1.6243	1.6822	1.6556	-.03565	-.01927
	48.66	1.5035	1.5865	1.5660	-.05520	-.04157
	45.40	1.3242	1.4310	1.4084	-.08065	-.06359
	43.19	1.2034	1.3218	1.3009	-.09839	-.08102
	38.30	.96695	1.0842	1.0671	-.12126	-.10357
	35.32	.84044	.94327	.92837	-.12235	-.10462
	31.59	.70249	.77424	.76199	-.10214	-.08470
	28.76	.58869	.65371	.64337	-.11045	-.09288
	17.91	.28608	.26712	.26291	.06628	.08099
	6.49	.10935	.03599	.03542	.67087	.67609
	0	.04514	0	0	1.0000	1.0000
5	47.44	1.4669	1.4666	1.5069	.00020	-.02727
	45.53	1.3391	1.3771	1.4147	-.02838	-.05646
	43.66	1.2354	1.2780	1.3240	-.03448	-.07172
	40.40	1.0815	1.1358	1.1670	-.05021	-.07906
	38.19	.96876	1.0333	1.0619	-.06662	-.09614
	36.11	.87179	.93939	.96487	-.07754	-.10677
	33.30	.75119	.81501	.83734	-.08496	-.11468
	30.32	.64331	.68893	.70796	-.07091	-.10050
	26.59	.52755	.54146	.55634	-.02637	-.05457
	12.91		.13512	.13866		
	1.49	.05907	.00180	.00187	.96953	.9683
	-5.00	.01349				
10	42.44	1.1847	1.1844	1.2651	.00025	-.06787
	40.53	1.0861	1.0988	1.1732	-.01169	-.08020
	38.66	1.0044	1.0111	1.0841	-.00667	-.07935
	37.65	.97537	.97060	1.0366	.00489	-.06278
	33.19	.77332	.77932	.83248	-.00776	-.07650
	31.11	.69165	.69478	.74162	-.00453	-.07225
	28.30	.59122	.58473	.62438	.01098	-.05609
	25.32	.49866	.47572	.50809	.04600	-.01891
	18.76	.31838	.26926	.28733	.15428	.09752
	7.91	.12903	.04935	.05261	.61753	.59227
	-3.51	.02800				
	-10.00	-.00539				
15	37.44	.55016		1.0264		-.86564
	35.53	.88899	.88917	.93814	-.00020	-.05529
	33.66	.78216	.80475	.85337	-.02888	-.09104
	30.40	.67104	.67408	.71137	-.00453	-.06010
	28.19	.60023	.58719	.61994	.02173	-.03284
	26.11	.54162	.51011	.53808	.05818	.00654
	20.32	.35969	.31733	.33438	.11777	.07037
	16.59	.28032	.21443	.22646	.23505	.19214
	13.76	.21988	.14907	.15717	.32204	.28520
	2.91	.07886	.00682	.00716	.91352	.90921
	-8.51	.00535				
	-15.00	-.01723				
20	32.44	.33612		.79936		-.13782
	30.53	.59208		.71684		-.21071
	28.66	.64583	.64609	.63900	-.00040	.00293
	25.40	.50655	.51657	.51113	-.01978	-.00904
	21.11	.37583	.36434	.36037	.03057	.04114
	18.30	.30863	.27680	.27388	.10313	.11259
	15.32	.25243	.19591	.19392	.22390	.23179
	11.59	.19562	.11320	.11213	.42133	.42680
	8.76	.15103	.06522	.06443	.56817	.57340
	-2.09	.04535				
	-13.51	-.01061				
	-20.00	-.02539				
25	27.44	.22042		.58993		-.16764
	25.53	.35559		.51597		-.45103
	23.66	.42654	.43934	.44738	-.03001	-.04886
	20.40	.38067	.33394	.33753	.12276	.11333
	18.19	.32623	.26765	.27072	.17957	.17016
	16.11	.27791	.21180	.21389	.23788	.23036
	13.30	.22226	.14545	.14701	.34559	.33857
	10.32	.17394	.08814	.08914	.49327	.48752
	6.59	.12807	.03612	.03658	.71797	.71437
	-7.09	.01504				
	-18.51	-.01988				
	-25.00	-.02906				

$\theta_{le} = 66^\circ$

α, deg	δ, deg	$C_{p,meas}$	C_p (a)	C_p (c)	$\frac{C_{p,meas} - C_p}{C_{p,meas}}$ (a)	$\frac{C_{p,meas} - C_p}{C_{p,meas}}$ (c)
0	63.64	1.7617	1.7615	1.7491	0.00011	0.00727
	61.49	1.6839	1.6942	1.6821	-.00612	.00107
	60.01	1.6280	1.6463	1.6345	-.01124	-.00399
	54.33	1.4190	1.4483	1.4379	-.02065	-.01332
	49.04	1.2112	1.2511	1.2422	-.03294	-.02559
	46.29	1.1146	1.1463	1.1381	-.02844	-.02108
	40.12	.88620	.91103	.90464	-.02802	-.02067
	35.76	.72216	.74432	.74401	-.03069	-.03027
	31.33	.58182	.59338	.58913	-.01987	-.01256
	18.37	.27806	.21787	.21631	.21646	.22207
	9.94	.14197	.06531	.06484	.53997	.54328
	0	.04659	0	0	1.0000	1.0000
5	58.64	1.6204	1.6202	1.5885	.00012	.01969
	56.49	1.5297	1.5447	1.5145	-.00981	.01520
	55.01	1.4675	1.4918	1.4624	-.01656	.00361
	49.33	1.2498	1.2785	1.2533	-.02296	-.00280
	44.04	1.3046	1.0736	1.0528	-.03770	-.019301
	41.29	.94268	.96736	.94843	-.02618	-.006301
	35.12	.72744	.73534	.72101	-.01086	.00884
	30.76	.57932	.58151	.56985	-.00378	.00211
	26.33	.45114	.43726	.42858	.03077	.05001
	13.37	.19600	.11878	.11649	.39398	.40566
	4.94	.09201	.01645	.01615	.82122	.82448
	-5.00	.01849				
10	53.64	1.4400	1.4398	1.4129	.00014	.01882
	51.49	1.3581	1.3593	1.3339	-.00088	.01782
	50.01	1.2944	1.3036	1.2788	-.00711	.01205
	44.33	1.0828	1.0844	1.0638	-.00148	.01755
	41.63	.97485	.98006	.96149	-.00534	.01370
	39.04	.86933	.88065	.86429	-.01302	.00580
	36.29	.78200	.77760	.76318	.00563	.02407
	30.12	.59158	.55904	.54857	.05501	.07270
	25.76	.45756	.41960	.41149	.08296	.10069
	8.37	.13919	.04700	.04616	.66233	.66837
	-.06	.05489				
	-10.00	-.00078				
15	48.64	1.2683	1.2680	1.2273	.00024	.03233
	46.49	1.1645	1.1839	1.1458	-.01666	.01606
	45.01	1.1058	1.1263	1.0897	-.01854	.01456
	39.33	.91586	.90444	.87510	.01247	.04450
	36.63	.81018	.80155	.77558	.01065	.04271
	31.29	.63242	.60705	.58967	.04012	.07076
	28.45	.55789	.51093	.49444	.08417	.11373
	25.12	.46504	.40562	.39262	.12777	.15572
	16.33	.25979	.17806	.17226	.31460	.33693
	3.37	.09119	.00776	.00802	.91490	.91205
	-5.06	.02643				
	-15.00	-.01395				
20	43.64	.64803		1.0376		-.60116
	41.49	1.0138	1.0135	.95612	.00030	.05689
	40.01	.93479	.95506	.90049	-.02168	.03669
	34.33	.72707	.73478	.69289	-.01060	.04701
	31.63	.63761	.63541	.59920	.00345	.06024
	29.04	.55550	.54406	.51334	.02059	.07590
	26.29	.48565	.45293	.42738	.06737	.11998
	20.12	.34227	.27324	.25779	.20168	.24682
	11.33	.17866	.08920	.08409	.50073	.52933
	-1.63	.05305				
	-10.06	.00526				
	-20.00	-.02311				
25	38.64	.39894		.84942		-1.1292
	36.49	.58573		.77040		-.31528
	35.01	.66105	.67500	.71706	-.02110	-.08473
	32.37	.64451	.58751	.62447	.08844	.03109
	29.33	.56674	.49200	.52171	.13188	.07945
	26.63	.48897	.41197	.43771	.15747	.10483
	21.29	.35180	.27010	.28721	.23223	.18360
	15.12	.23667	.13943	.14822	.41087	.37373
	6.33	.11971	.02495	.02648	.79158	77880
	-6.63	.02418				
	-15.06	-.00968				
	-25.00	-.02879				

[a,c]See footnotes at end of table.

TABLE II.- MEASURED AND THEORETICAL VALUES OF PRESSURE COEFFICIENTS FOR

TWO-DIMENSIONAL AERODYNAMICALLY BLUNT BODIES - Concluded

(d) Circular arc bodies - upper surface - Concluded

$\theta_{le} = 78^{\circ}$						
α, deg	δ, deg	$C_{p,meas}$	C_p (a)	C_p (c)	$\frac{C_{p,meas} - C_p}{C_{p,meas}}$ (a)	$\frac{C_{p,meas} - C_p}{C_{p,meas}}$ (c)
0	75.11	1.8010	1.8012	1.7758	-0.00011	0.01399
	72.89	1.7651	1.7613	1.7365	.00215	.01620
	70.46	1.7181	1.7128	1.6887	.00308	.01711
	67.10	1.6488	1.6363	1.6133	.00758	.02153
	60.56	1.4718	1.4627	1.4421	.00618	.02018
	57.11	1.3604	1.3599	1.3408	.00037	.01441
	49.76	1.1135	1.1238	1.1080	-.00925	.00494
	43.16	.92354	.90250	.88980	.02278	.03653
	37.08	.72057	.70109	.69124	.02703	.04070
	31.47	.55906	.52544	.51805	.06014	.07336
	9.82	.15683	.05607	.05526	.64248	.64764
	0	.05349	0	0	1.0000	1.0000
5	70.11	1.7277	1.7279	1.6812	-.00012	.02691
	67.89	1.6757	1.6769	1.6318	-.00716	.02620
	65.46	1.6127	1.5908	1.5733	.01358	.02443
	62.10	1.5330	1.5260	1.4849	.00457	.03138
	55.56	1.3352	1.3292	1.2931	.00449	.03153
	52.11	1.2091	1.2171	1.1841	-.00662	.02068
	44.76	.95943	.96898	.94265	-.00995	.017490
	38.16	.76474	.74611	.72580	.02436	.05092
	32.08	.58303	.55122	.53629	.05456	.08017
	26.47	.44088	.38809	.37774	.11974	.14321
	4.82	.10467	.01377	.01342	.86844	.87179
	-5.00	.02494				
10	65.11	1.6038	1.6040	1.5644	-.00012	.02457
	62.89	1.5432	1.5441	1.5064	-.00058	.02385
	60.46	1.4740	1.4755	1.4391	-.00102	.02368
	57.10	1.3948	1.3740	1.3402	.01491	.03915
	50.56	1.1858	1.1627	1.1339	.01948	.04377
	43.34	.93530	.91787	.89553	.01864	.04252
	36.37	.70586	.68527	.66856	.02917	.05284
	33.16	.62237	.58333	.56883	.06273	.08603
	27.08	.46406	.40401	.39400	.12940	.15097
	21.47	.34099	.26103	.25470	.23449	.25306
	-.18	.06455				
	-10.00	.00364				
15	60.11	1.4596	1.4597	1.4290	-.00007	.02096
	57.89	1.3997	1.3930	1.3641	.00479	.02543
	55.46	1.3285	1.3178	1.2900	.00805	.02898
	52.10	1.2517	1.2091	1.1837	.03403	.05433
	45.56	1.0445	.99012	.96920	.05206	.07209
	42.11	.91903	.87337	.85489	.04968	.06979
	38.34	.79294	.74701	.73158	.05792	.07736
	31.37	.57758	.52610	.51519	.08913	.10802
	28.16	.50330	.43268	.42346	.14031	.15863
	16.47	.25361	.15603	.15282	.38476	.39742
	-5.18	.03451				
	-15.00	-.01018				
20	55.11	1.2715	1.2717	1.2792	-.00016	-.00606
	52.89	1.2234	1.2017	1.2091	.01774	.01169
	50.46	1.1515	1.1241	1.1307	.02380	.01806
	47.10	1.0859	1.0141	1.0201	.06612	.06059
	40.56	.88588	.79926	.80387	.09778	.09257
	37.11	.76401	.66816	.69210	.12546	.09412
	33.34	.64526	.57065	.57428	.11563	.11000
	29.76	.53588	.46580	.46843	.13078	.12587
	23.16	.38838	.29248	.29409	.24692	.24278
	11.47	.17651	.07469	.07518	.57685	.57407
	-10.18	.01251				
	-20.00	-.01912				
25	50.11	1.0198	1.0200	1.1193	-.00020	-.09757
	47.89	.99127	.95316	1.0464	.00384	-.05562
	45.46	.92507	.88023	.96589	.04847	-.04413
	42.10	.86680	.77860	.85453	.08820	.01419
	38.91	.79212	.68358	.75001	.13702	.05316
	35.56	.69194	.58606	.64303	.15302	.07068
	32.11	.58690	.48963	.53719	.16574	.08470
	28.34	.48732	.39020	.42840	.19929	.12091
	21.37	.32217	.22994	.25244	.28628	.21644
	6.47	.11377	.02197	.02414	.81502	.79675
	-15.18	-.00642				
	-25.00	-.02719				

$\theta_{le} = 90^{\circ}$						
α, deg	δ, deg	$C_{p,meas}$	C_p (a)	C_p (c)	$\frac{C_{p,meas} - C_p}{C_{p,meas}}$ (a)	$\frac{C_{p,meas} - C_p}{C_{p,meas}}$ (c)
0	87.45	1.8164	1.8164	1.8140	0	0.00132
	85.13	1.8103	1.8069	1.8045	.00188	.00320
	82.07	1.7864	1.7853	1.7830	.00062	.00190
	78.73	1.7510	1.7505	1.7482	.00029	.00160
	71.05	1.6173	1.6281	1.6259	-.00668	-.00532
	61.88	1.4006	1.4158	1.4138	-.01085	-.00950
	57.39	1.2767	1.2912	1.2897	-.01136	-.01003
	53.40	1.1546	1.1730	1.1715	-.01594	-.01464
	43.82	.86764	.87242	.87138	-.00551	-.00418
	36.02	.64176	.62931	.62858	.01940	.02071
	14.27	.19121	.11053	.11043	.42194	.42273
	0	.05446	0	0	1.0000	1.0000
5	82.45	1.7782	1.7800	1.7863	-.00101	-.01041
	80.13	1.7520	1.7581	1.7642	-.00348	-.00696
	77.07	1.7154	1.7205	1.7266	-.00297	-.00652
	73.73	1.6624	1.6691	1.6749	-.00403	-.00752
	66.05	1.4948	1.5128	1.5181	-.01204	-.01559
	60.96	1.3632	1.3846	1.3894	-.01570	-.01922
	52.39	1.1219	1.1364	1.1406	-.01292	-.01667
	43.51	.85802	.85875	.86157	-.00085	-.00414
	38.82	.71603	.71167	.71428	.00609	.00244
	31.02	.51311	.48093	.48085	.06272	.06287
	9.27	.13712	.04696	.04717	.65753	.65672
	-5.00	.02499				
10	77.45	1.7143	1.7143	1.7318	0	-.01021
	75.13	1.6756	1.6808	1.6979	-.00310	-.01331
	72.07	1.6166	1.6287	1.6453	-.00748	-.01775
	68.73	1.5546	1.5626	1.5784	-.00515	-.01531
	61.05	1.3555	1.3777	1.3917	-.01638	-.02671
	55.96	1.2192	1.2357	1.2481	-.01353	-.02379
	47.39	.97286	.97439	.98453	-.00157	-.01200
	43.40	.84447	.84942	.85809	-.00586	-.01613
	38.51	.71119	.69777	.70468	.01887	.00915
	33.82	.57974	.57726	.56308	.00424	.02874
	26.02	.39853	.34615	.34978	.13143	.12232
	-10.00	.00431				
15	72.45	1.6341	1.6341	1.6524	0	-.01120
	70.13	1.5839	1.5899	1.6076	-.00379	-.01496
	67.07	1.5139	1.5246	1.5417	-.00707	-.01836
	63.73	1.4440	1.4455	1.4622	-.00104	-.01260
	56.05	1.2297	1.2369	1.2507	-.00586	-.01708
	50.96	1.0879	1.0846	1.0966	.00303	-.00799
	46.88	.96905	.95783	.96837	.01158	.00070
	38.40	.71456	.69353	.70130	.02943	.01856
	33.51	.58483	.54808	.55400	.06236	.05272
	28.82	.46998	.41763	.42238	.11139	.10128
	21.02	.30960	.23121	.23385	.25320	.24467
	-15.00	-.00689				
20	67.45	1.5304	1.5304	1.5503	0	-.01300
	65.13	1.4686	1.4770	1.4961	-.00572	-.01737
	62.07	1.3925	1.4005	1.4188	-.00575	-.01889
	58.75	1.3158	1.3109	1.3279	.00372	-.00920
	51.05	1.0881	1.0852	1.0993	.00267	-.01029
	41.88	.81674	.79973	.81000	.02083	.00825
	37.39	.68885	.66141	.67021	.03983	.02706
	33.40	.57843	.54372	.55080	.06001	.04777
	28.51	.46240	.40895	.41410	.11560	.10446
	16.02	.22410	.13660	.15660	.39045	.30120
	-5.73	.02759				
	-20.00	-.02063				
25	62.45	1.4028	1.4028	1.4288	0	-.01853
	60.13	1.3384	1.3420	1.3668	-.00269	-.02122
	57.07	1.2522	1.2571	1.2805	-.00391	-.02260
	53.73	1.1722	1.1601	1.1815	.01032	-.00793
	46.05	.93903	.92498	.94211	.01496	-.00322
	40.96	.78965	.76708	.78108	.02858	.01085
	32.39	.55715	.51191	.52155	.08120	.06390
	28.40	.45715	.40371	.41117	.11690	.10058
	23.51	.35528	.28412	.28924	.20029	.18588
	18.82	.26590	.18565	.18916	.30181	.28860
	-10.73	.00565				
	-25.00	-.02723				

[a]Computed by using generalized Newtonian theory with the maximum pressure coefficient at its actual location on each surface,

$$C_p = C_{p,max} \frac{\sin^2\delta}{\sin^2\delta_{max}}.$$

[b]Computed by using generalized Newtonian theory with the lower-surface maximum pressure coefficient at its geometric location,

$$C_p = C_{p,max} \frac{\sin^2\delta}{\sin^2\delta_{max,geom}}.$$

[c]Computed by using generalized Newtonian theory with both the maximum pressure coefficient and leading-edge angle at $\alpha = 0^{\circ}$,

$$C_p = C_{p,max(\alpha=0^{\circ})} \frac{\sin^2\delta}{\sin^2\delta_{le(\alpha=0^{\circ})}}.$$

24

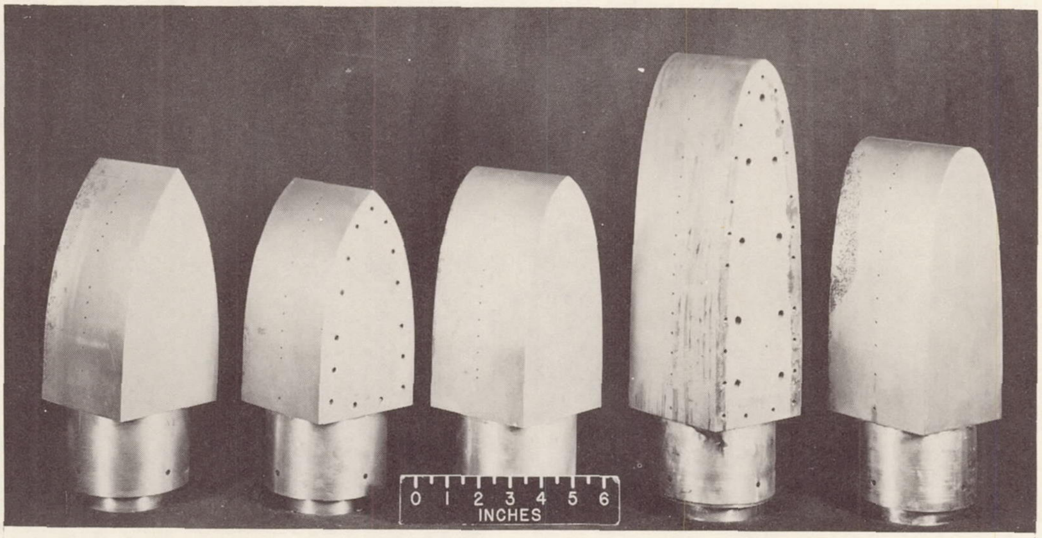

(a) Parabolic arc models.

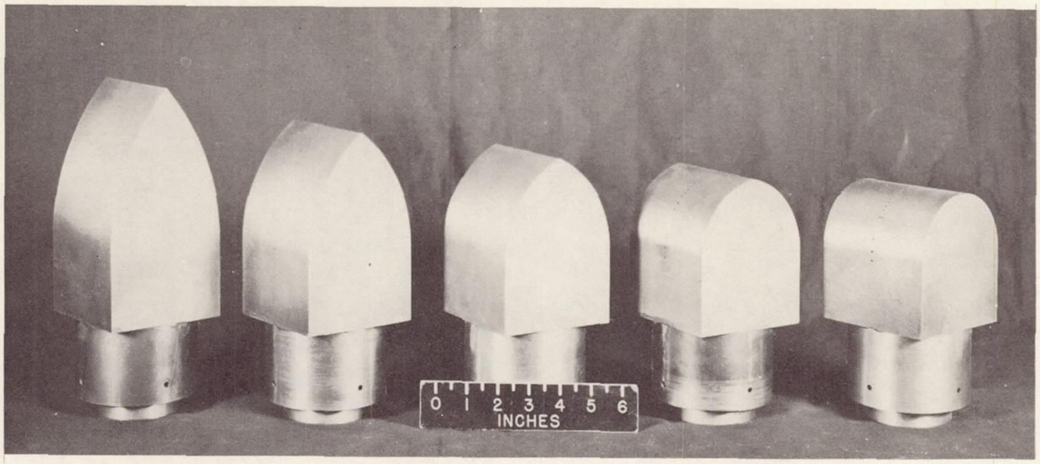

(b) Circular arc models.

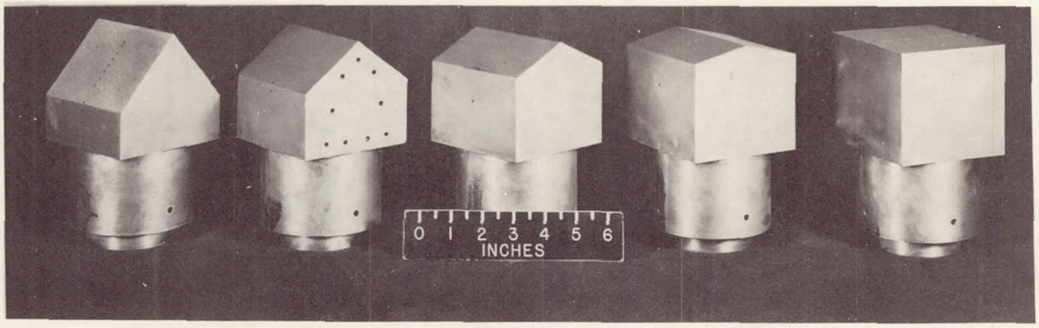

(c) Wedge models.

L-63-83

Figure 1.- Photograph of two-dimensional aerodynamically blunt bodies.

25

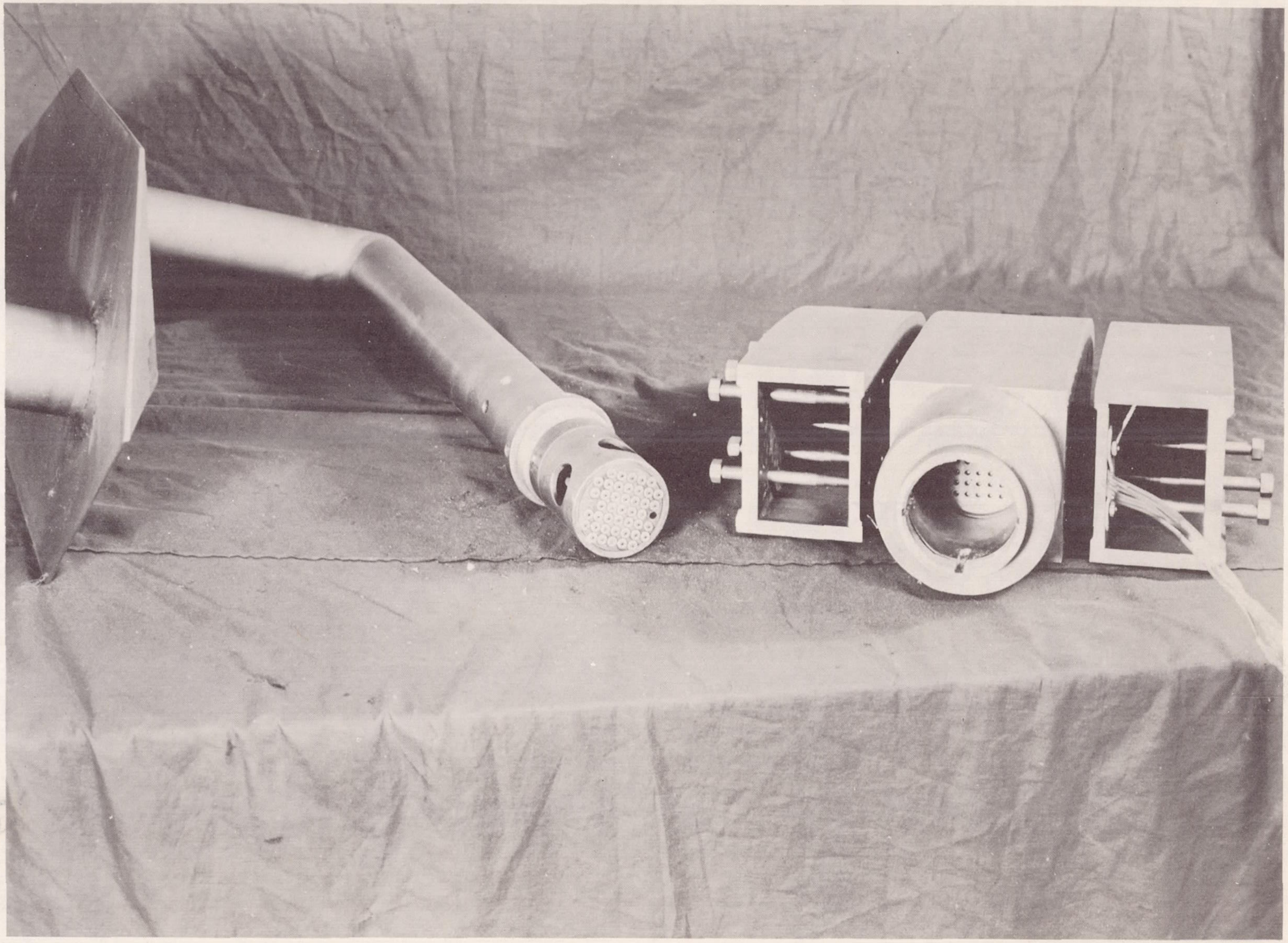

L-62-872

Figure 2.- Photograph of 78° parabola with extensions and support.

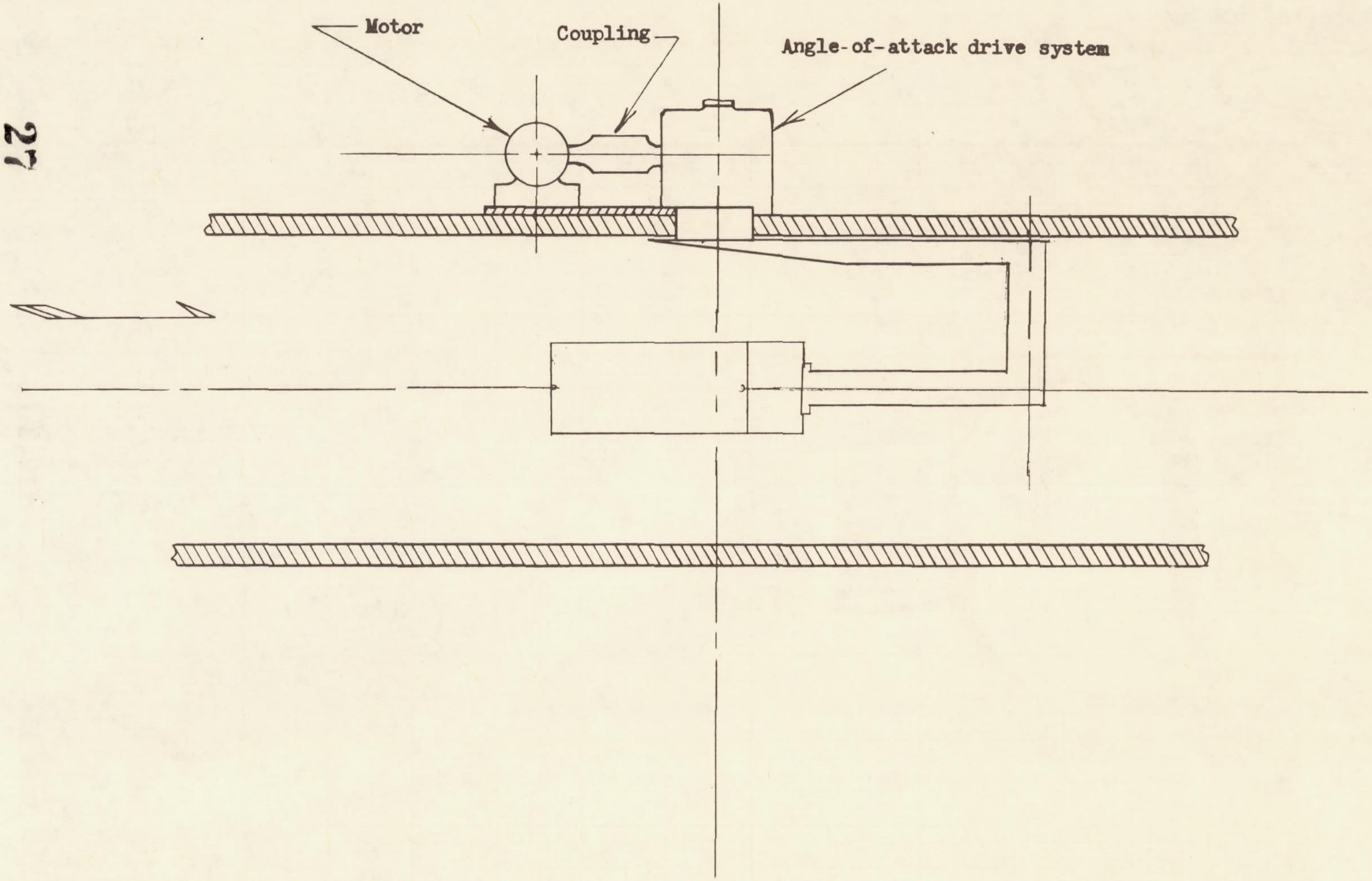

Figure 3.- Schematic diagram of model support system.

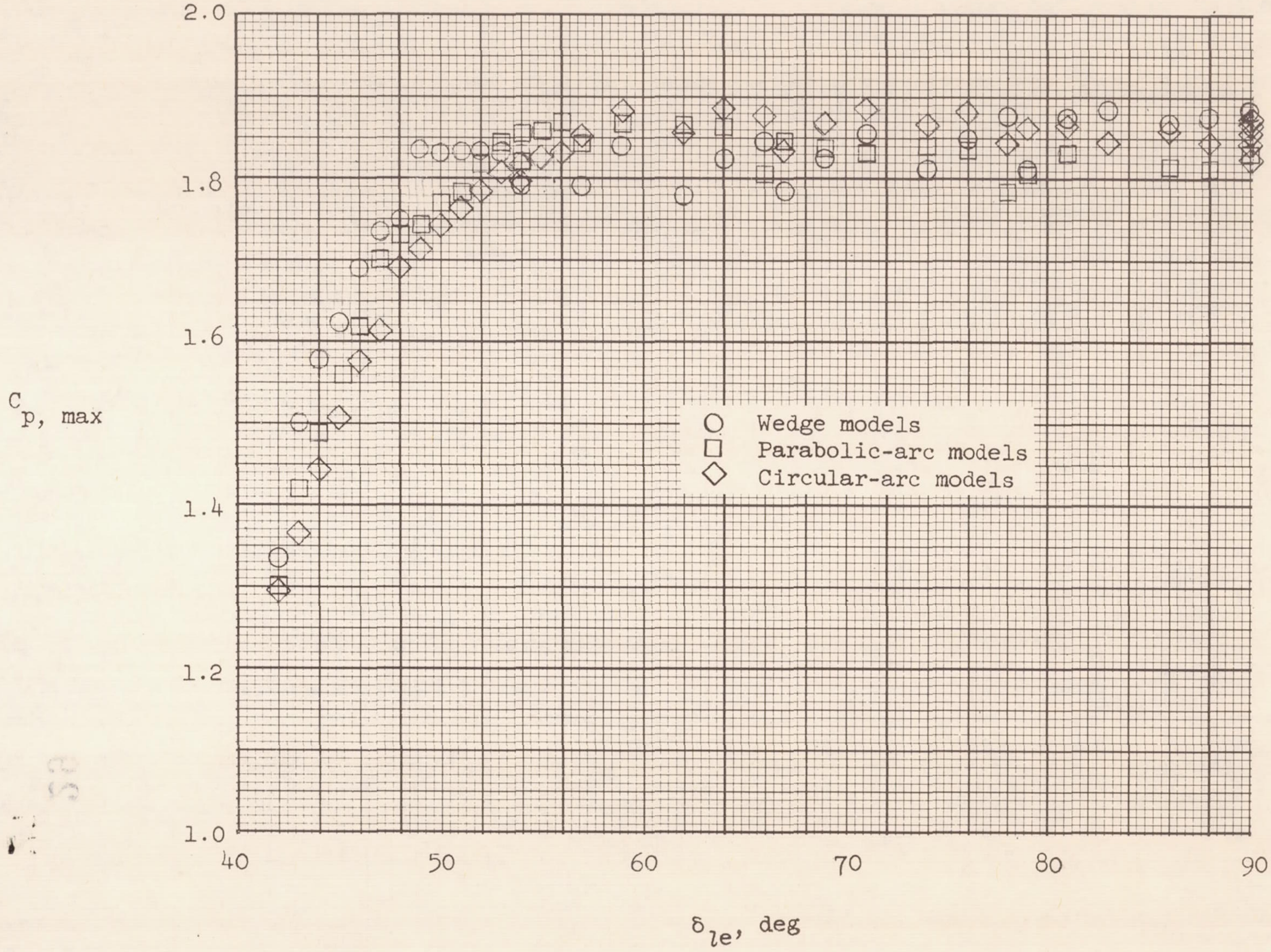

Figure 4.- Maximum pressure coefficients based upon an assumed Mach number of 6.

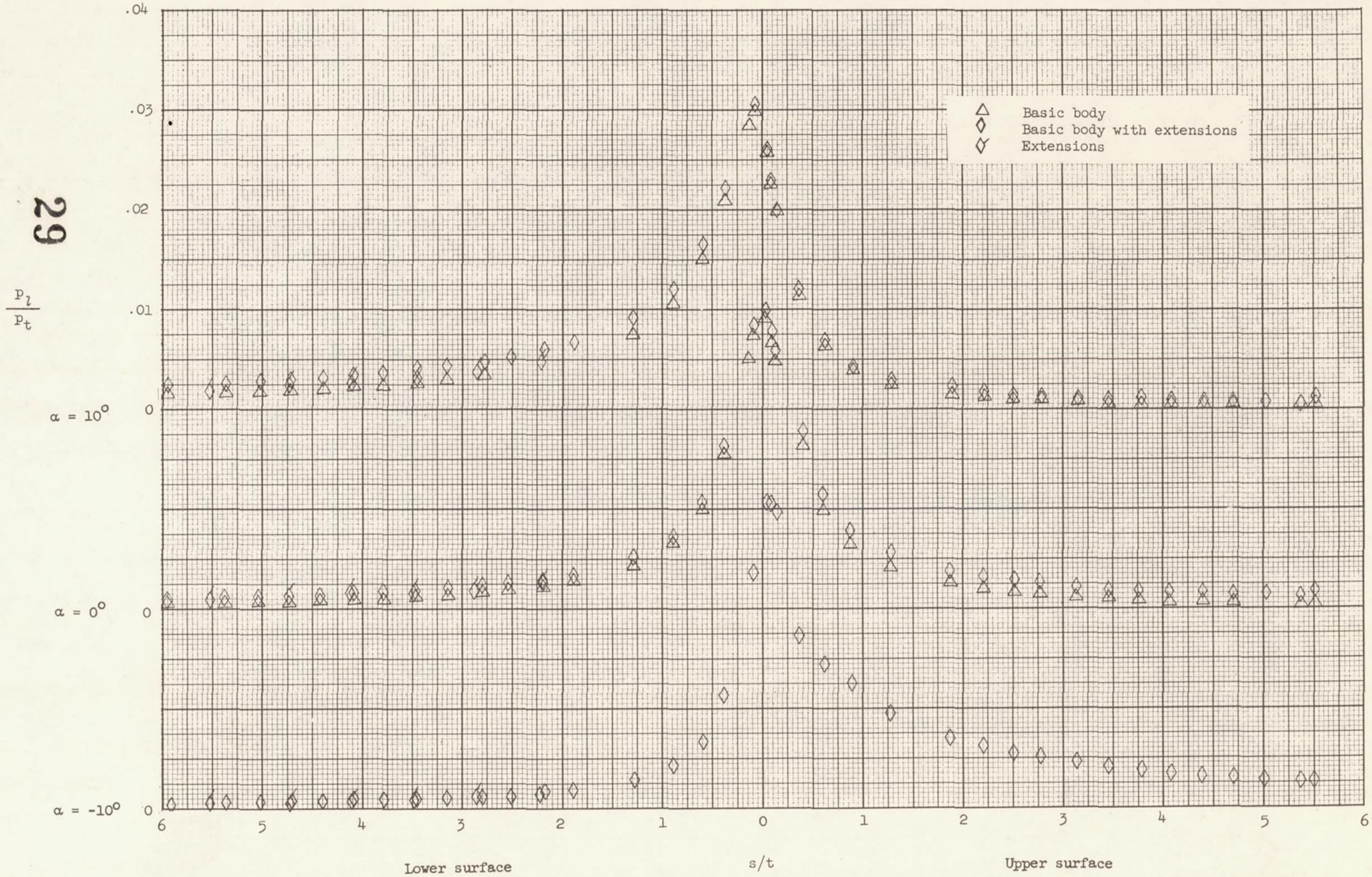

Figure 5.- Pressure distributions of two-dimensional 78° parabola with and without extensions.

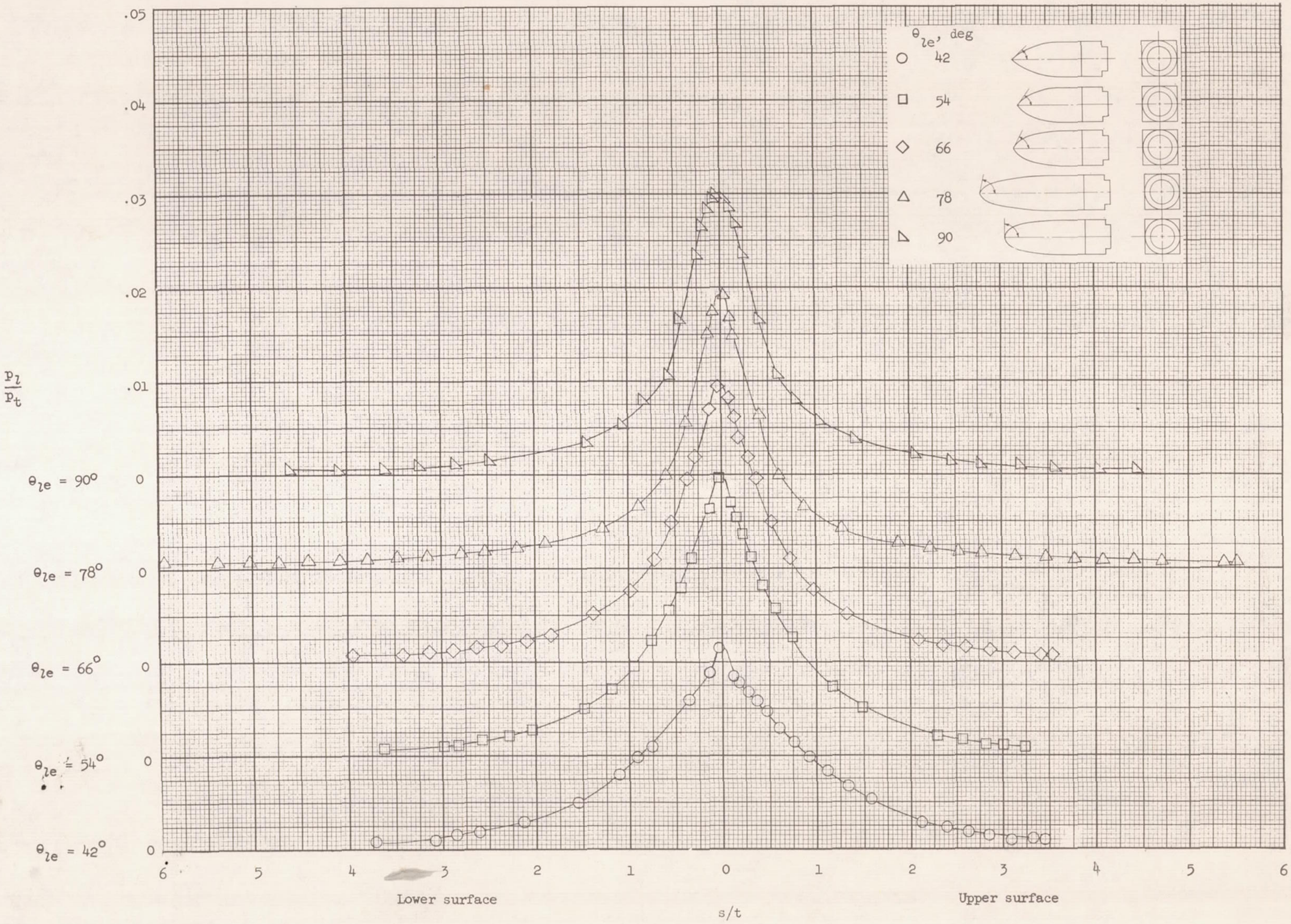

(a) $\alpha = 0^{\circ}$.

Figure 6.- Pressure distributions of two-dimensional parabolas.

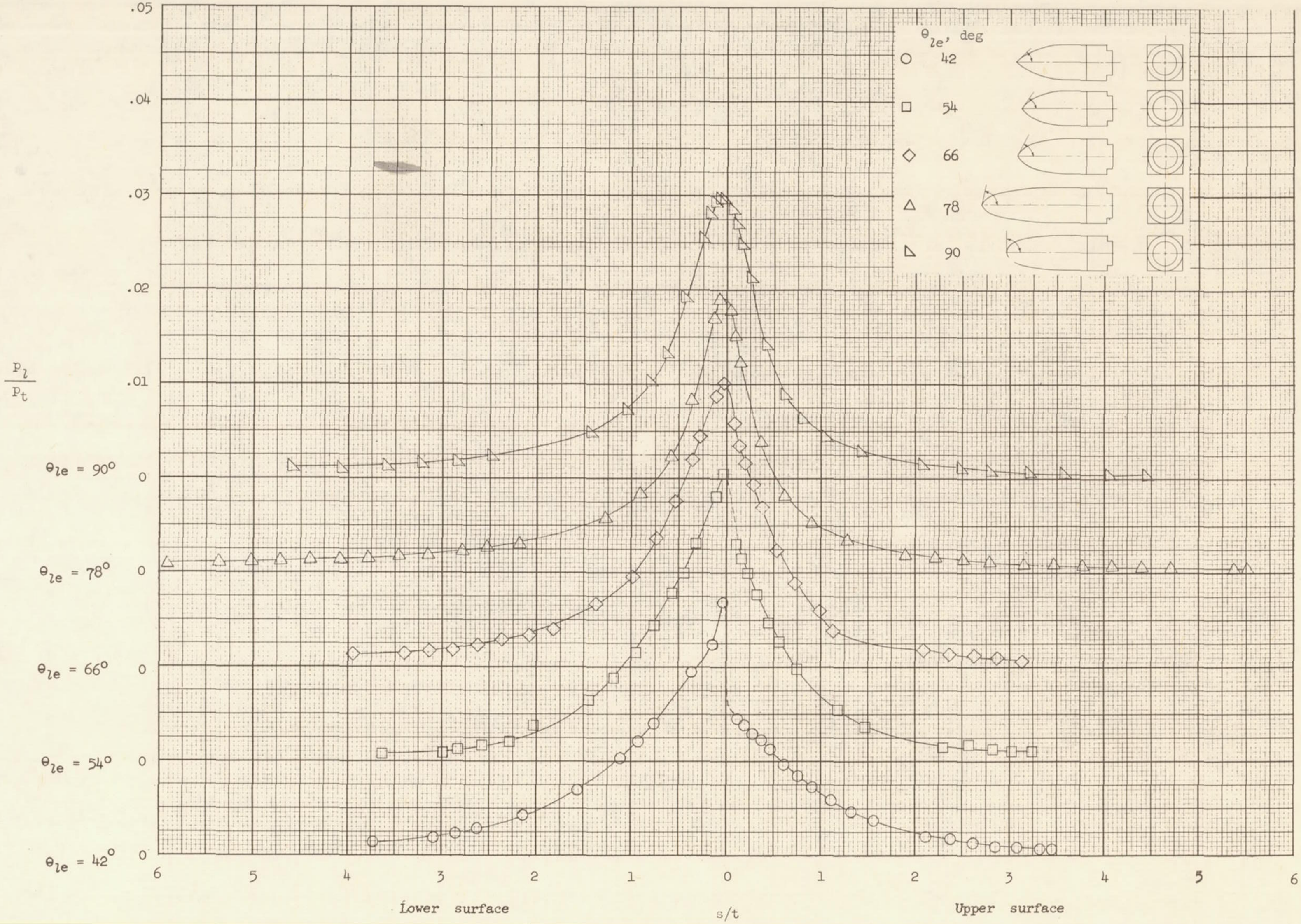

(b) $\alpha = 5^\circ$.

Figure 6.- Continued.

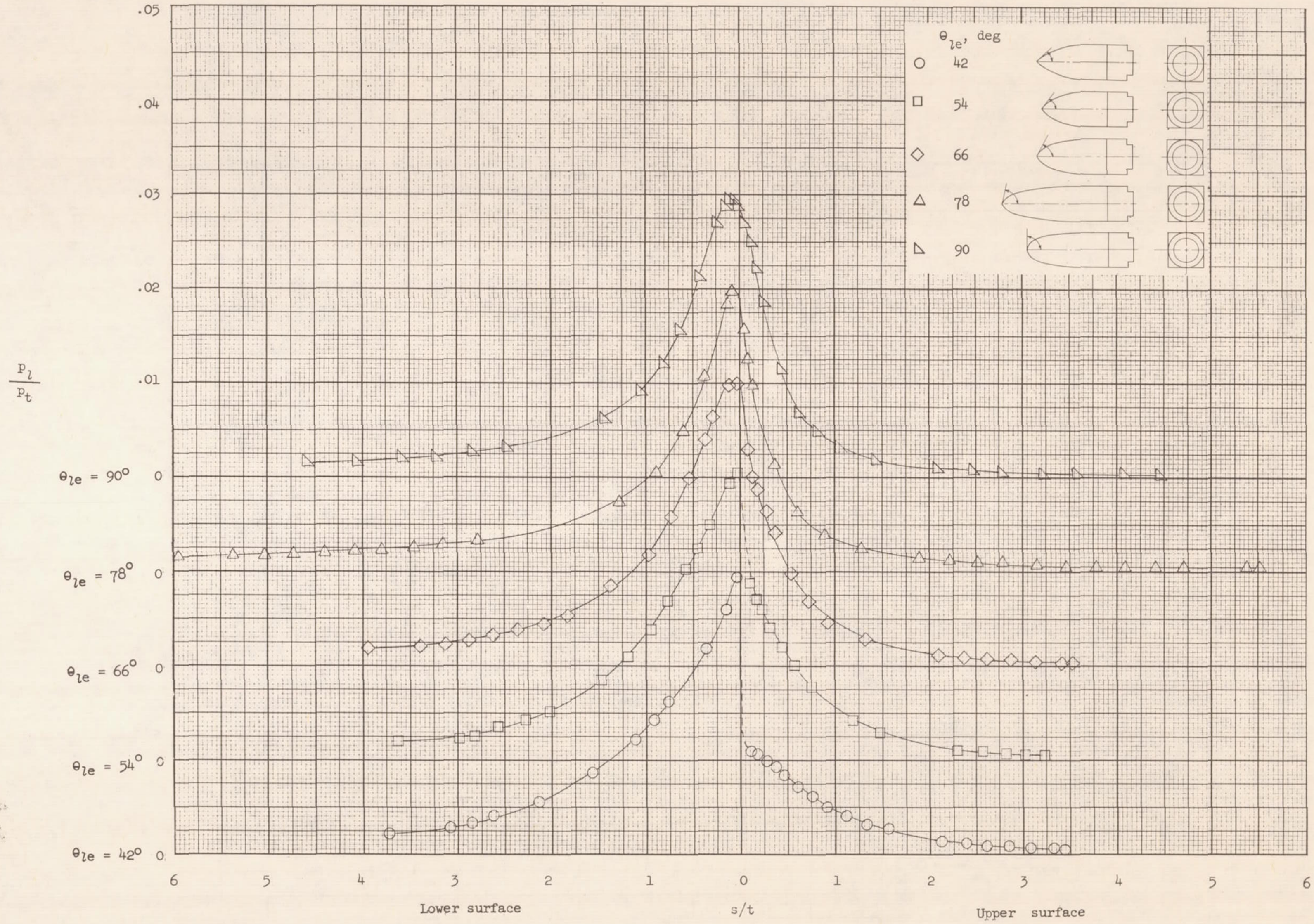

(c) $\alpha = 10^{\circ}$.

Figure 6.- Continued.

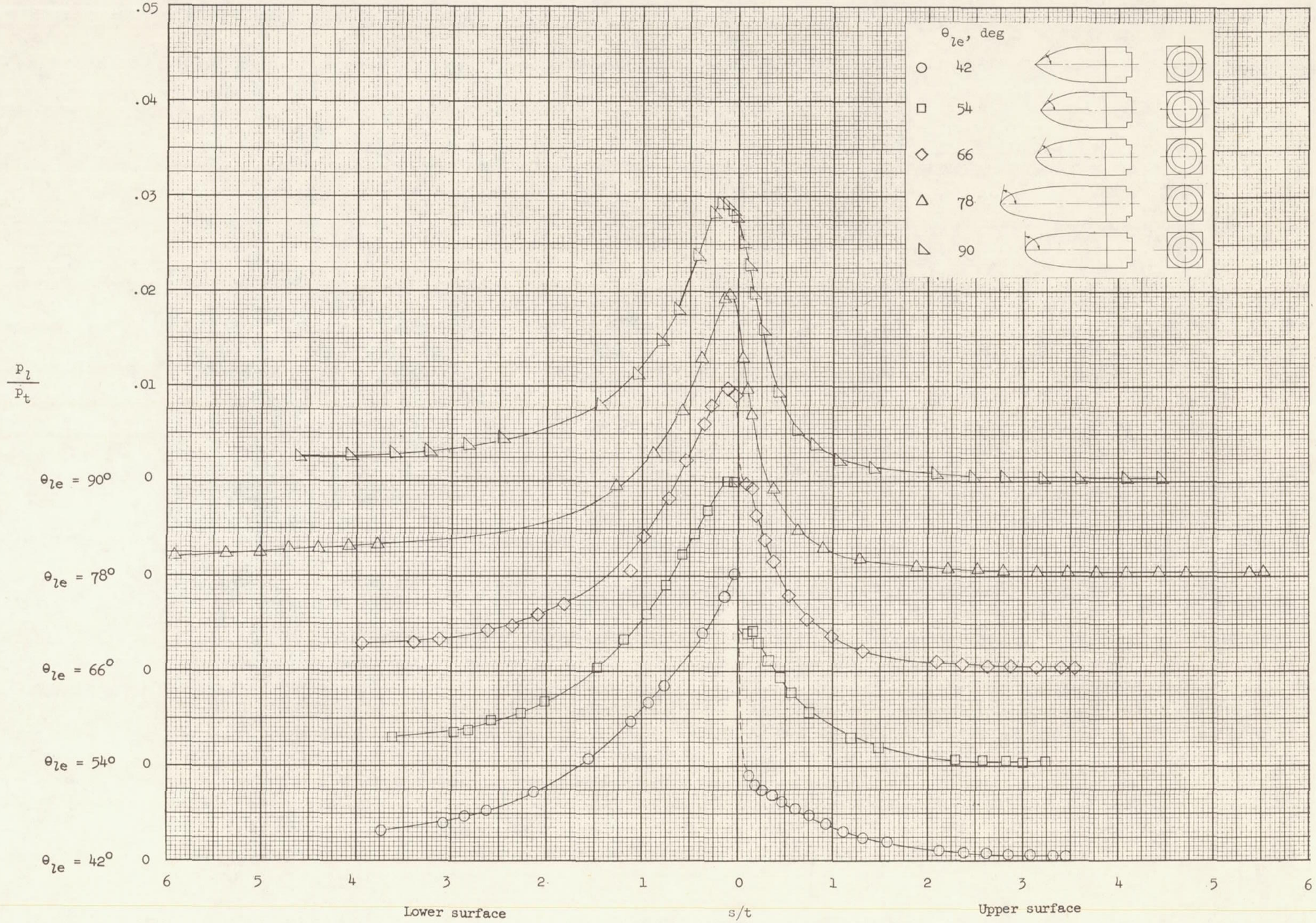

(d) $\alpha = 15^{\circ}$.

Figure 6.- Continued.

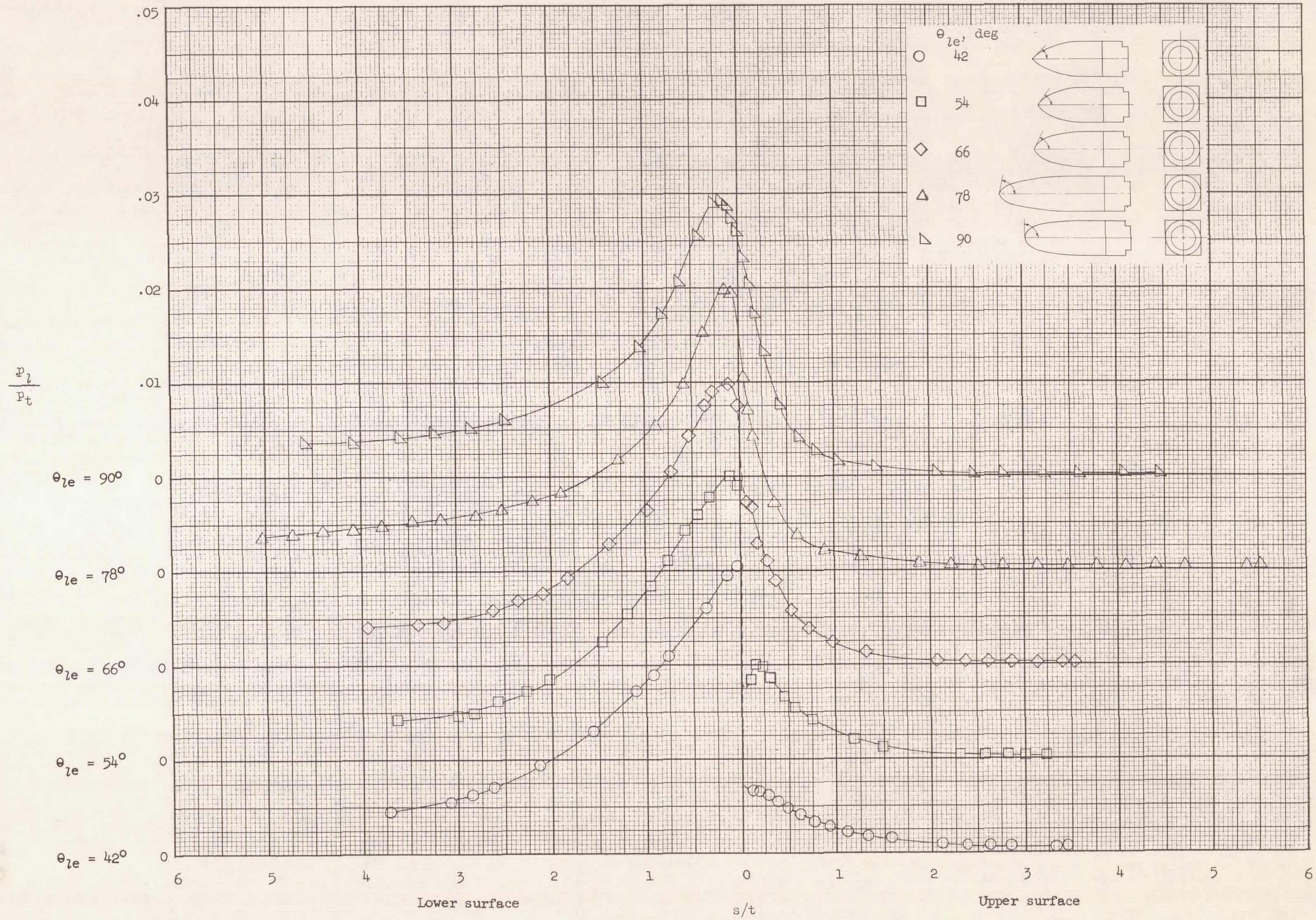

(e) $\alpha = 20^\circ$.

Figure 6.- Continued.

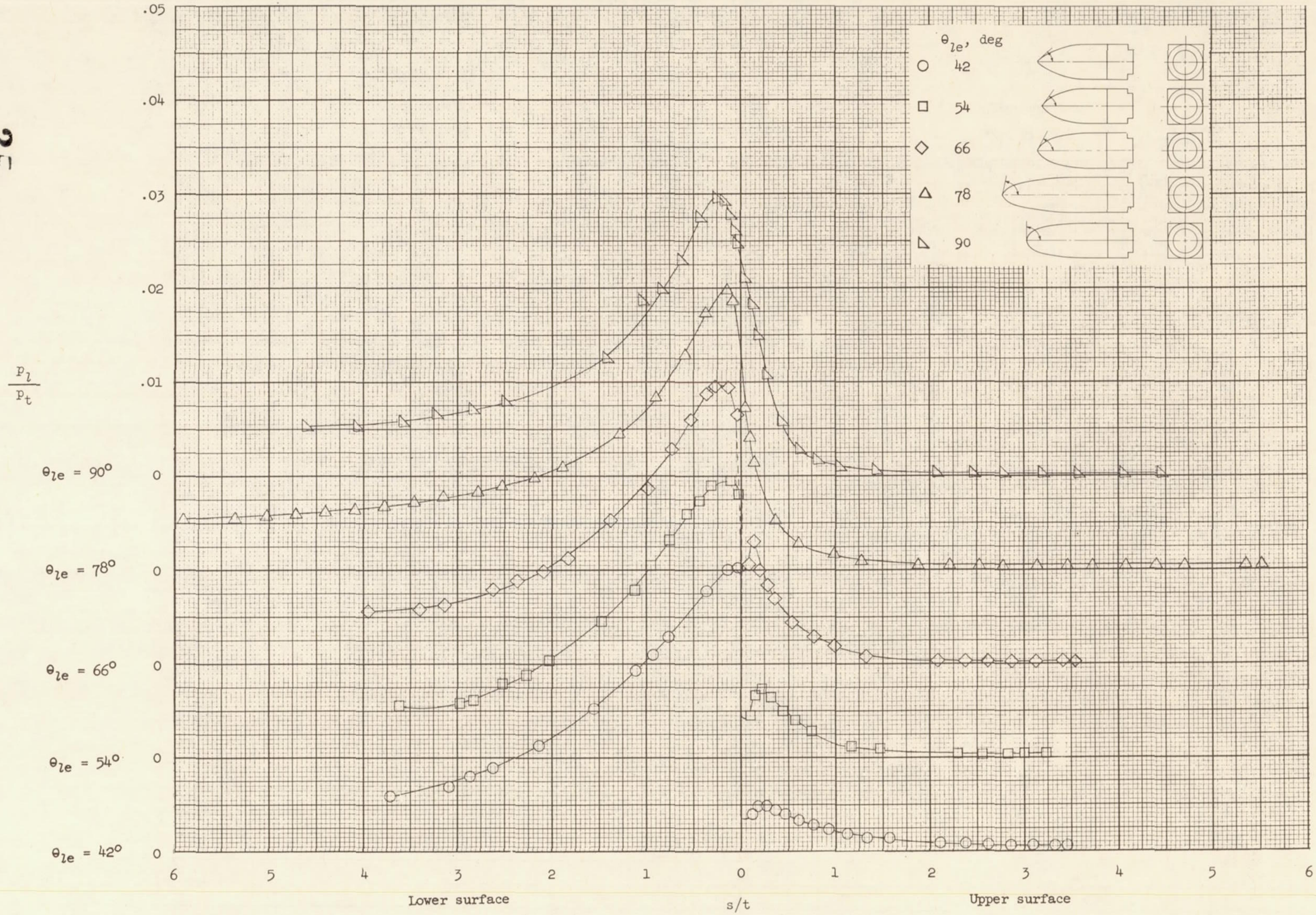

(f) $\alpha = 25^{\circ}$.

Figure 6.- Concluded.

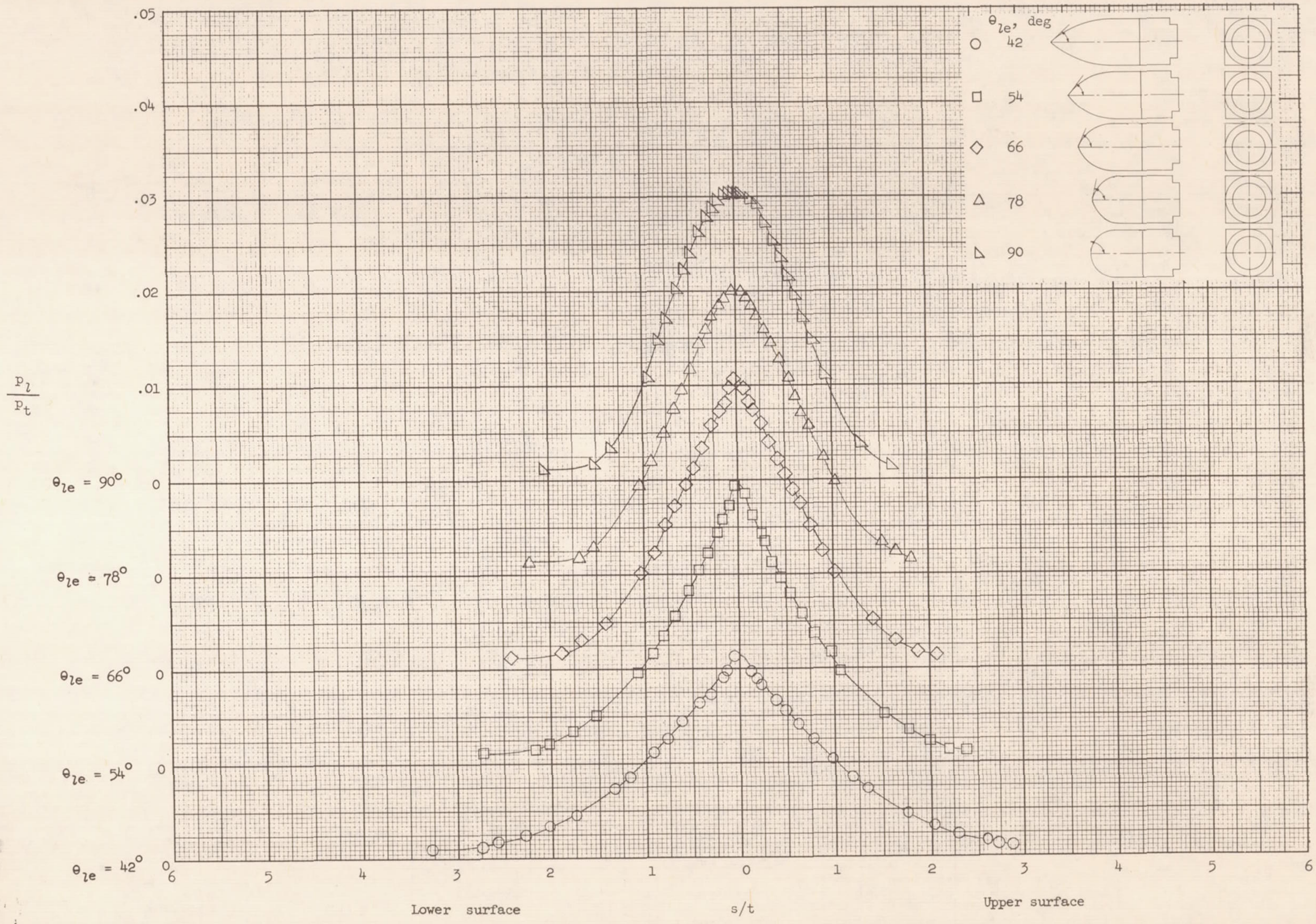

(a) $\alpha = 0^\circ$.

Figure 7.- Pressure distributions of two-dimensional circular arcs.

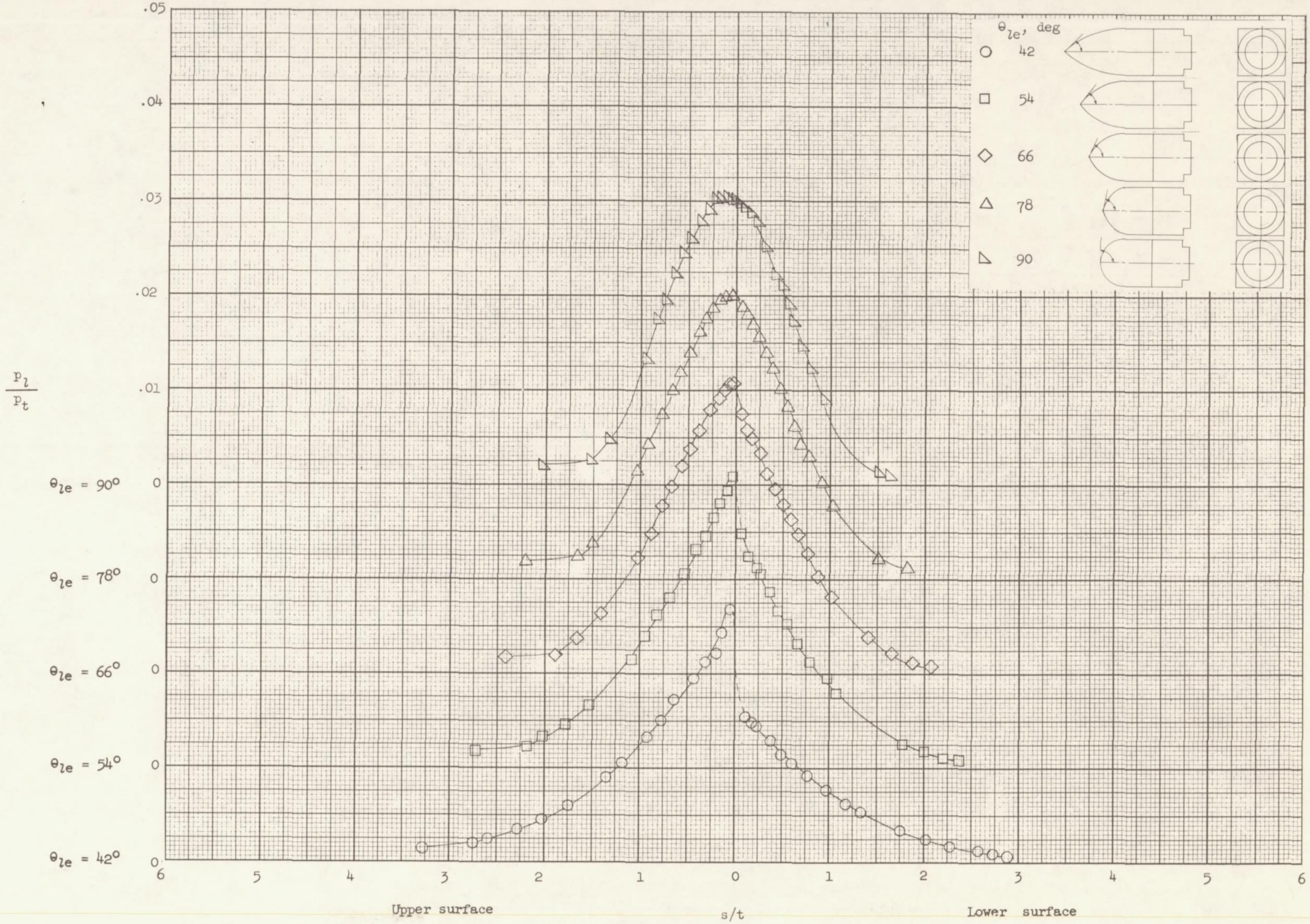

(b) $\alpha = 5^\circ$.

Figure 7.- Continued.

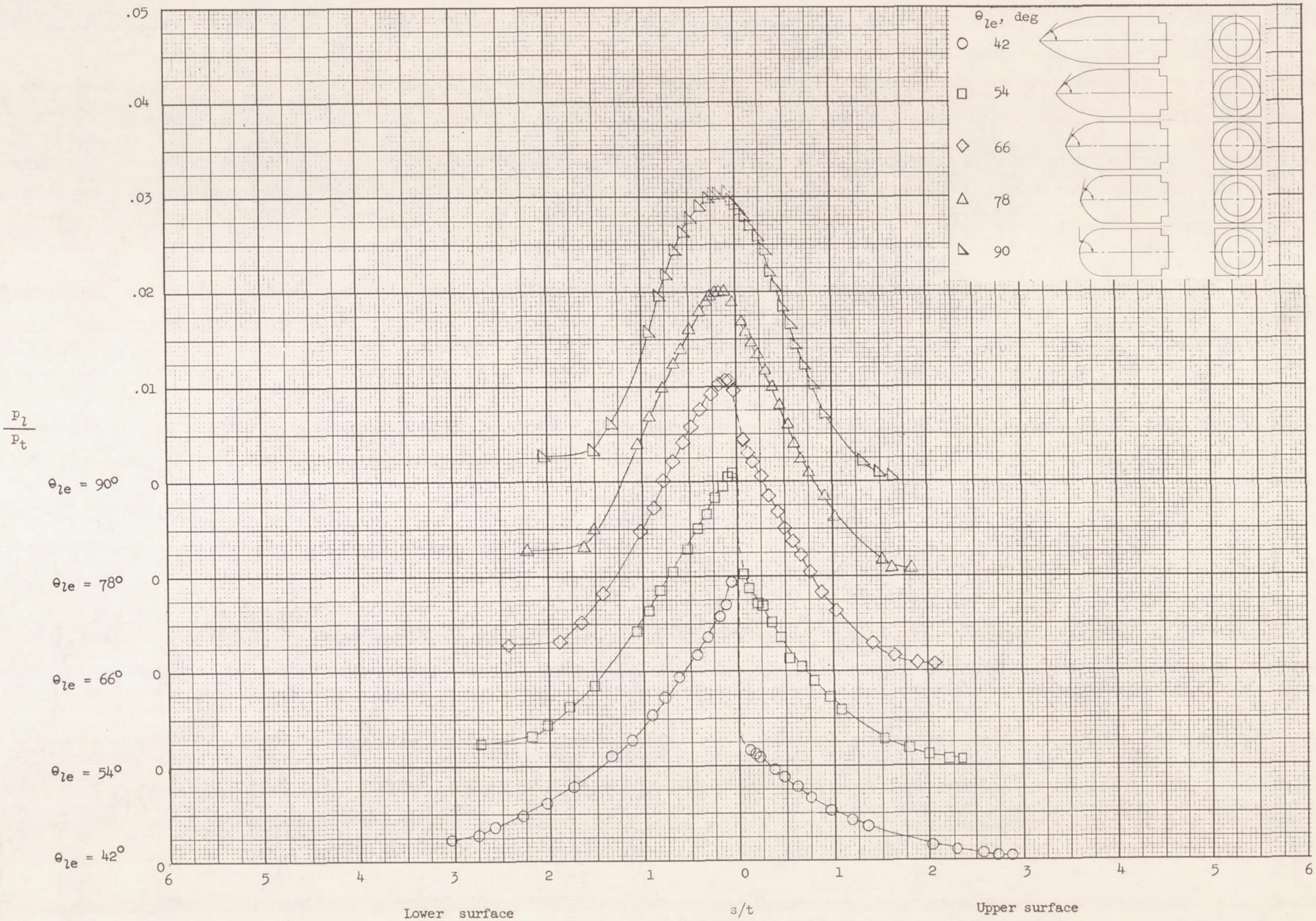

(c) $\alpha = 10^{\circ}$.

Figure 7.- Continued.

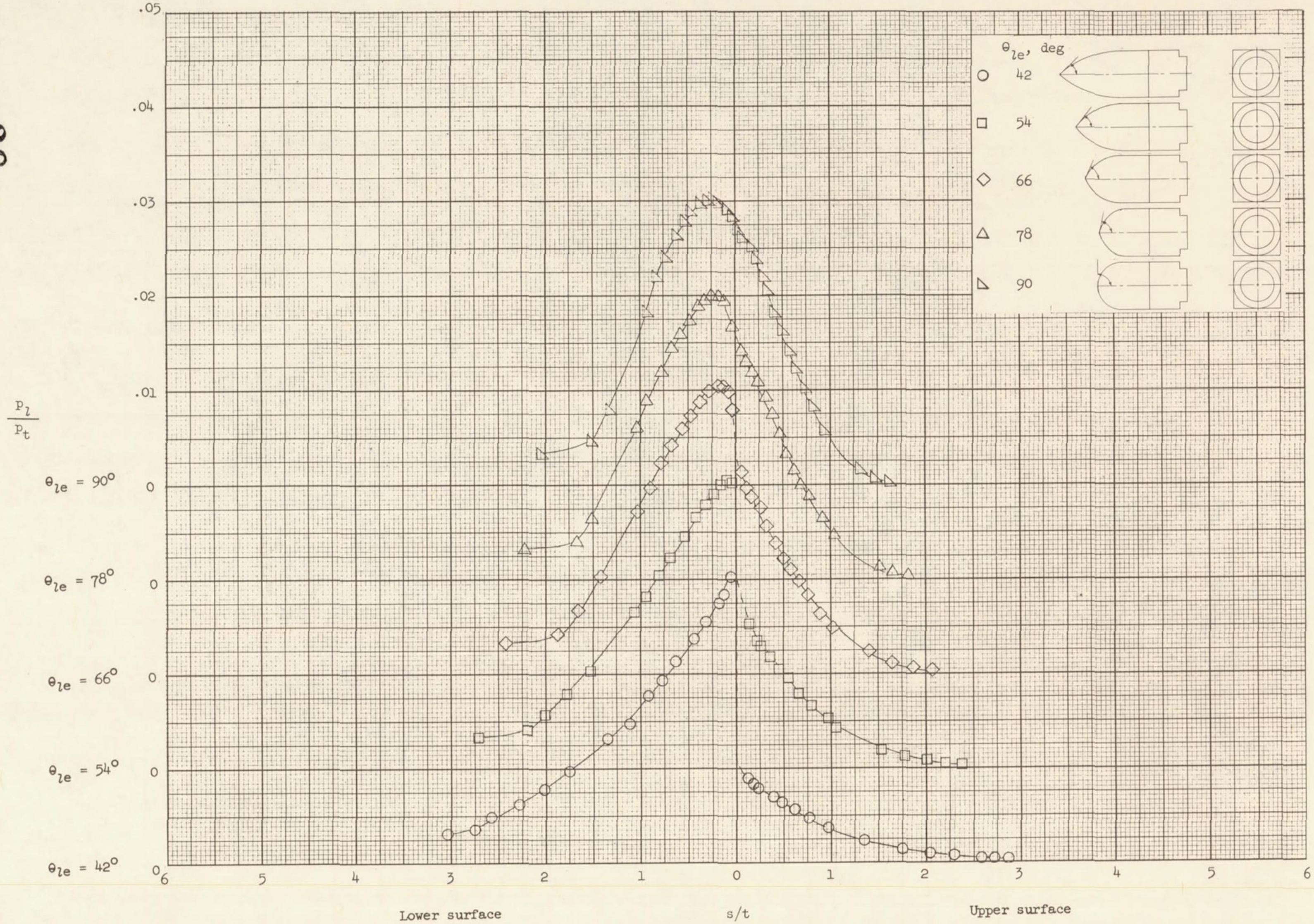

(d) $\alpha = 15^{\circ}$.

Figure 7.- Continued.

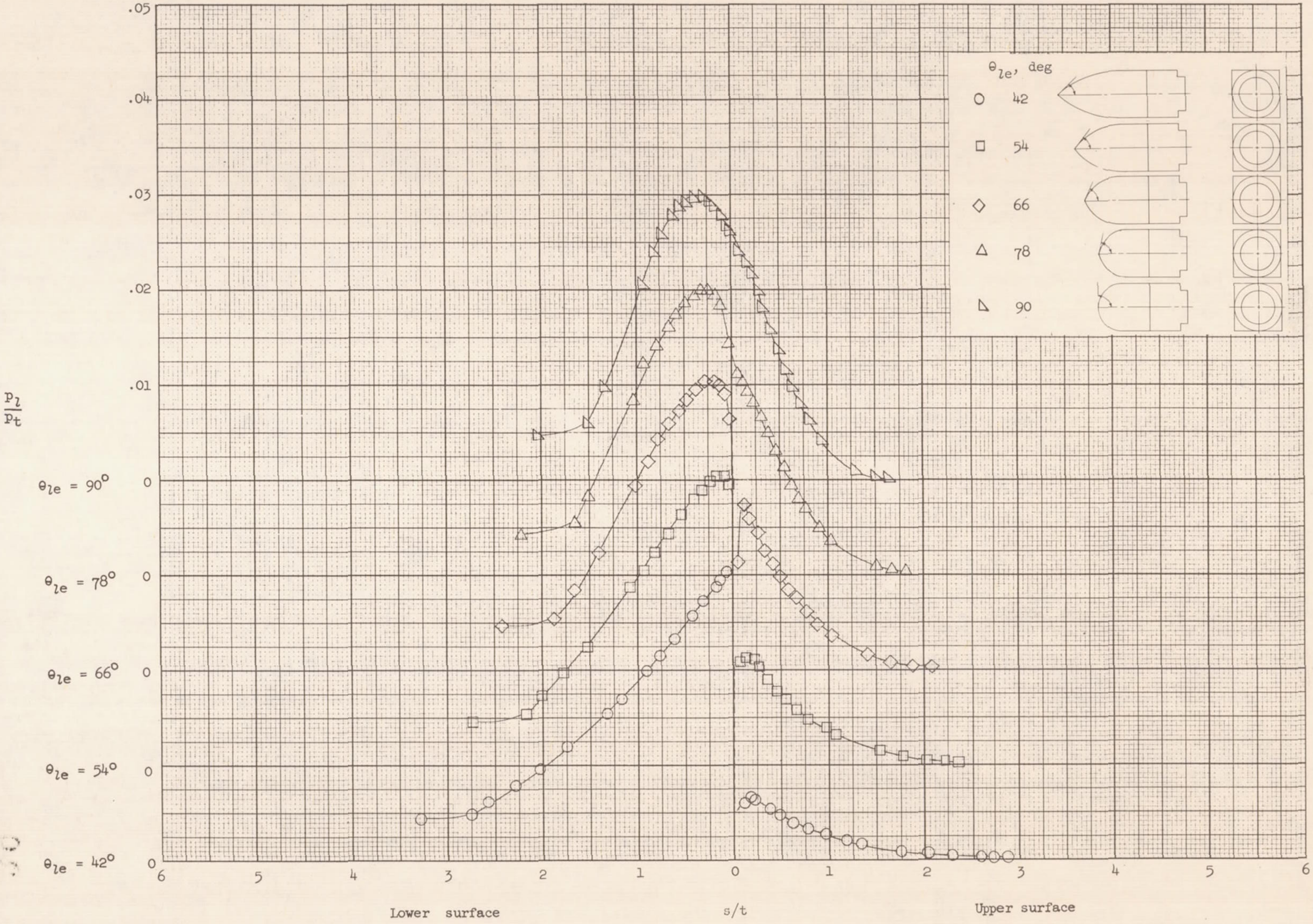

(e) $\alpha = 20^{\circ}$.

Figure 7.- Continued.

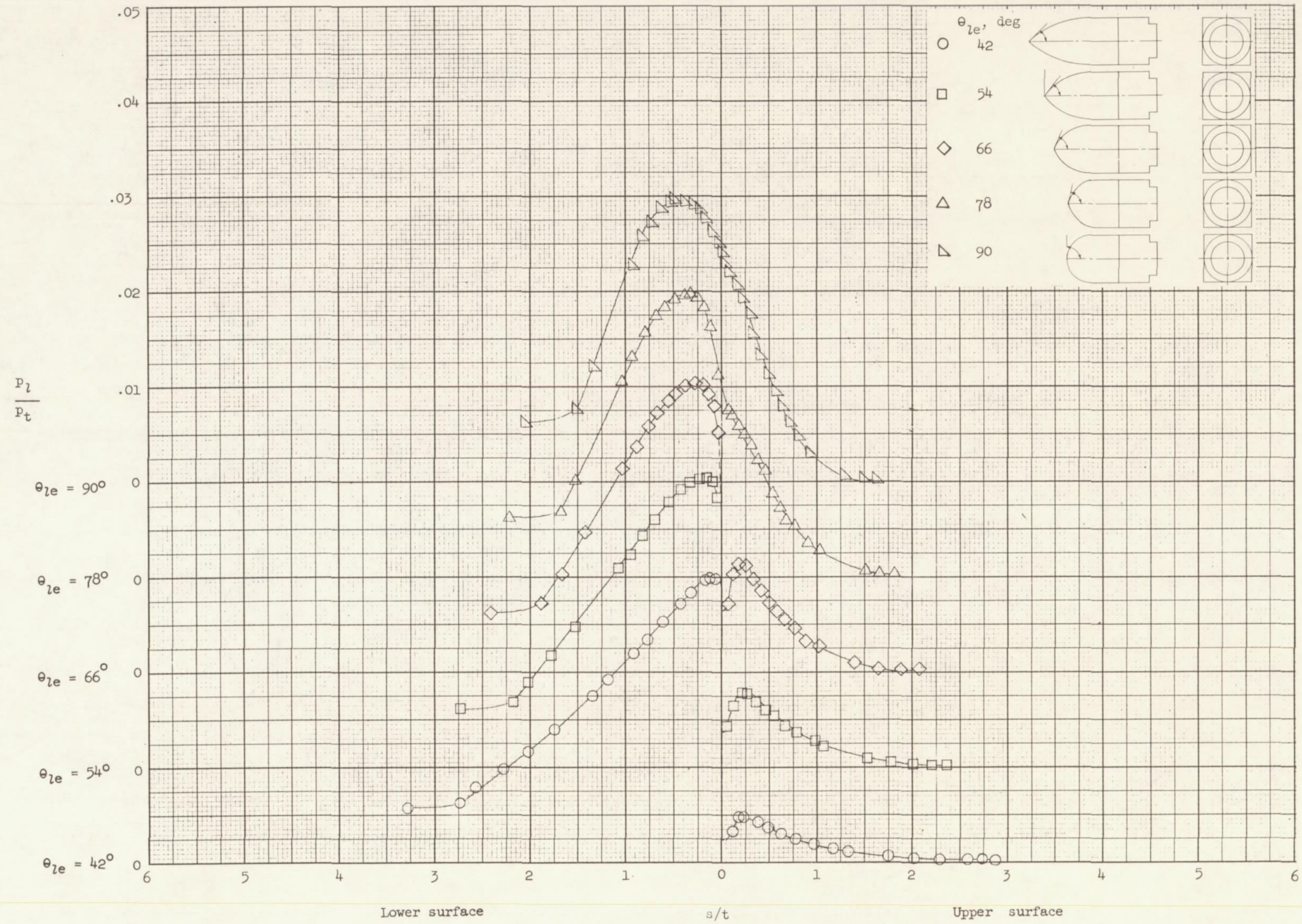

(f) $\alpha = 25^{\circ}$.

Figure 7.- Concluded.

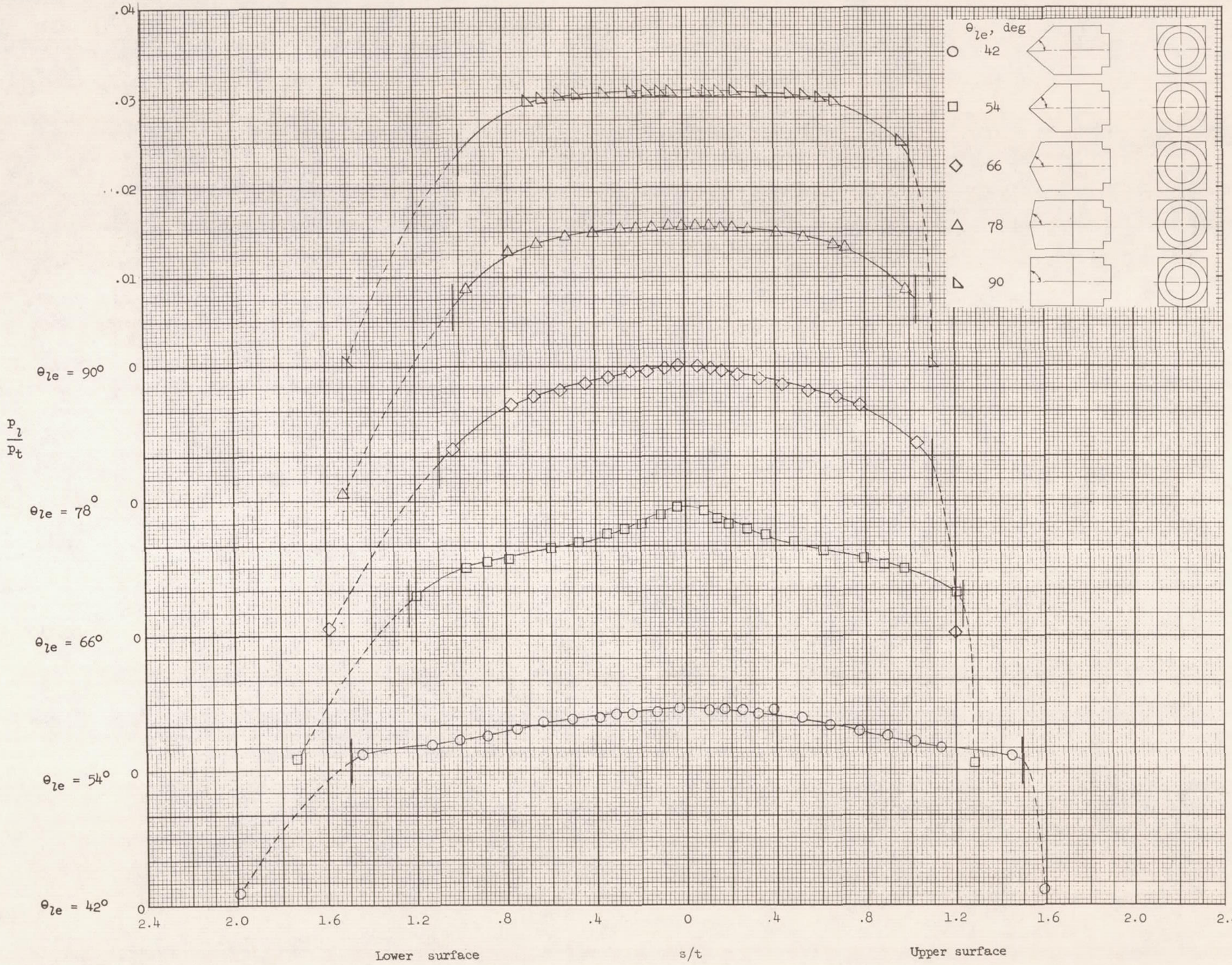

(a) $\alpha = 0^\circ$.

Figure 8.- Pressure distributions of wedges.

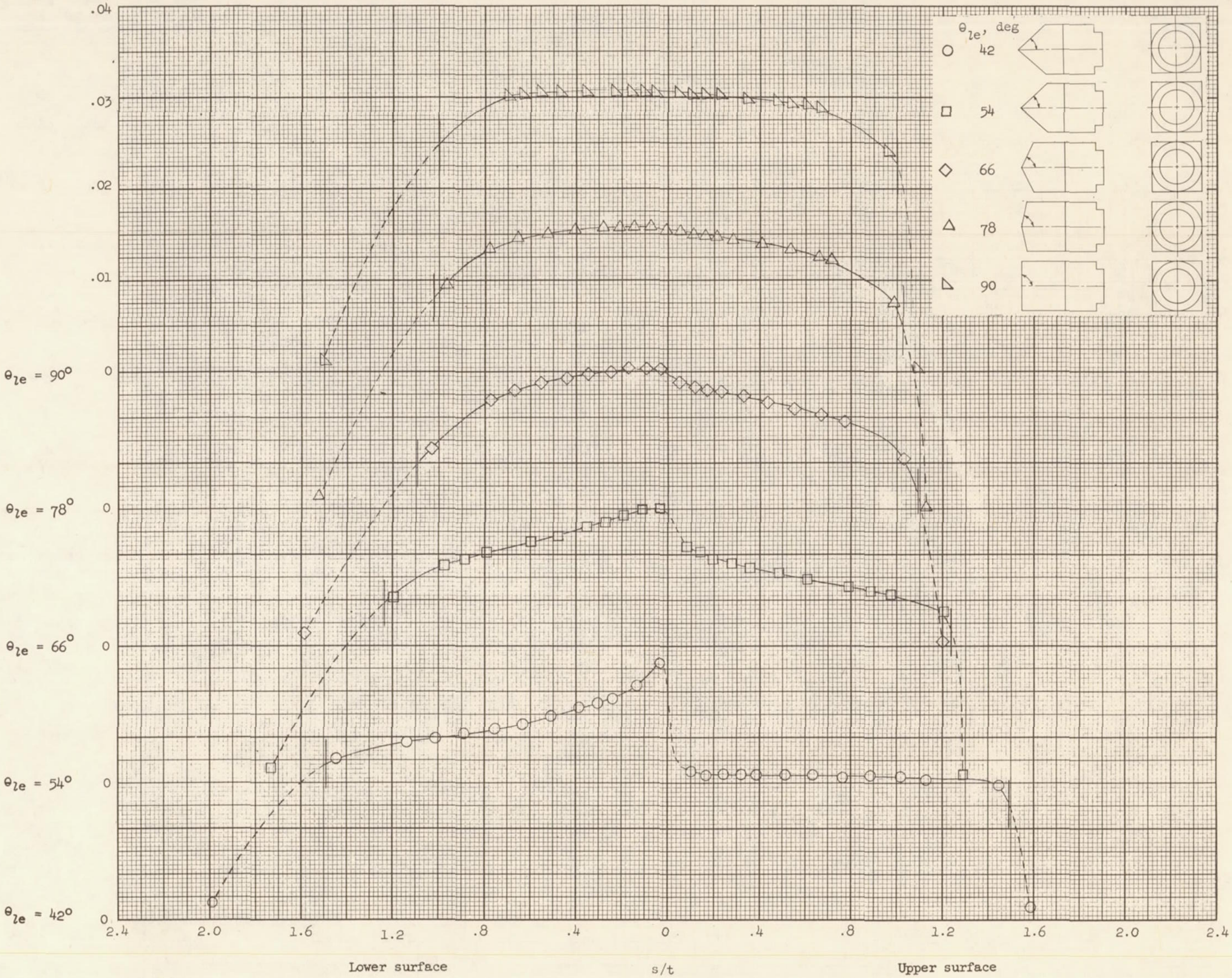

(b) $\alpha = 5^{\circ}$.

Figure 8.- Continued.

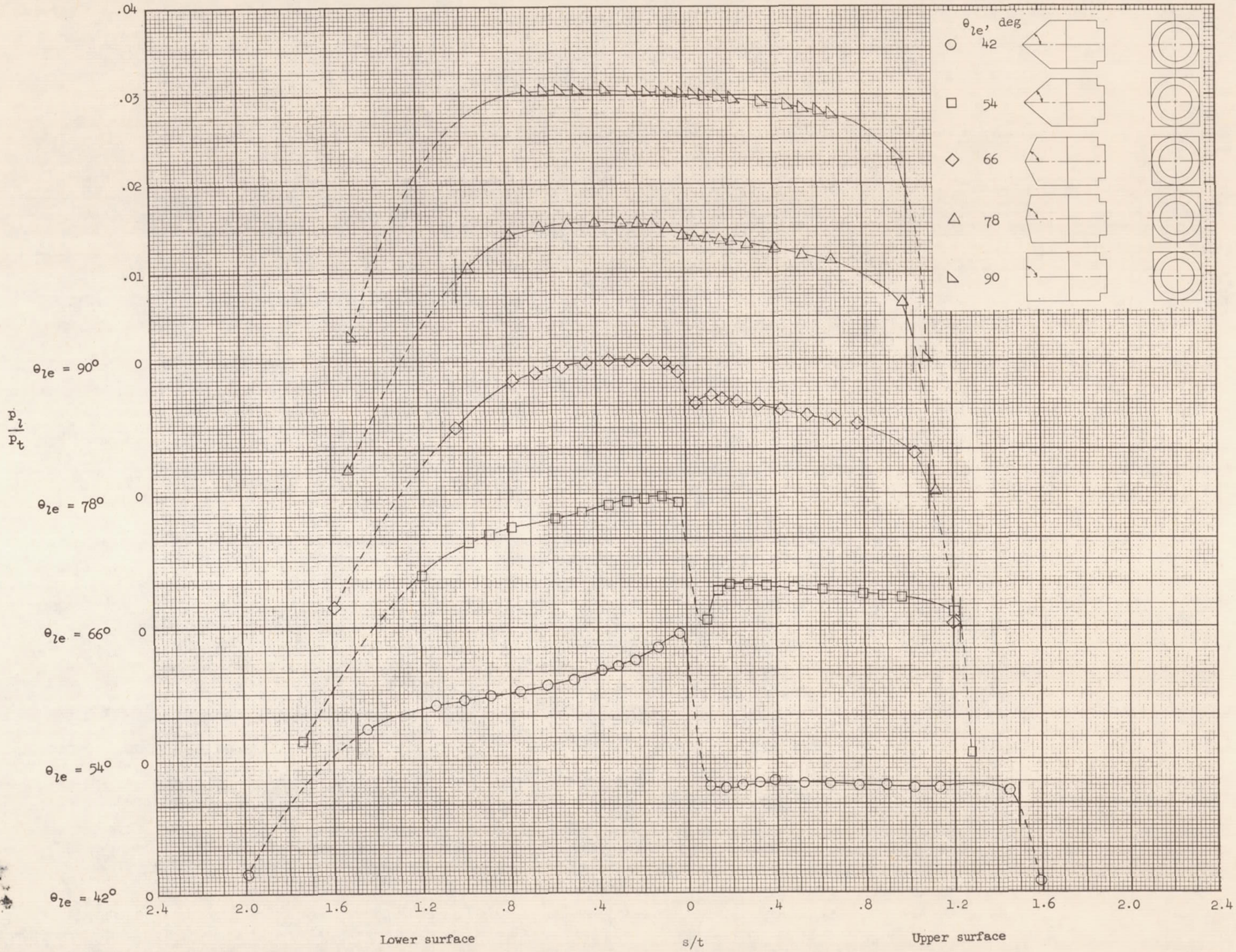

(c) $\alpha = 10^{\circ}$.

Figure 8.- Continued.

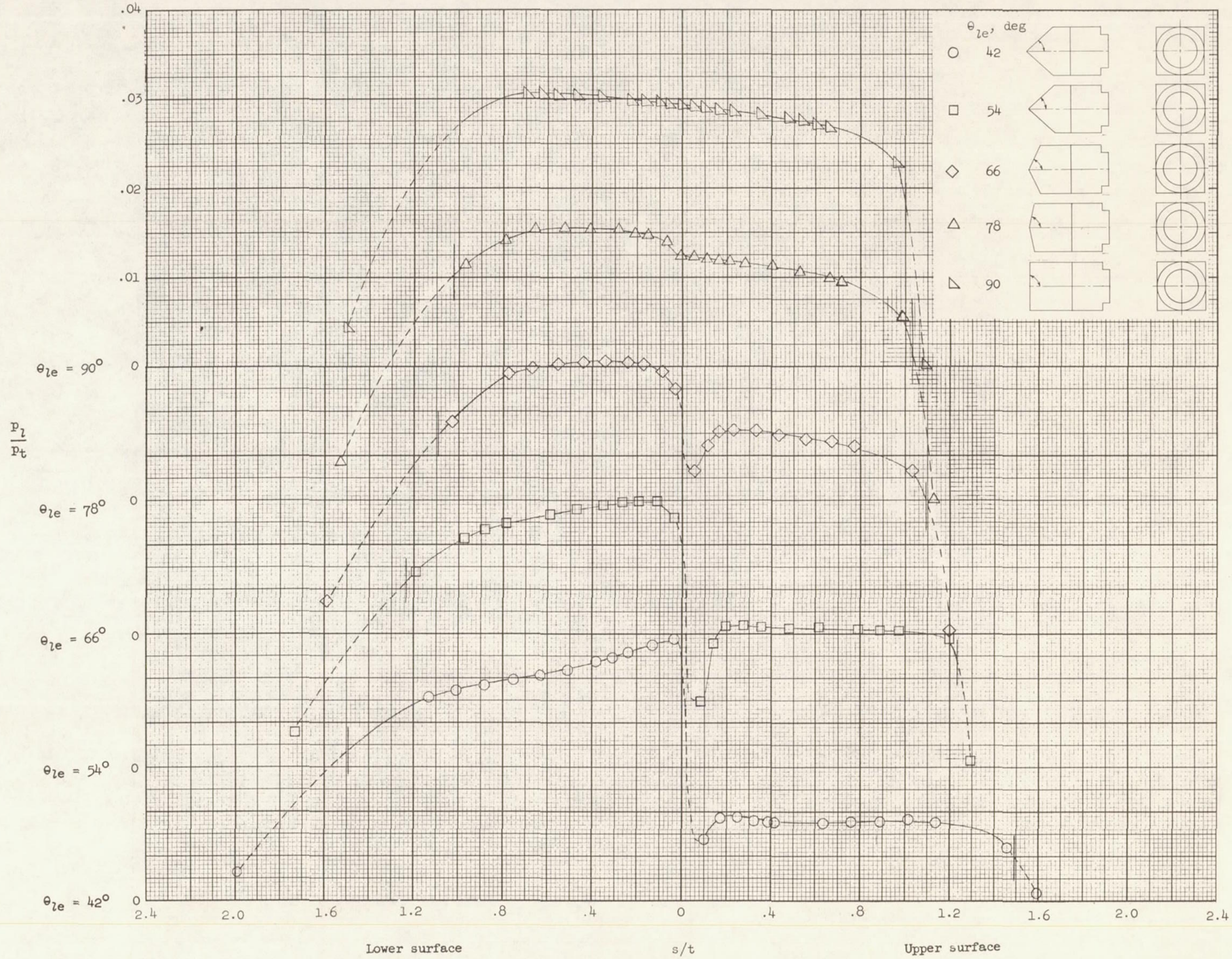

(d) $\alpha = 15^{\circ}$.

Figure 8.- Continued.

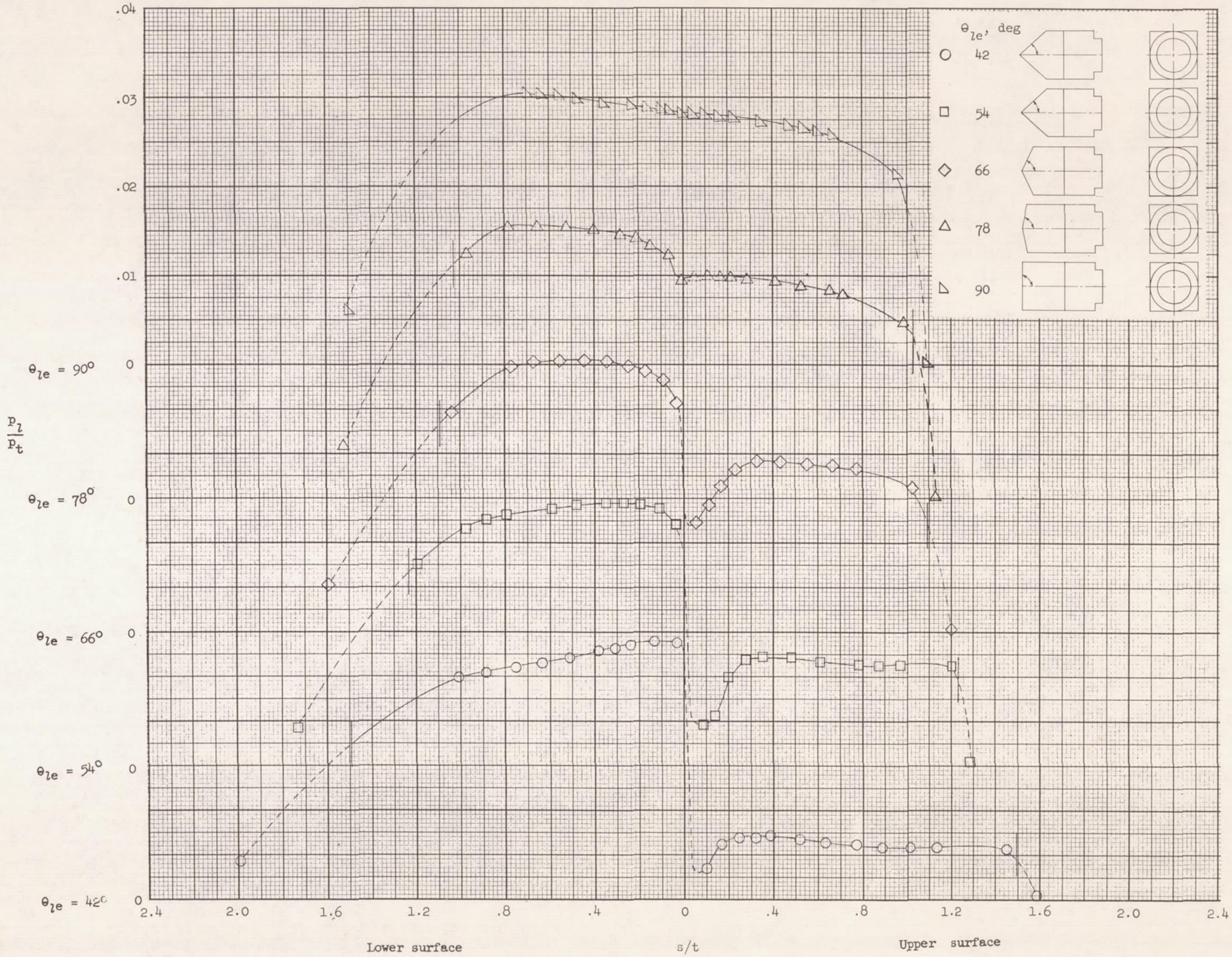

(e) $\alpha = 20^{\circ}$.

Figure 8.- Continued.

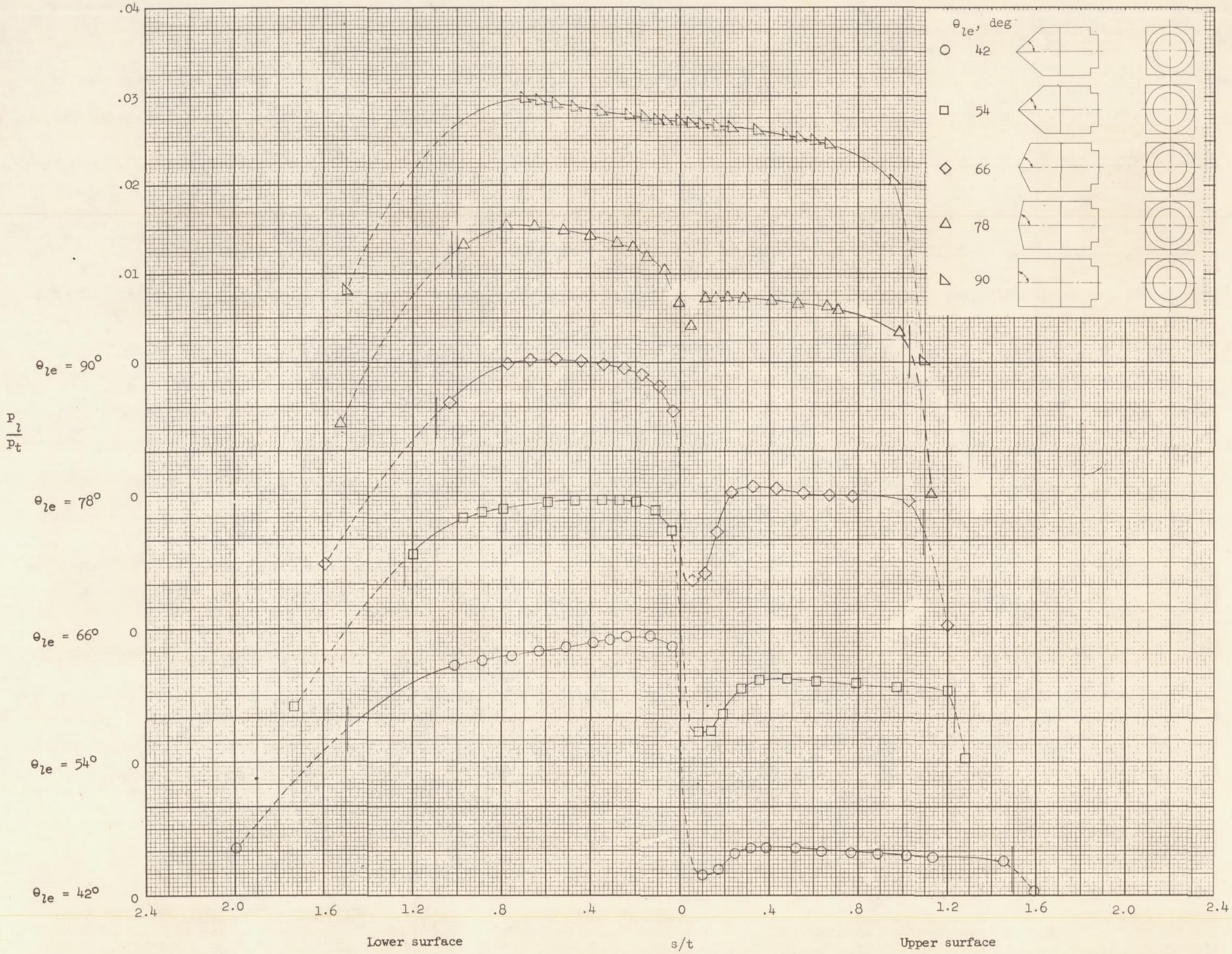

(f) $\alpha = 25^{\circ}$.

Figure 8.- Concluded.

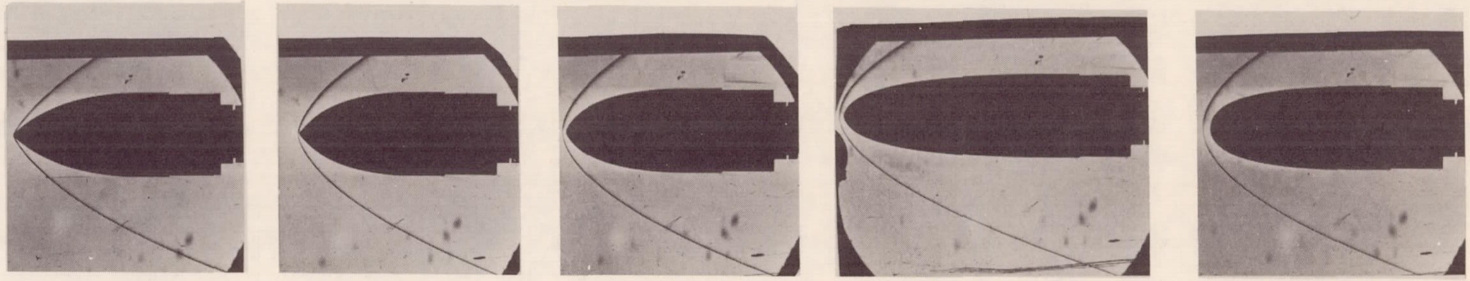

$\theta_{le} = 42^{\circ}$ $\theta_{le} = 54^{\circ}$ $\theta_{le} = 66^{\circ}$ $\theta_{le} = 78^{\circ}$ $\theta_{le} = 90^{\circ}$

(a) Parabolic arc models.

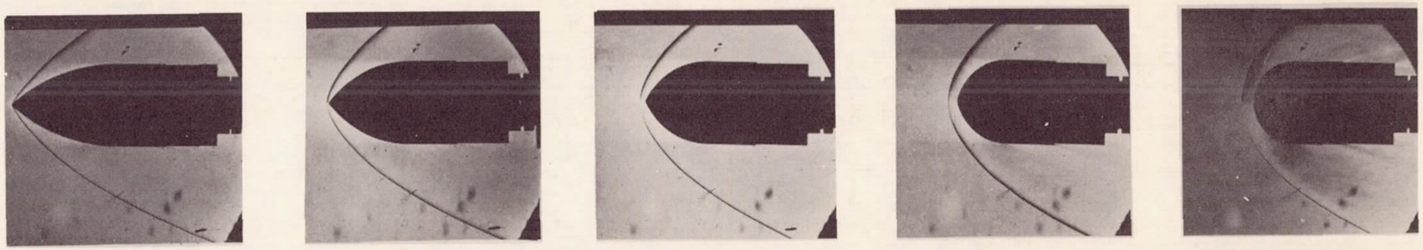

$\theta_{le} = 42^{\circ}$ $\theta_{le} = 54^{\circ}$ $\theta_{le} = 66^{\circ}$ $\theta_{le} = 78^{\circ}$ $\theta_{le} = 90^{\circ}$

(b) Circular arc models.

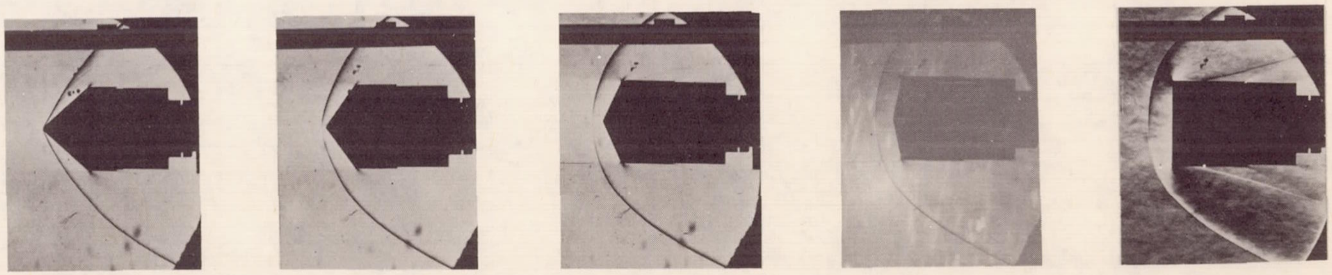

$\theta_{le} = 42^{\circ}$ $\theta_{le} = 54^{\circ}$ $\theta_{le} = 66^{\circ}$ $\theta_{le} = 78^{\circ}$ $\theta_{le} = 90^{\circ}$

(c) Wedge models.

L-63-82

Figure 9.- Schlieren photographs of aerodynamically blunt bodies near 0° angle of attack.

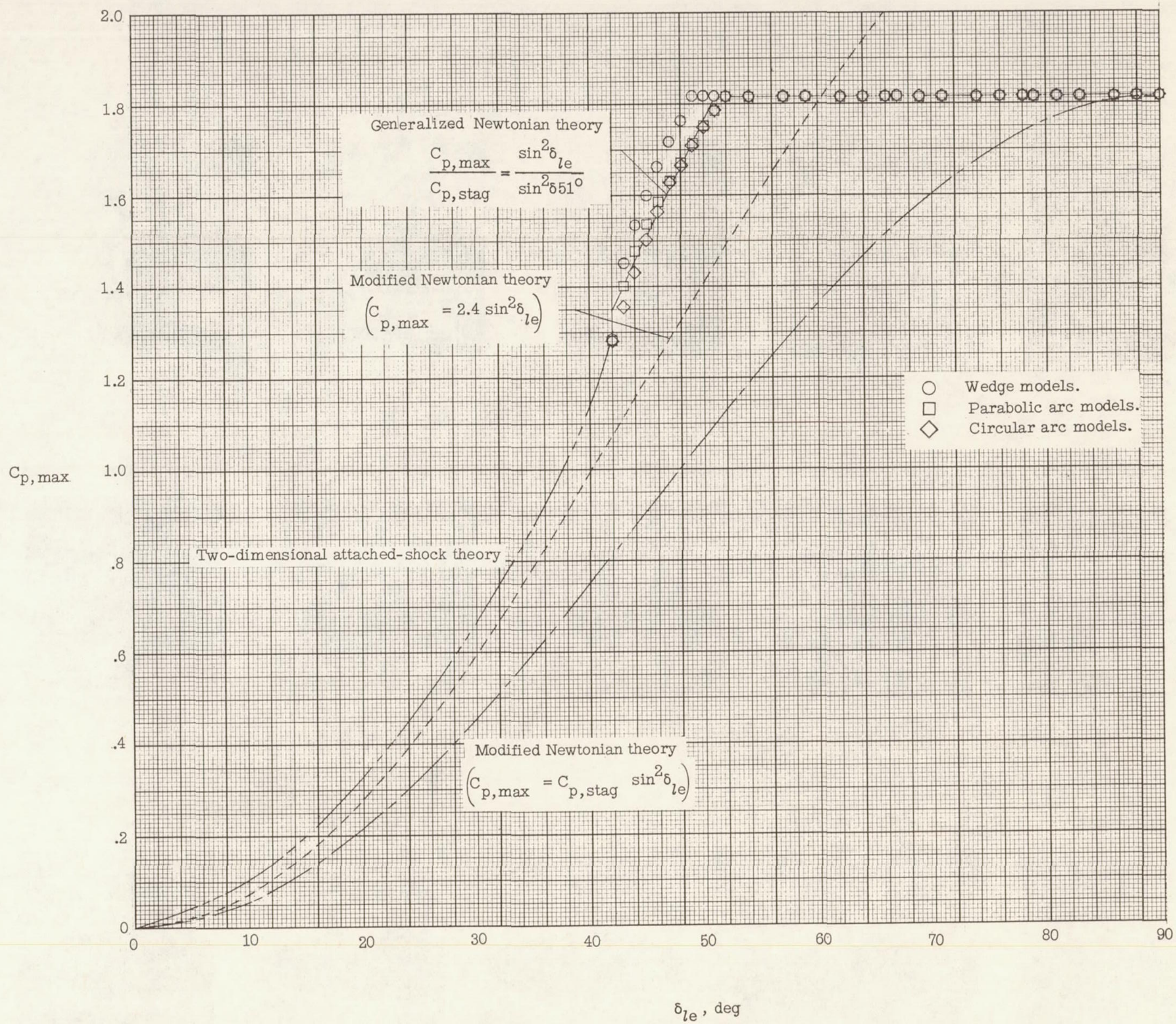

Figure 10.- Comparison of measured and predicted pressure coefficients on the lower surface for aerodynamically blunt bodies.

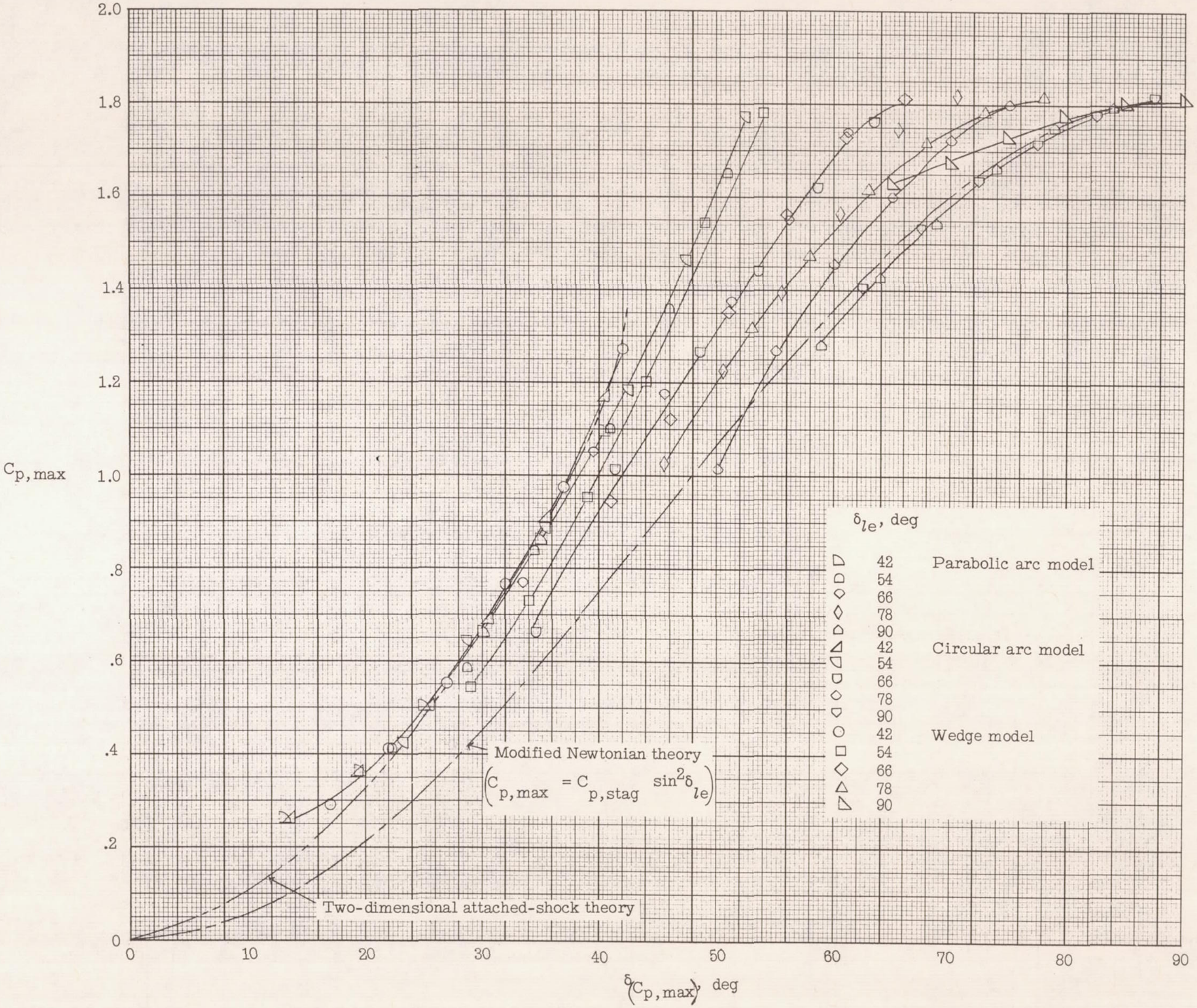

Figure 11.- Comparison [illegible]easured and predicted maximum pressure coefficients on the upper surface for aerodynamically blunt bodies.

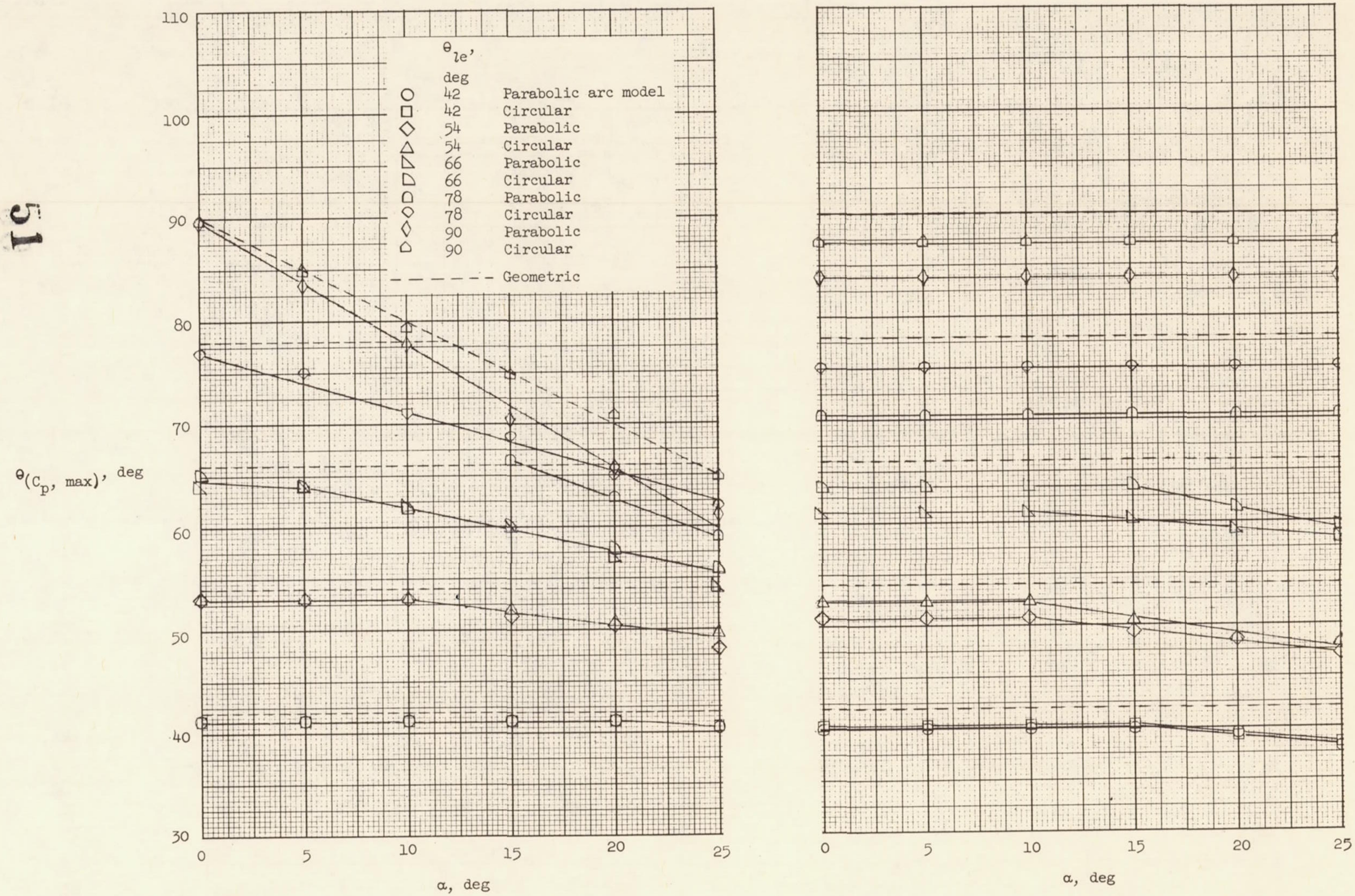

(a) Lower surface

(b) Upper surface

Figure 12.- Comparison of geometric and measured slopes at which maximum pressure occurred for various angles of attack on the parabolic and circular arc bodies.

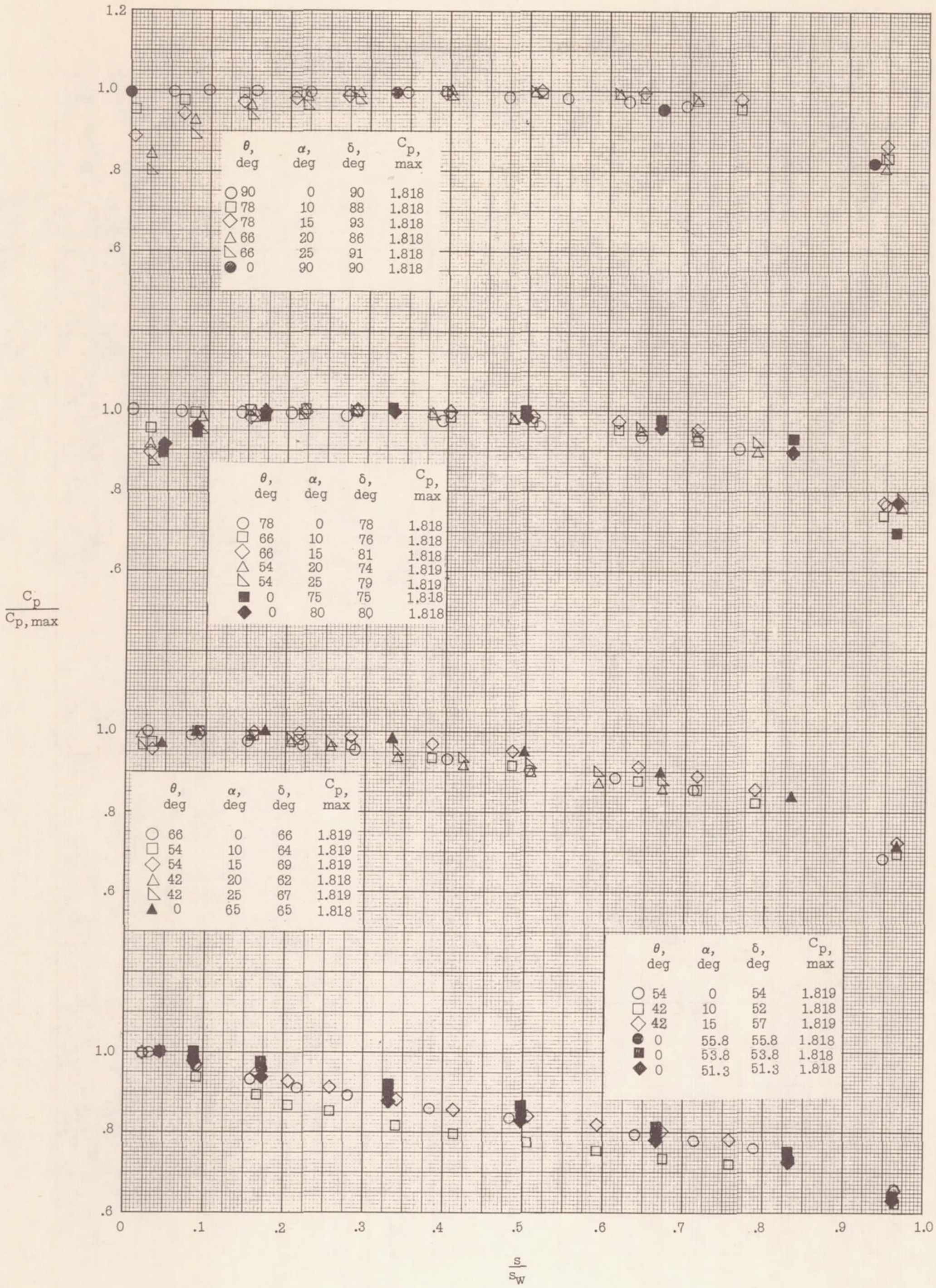

(a) Lower surface.

Figure 13.- Comparison of pressure distributions on wedges with constant deflection angles. Solid symbols are for flat-plate data at approximately the same deflection angles (ref. 2).

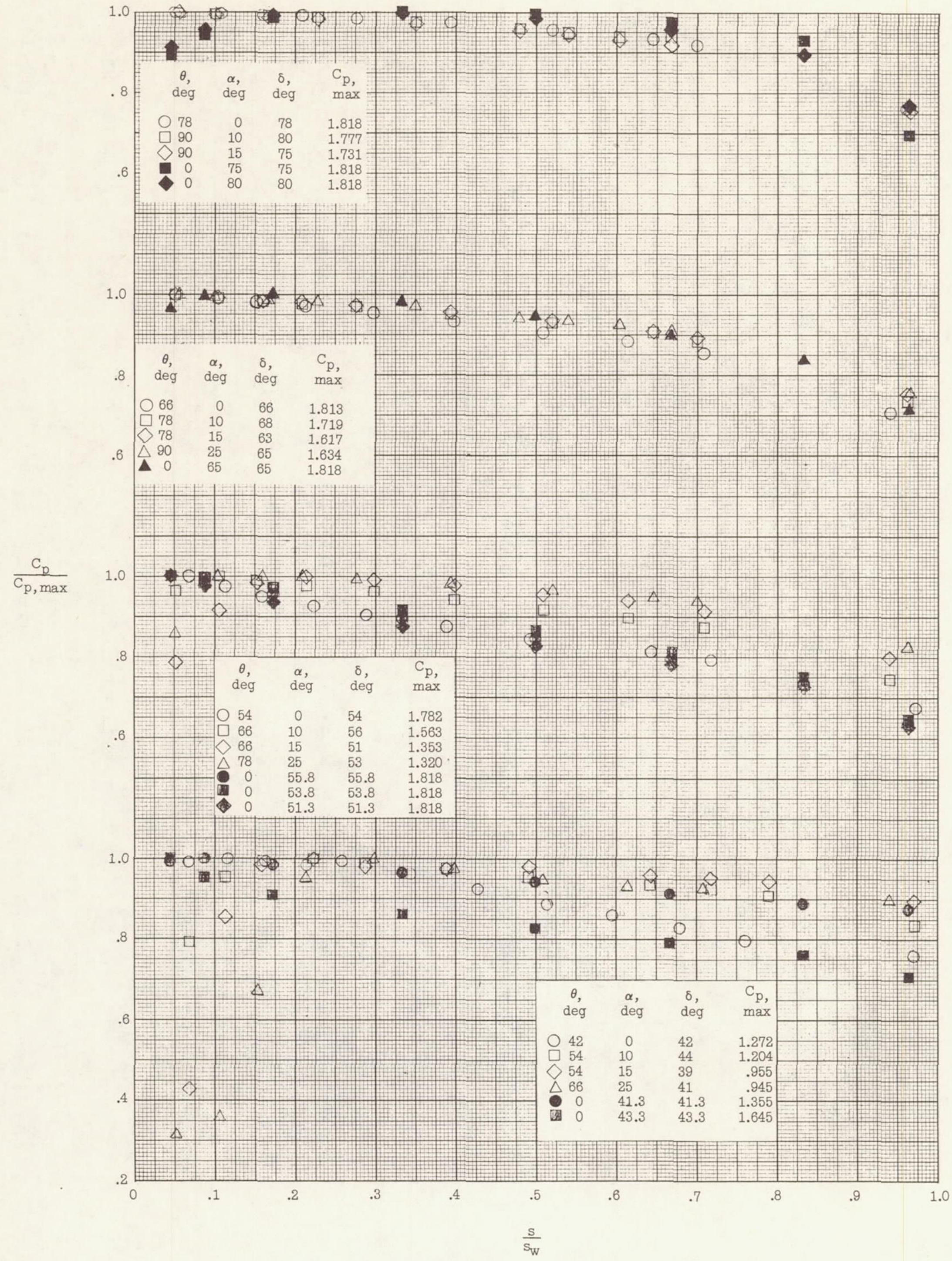

(b) Upper surface.

Figure 13.- Continued.

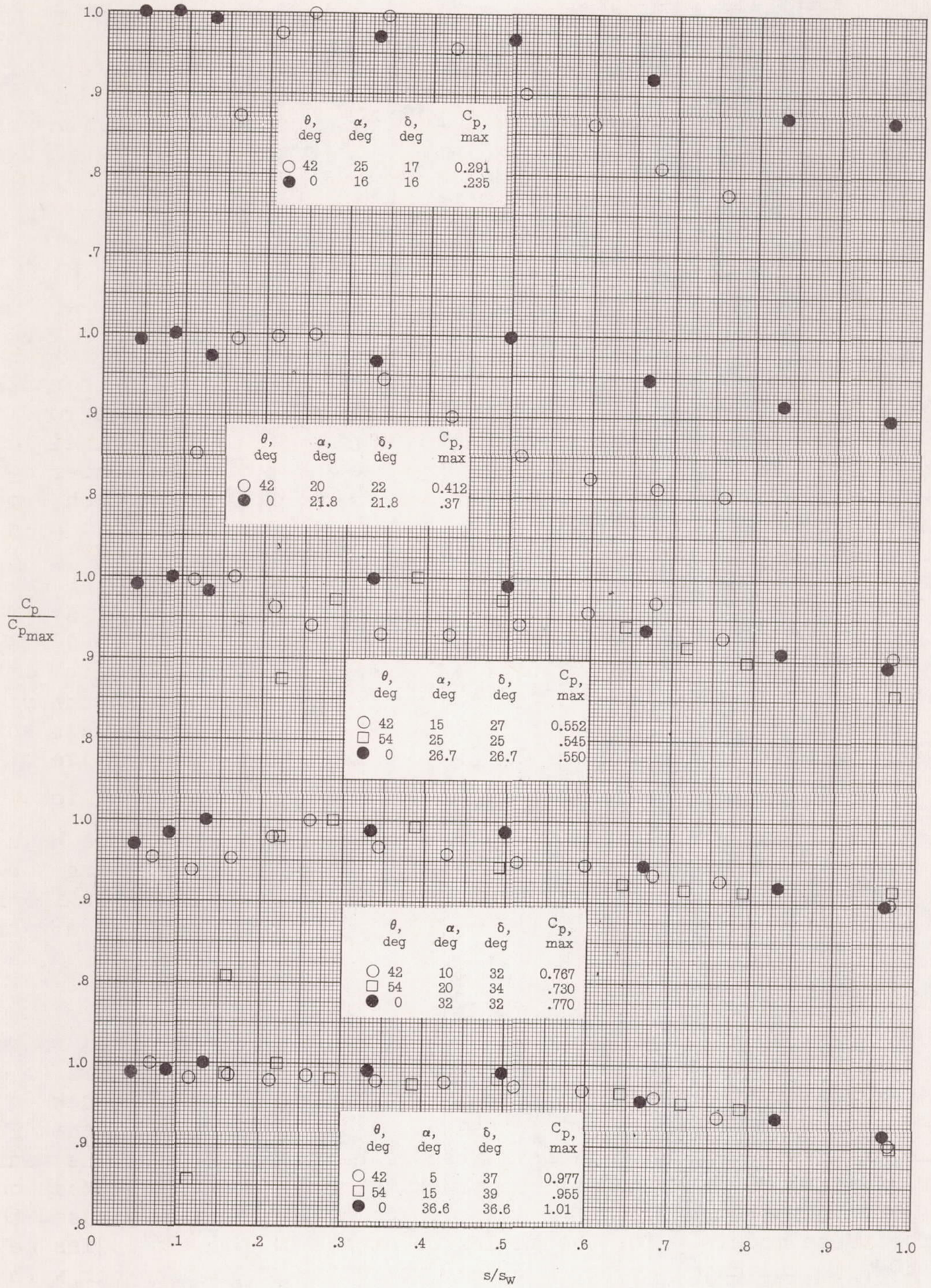

(b) Concluded.

Figure 13.- Concluded.

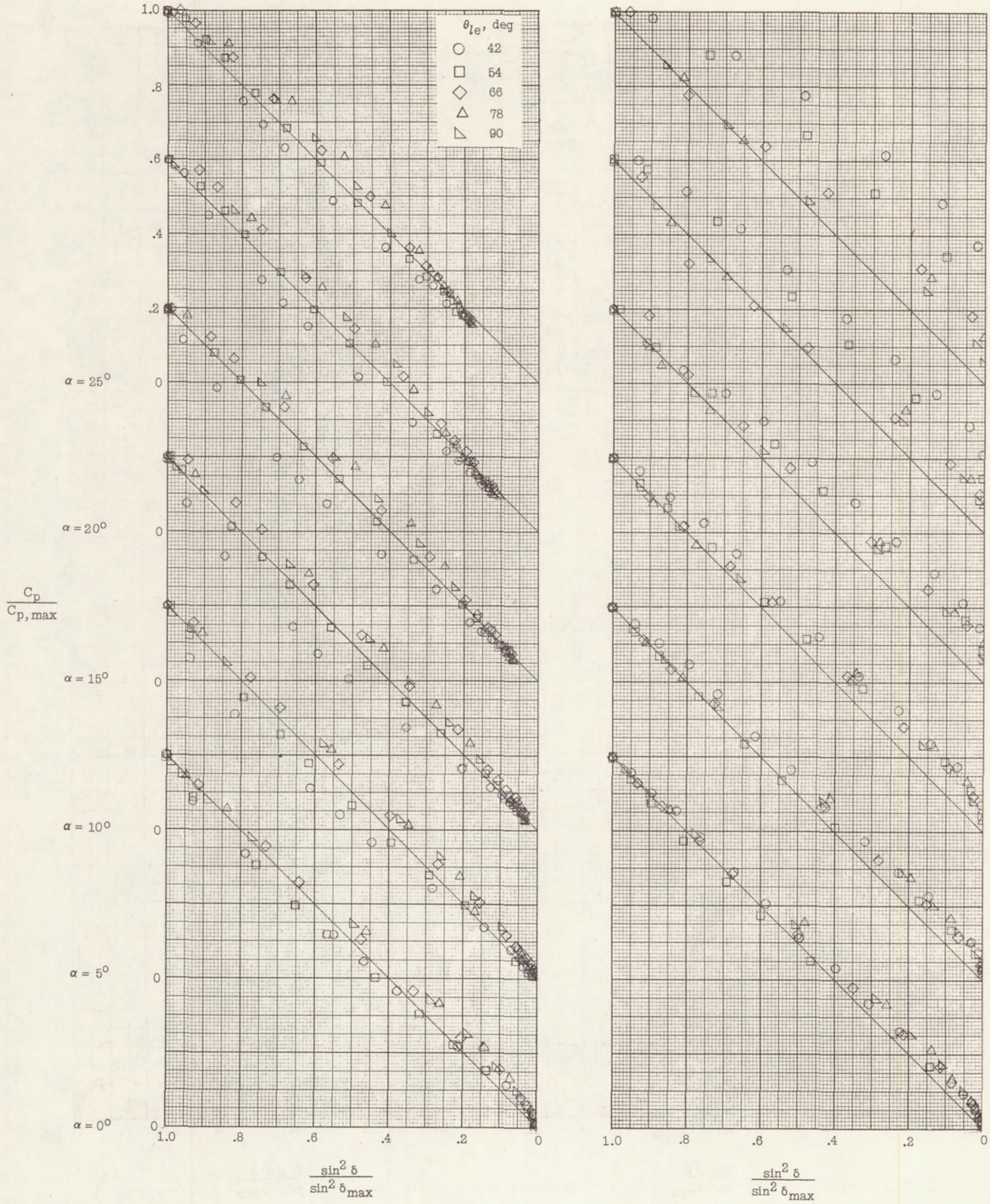

(a) Lower surface.

(b) Upper surface.

Figure 14.- Correlation of pressure distributions with generalized Newtonian theory for two-dimensional parabolic arc models.

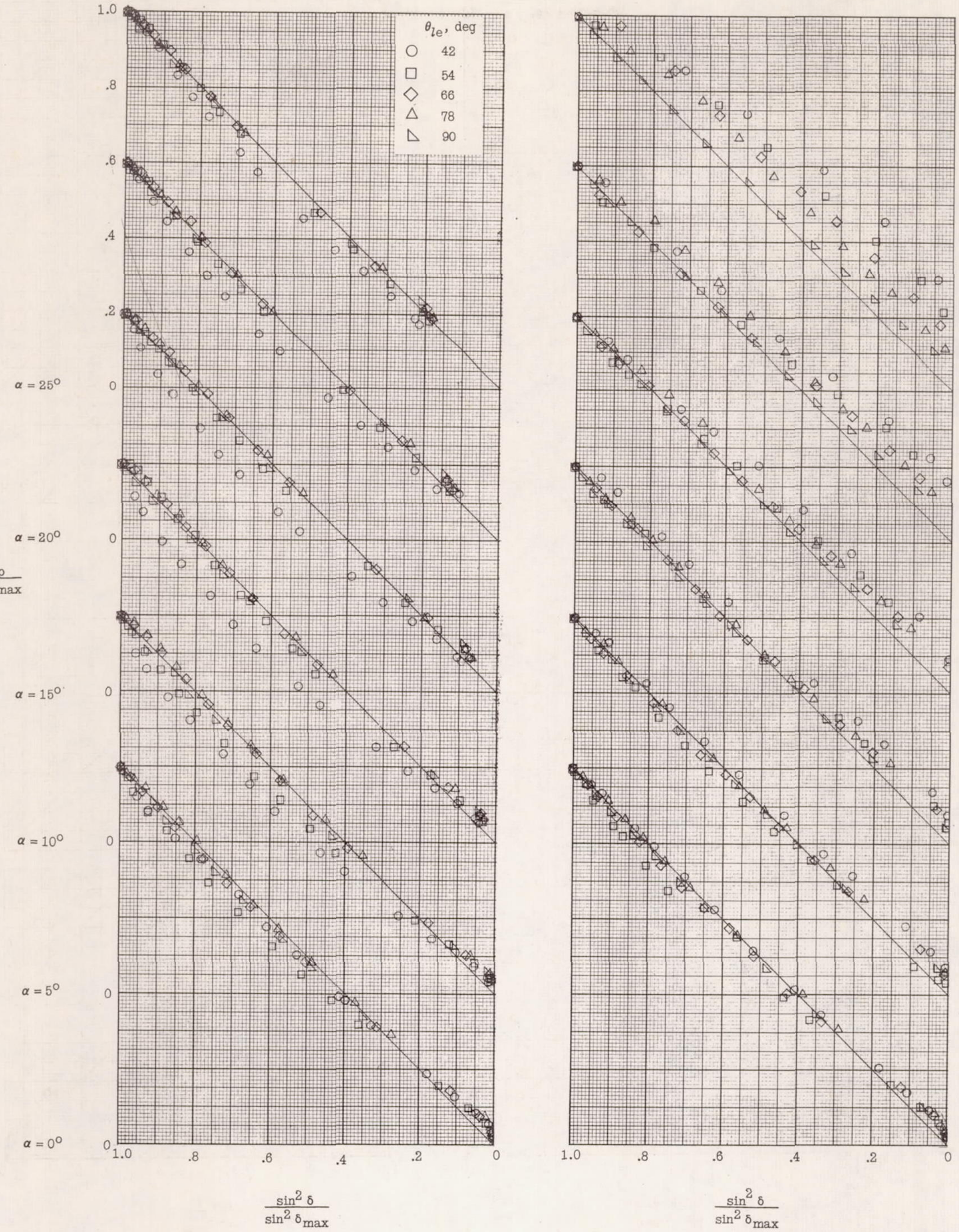

(a) Lower surface.

(b) Upper surface.

Figure 15.- Correlation of pressure distributions with generalized Newtonian theory for two-dimensional circular arc models.